EYE MOVEMENTS AND REWARD, SEQUENTIAL STATES, AND CONTEXT-DEPENDENT TARGET SELECTION

Thesis by

Michael Campos

In Partial Fulfillment of the Requirements

for the Degree of

Doctor of Philosophy

California Institute of Technology

Pasadena, California

2007

(Defended October 24, 2006)

ACKNOWLEDGEMENTS

I am thankful for my scientific lineage, from the earliest progenitors of inquiry and discovery, to the pioneers of neuroscience, to my thesis advisor, Richard Andersen. Under Richard's guidance I matured into a committed neurophysiologist and was continually inspired to refine and clarify my projects, papers, and analysis. I am grateful for the guidance and feedback provided by my thesis committee: Shin Shimojo, Christof Koch, Wolfram Schultz, and John O'Doherty. Throughout my graduate work I received additional encouragement, assistance and support from many other professors. Thank you: Joel Burdick, Erik Winfree, Kenji Doya, Masamichi Sakagami, Larry Pinto, and Mark Segraves. I spent my formative years as a scientist in the company of brilliant and dedicated mentors.

The Andersen Lab always felt like a nurturing family, and I am indebted to all of my colleagues over the last five years. Thanks to Alex Gail, Brian Corneil, Zoltan Nadasdy, Rodrigo Quian-Quiroga, Marina Brozovich, Dan Rizzuto, Sam Musallam, Bradley Gregor, Kelsie Pejsa, Nicole Sammons, Viktor Shcherbatyuk, Tessa Yao, and my grad student crew, Rajan Bhattacharyya, Grant Mulliken, Brian Lee, Eddie Branchaud, Hilary Glidden, Matt Nelson, and Asha Iyer. Extra special thanks must go to Boris Breznen. Our relationship began as an apprenticeship and, over the last three years, transitioned gracefully into a collaborative partnership.

My colleagues in the Computation and Neural Systems program are as diverse as they are driven. I felt supported by the bond keeping us together. Thank you Carl Gold,

Alan Hampton, Alex Holub, Kerstin Preuschoff, Sidney Cox, Tosin Otitoju, Ulrik Beierholm, and Vivek Jayaraman.

My family has supported me unconditionally along my journey. My father, George, has become one of my best friends, and my mother, Virginia, has been a patient and loving teacher who inspired me to approach problems creatively. My siblings Sara, Katie, and Christian, have always added sparkle and joy to my world. I welcome Julie to the family and acknowledge my grandparents, Alice Couturier, Aba (mi jovencita), and Abo, who I will always miss. Also, I thank my uncle, Vincent Takas, who welcomed me into his home when I first moved to California. The monks and nuns of Deer Park monastery, teachers in the tradition of Zen Master Thich Nhat Hahn, have given me support and guidance on all levels from their mountaintop sanctuary. And thank you to my new family, Virginia and David Tobias, my in-laws, who have shown great pride and caring, and to my aunts, uncles, cousins, niece, nephew, and goddaughter.

Finally, my wife, Elizabeth Tobias, the great woman behind this man, has been inspiring in countless ways. I thank her for the past four years, but I thank her more for the promise of the future.

ABSTRACT

The eye movement system is a complete sensorimotor loop from sensation to action, which includes a large number of distinct cortical and subcortical regions and participates in both reflexive and voluntary behaviors. This dissertation elucidates some of the functions of three cortical areas known to participate in eye movement behavior: the supplementary eye fields (SEF), motor area (SMA), and the lateral intraparietal area (LIP). In the course of executing eye movements, the eye movement circuitry interfaces with other functional circuits, including the networks of brain structures involved in reward processing, the temporal organization of behavior, target selection, and object perception. Here it is shown how LIP, SEF, and SMA participate in these multiple functional circuits, and complement each other during eye movement tasks. First, it is shown that neurons in the SMA carry a reward expectancy signal in the post-saccadic period of oculomotor tasks. Second, the neurons of SEF, but not LIP, are shown to collectively encode the temporal progression of the task. Third, in a target selection task, most LIP neurons are shown to respond to both cue and distractor stimuli, while most SEF neurons respond selectively only to the cue. Finally, fourth, the spatial tuning of parietal neurons is investigated in more natural circumstances, and the directional tuning preferences of cells in parietal cortex are found to be task dependent. These results extend the understanding of how these cortical brain areas that participate in eye movement behavior specialize and complement each other, and how they interface with other brain circuits, to support the organism in successfully completing a variety of instructed tasks.

TABLE OF CONTENTS

Acknowledgements……...…….iii

Abstract……...……...…..v

Table of Contents……..…….….vi

List of Illustrations and Tables……..…….…...…vii

Introduction……..……..…..1

Chapter 1: Supplementary Motor Area Encodes Reward Expectancy in Eye-Movement Tasks……..…..5

Chapter 2: Neural Representation of Sequential States within an Instructed Task…….……..……...…..40

Chapter 3: Selection of Targets and Disregard of Irrelevant Stimuli in monkey LIP and SEF…….....……82

Chapter 4: Individual LIP Neurons Remap Directional Tuning Preferences in Different Task Contexts……...……104

Conclusion…..……..…….……..….133

LIST OF ILLUSTRATIONS AND TABLES

Figure 1.1. Time course of oculomotor tasks……...…….10

Figure 1.2. Sites of neural recording……..17

Figure 1.3. Shift in burst onset times……...…….20

Figure 1.4. Histograms of burst onset times…….21

Figure 1.5. Example response to control trials……..24

Table 1.1. Total number of recorded neurons for both monkeys……..……15

Table 1.2. Cell counts for spatial tuning properties of recorded neurons…….....16

Figure 2.1. Time course of oculomotor tasks……49

Figure 2.2. Example SEF neurons……56

Figure 2.3. Continuous measures of activation, suppression, and spatial tuning…….....58

Figure 2.4. Temporal decode performance……..…….60

Figure 2.5. Summary temporal and spatial decode results…….……..63

Table 2.1. Cell counts for the neuronal database……..……54

Supplementary Figure 2.S1. Example LIP neurons……...….76

Supplementary Figure 2.S2. Activity types exhibited by individual neurons……77

Supplementary Figure 2.S3. Variety of event detection activity in SEF…...…….78

Supplementary Figure 2.S4. Variety of anticipation activity in SEF…….….80

Supplementary Figure 2.S5. Variety of state encoders in SEF……..….81

Figure 3.1. Time course of oculomotor tasks……...…….88

Figure 3.2. Responses to a distractor……92

Figure 3.3. Continuous measures of activation, suppression, and spatial tuning…...….94

Figure 3.4. Variety of state encoding neurons in SEF…….…….96

Figure 3.5. Spatial decode performance for cue and distractor positions…….97

Table 3.1. Cell counts for the neuronal database……...……..…….91

Figure 4.1. Behavioral tasks used in the experiment……...……...109

Figure 4.2. Sample cell recorded form monkey R…….…….115

Figure 4.3. Cells' spatial tuning compared across the two tasks……...…….118

Figure 4.4. Population vector decode of the direction of saccades……...…….…….119

Figure 4.5. ROC analysis of object-centered location of the cue discriminability…..120

Figure 4.6. Object orientation discrimination…….……122

INTRODUCTION

Eye movements can be made reflexively or voluntarily, and because they can be made voluntarily, the study of eye movements offers a window into the mechanisms of many high-level brain functions. With the development of awake-behaving neurophysiology techniques, the field of neuroscience became equipped to probe the working brain. Mainly in the last half-century, neurophysiologists have detailed the brain structures involved in eye movement control. At this stage it remains a challenge to understand how the different parts complement each together, and how they interface with other functional circuits in the brain, to support an organism in successfully completing the variety of tasks involved in normal behavior. In this dissertation we characterize some of the properties of two cortical nodes of the eye movement network, the supplementary eye fields (SEF) and the lateral intraparietal area (LIP), as well as a brain area that is just adjacent to SEF, the supplementary motor area (SMA), as they interface with (and participate in) other functional networks, particularly those supporting reward processing, the temporal organization of behavior, target selection, and object perception.

The first study describes the confluence of eye movement and reward circuitry in supplementary motor cortex. We found signals related to the expectation of reward in the SMA, which complement similar findings in SEF. These results suggest a reinforcement mechanism to learn new, coordinated behavior between different body parts.

The expectation of reward implies a sense of when the positive consequence of the movement will occur. We investigated this further in SEF and LIP, and in SEF we

found that the neural expectation of events is not limited to the arrival of rewards, but also precedes all perceptual and motor events within the task. Furthermore, there was a representation of temporal states, meaning neurons activate for the duration between events. These results suggest that SEF, much more so than LIP, is likely to participate in the temporal organization of perception and behavior.

In the third study we compared LIP and SEF neurons during the performance of a target selection paradigm. We found a clear qualitative distinction, with individual LIP neurons representing the location of both cue and distractor stimuli and SEF neurons tending to respond to only one, suggesting complementary roles in target selection.

In the final study we compare the representation of eye movements made in different contexts, putting object perception and movement planning together to investigate how neurons respond when the monkey is instructed to look to a portion of an object. This study revealed that LIP encodes the same eye movements in very different ways based on the context in which the movement was instructed, suggesting that the influences of other networks can have dramatic effects on how eye movements are represented in LIP.

The studies presented here offer comparisons between two eye movement areas, first describing a role of SEF in representing temporal states that is not typically shared with LIP, and second, describing complementary roles of LIP and SEF in the process of target selection. These results also explore the relationships between different functional circuits brought together in eye movement behavior, first detailing the coexistence of reward processing and motor representations in supplementary motor cortex, and second,

detailing the effects of task context, which is dependent on object recognition, on the representation of eye movements in LIP.

Establishing the author's major contribution

The observation that the SMA encodes reward expectancy, the subject of Chapter 1, was made in a conversation with senior staff scientist, Dr. Boris Breznen, with whom I apprenticed in monkey neurophysiology. Boris was happy to let me follow up on the observation, which became a Society for Neuroscience meeting abstract, and eventually a paper in the *Journal of Neurophysiology* with me as the first author. Boris and I worked closely together to devise new control experiments to assess our interpretation, and with his oversight I collected the majority of a complete dataset from two monkeys. I also performed the analysis and writing for this paper. Before publication we also enlisted the help of M.D.-Ph.D. student Kyle Bernheim to perform MRI scans.

Chapters 2 and 3 grew out of my official thesis project, and these results are more fully my own work. I trained both of the monkeys, mapped the chambers (with assistance from MRI scans), implemented the task paradigms, executed the neural recording experiments, performed the analysis, prepared the figures, and did all of the writing. I still enjoyed occasional experimental assistance from Boris, as well as conversations about the results. In addition, I benefited tremendously from my relationship with the post-doctoral scholar, Dr. Alex Gail, with whom I shared experimental space, in particular because of his instruction in multiple electrode recording.

The official thesis proposal was planned over many conversations with Professor Richard Andersen, as well as Boris, and received much helpful insight from my thesis

committee. As the results came to light, however, it appeared that the questions that we were as asking did not logically precede the answers the neural recordings were giving. For example, whereas we wanted to know how SEF neurons were representing eye movement vectors made to portions of objects, it turned out that the majority of SEF neurons were not representing eye movement vectors at all. Instead they were representing temporal states within the task and the transitions from one state to the next. The stories presented in Chapters 2 and 3, therefore, did not make use of the extensive planning that went into the task designs, but were instead discovered through data analysis and visualization and refined in conversations with Richard, Boris, and other members of the Andersen Lab, where all of the work was carried out.

Chapter 4 is almost entirely Boris' work, and when we submit it for publication he will be the first author (and will be the second author when Chapters 2 and 3 are submitted). For that chapter, Boris performed the experiments and data analysis, prepared the figures, and wrote the Results and Methods sections. I assisted in various ways over the course of my apprenticeship and made substantial writing contributions to the Introduction and Discussion sections.

CHAPTER I

SUPPLEMENTARY MOTOR AREA ENCODES REWARD EXPECTANCY IN EYE-MOVEMENT TASKS[1]

ABSTRACT

Neural activity signifying the expectation of reward has been found in many parts of the brain, including midbrain and cortical structures. These signals can facilitate goal-directed behavior or the learning of new skills based on reinforcements. Here we show that neurons in the supplementary motor area (SMA), an area concerned with movements of the body and limbs, also carry a reward expectancy signal in the post-saccadic period of oculomotor tasks. While the monkeys performed blocks of memory-guided and object-based saccades, the neurons discharged a burst after a ~200 ms delay following the target acquiring saccade in the memory task, but often fired concurrently with the target acquiring saccade in the object task. The hypothesis that this post-saccadic bursting activity reflects the expectation of a reward was tested with a series of manipulations to the memory-guided saccade task. It was found that, while the timing of the bursting activity corresponds to a visual feedback stimulus, the visual feedback is not required for the neurons to discharge a burst. Second, blocks of no-reward trials reveal an extinction

[1] Published in the Journal of Neurophysiology, April 20, 2005. Campos M, Breznen B, Bernheim K, Andersen RA (2005) Supplementary Motor Area Encodes Reward Expectancy in Eye-Movement Tasks. *J Neurophysiol* **94**:1325-1335. Used with permission.

of the bursting activity as the monkeys come to understand that they would not be rewarded for properly generated saccades. Finally, the delivery of unexpected rewards confirmed that, in many of the neurons, the activity is not related to a motor plan to acquire the reward (e.g., licking). Thus, we conclude that reward expectancy is represented by the activity of SMA neurons, even in the context of an oculomotor task. These results suggest that the reward expectancy signal is broadcast over a large extent of motor cortex and may facilitate the learning of new, coordinated behavior between different body parts.

INTRODUCTION

There has been substantial progress in recent years on the identification and characterization of the network of brain areas that are involved in the processing of reward. Reward expectancy signals have been found in many cortical areas such as the medialfrontal (Matsumoto et al. 2003; Shidara and Richmond 2002), dorsolateral prefrontal (Barraclough et al. 2004; Kobayashi et al. 2002), orbitofrontal (Hikosaka and Watanabe 2000; Tremblay and Schultz 2000), and parietal cortices (Musallam et al. 2004; Platt and Glimcher 1999; Sugrue et al. 2004). Subcortical regions expressing reward expectancy include the caudate (Watanabe et al. 2003), striatum (Cromwell and Schultz 2003; Hassani et al. 2001; Tremblay et al. 1998), superior colliculus (Ikeda and Hikosaka 2003), and midbrain dopamine neurons (Satoh et al. 2003; Schultz et al. 1997). Reward related signals have also been found in the dorsomedial frontal cortex (DMFC),

an anatomical region that includes our current area of interest, the supplementary motor area (SMA).

The DMFC has been shown to participate in volitional (Schlag and Schlag-Rey 1985) or goal-oriented motor acts (Mann et al. 1988). It contains at least three well-studied motor-representation areas that are thought to be involved in higher order control of behavior: the SEF (Schlag and Schlag-Rey 1987, 1985), the SMA (Luppino et al. 1991; Matsuzaka et al. 1992), and the presupplementary motor area (pre-SMA) (Fujii et al. 2002; Nakamura et al. 1998; Shima and Tanji 2000). These three motor areas of DMFC can be distinguished based on anatomical connectivity (Luppino et al. 1993; Parthasarathy et al. 1992) and physiological responsivity (Matsuzaka et al. 1992). The SMA and pre-SMA are located in the DMFC on and above the medial wall in the frontal lobe. An orofacial region occupies the rostral end of the SMA, and further rostral is the pre-SMA. Intracortical microstimulation evokes movements in both areas, though the movements evoked in the pre-SMA require longer trains of pulses that produce more complex movements (Fujii et al. 2002). The pre-SMA has been implicated in planned motor acts (Matsuzaka and Tanji 1996) and the acquisition (Nakamura et al. 1998), planning, and regulating (Shima and Tanji 2000) of sequential procedures. Additionally, pre-SMA neurons respond more often to visual stimulation compared to SMA neurons. The SMA consists of a rostrocaudal progression of orofacial, forelimb, and hindlimb movement representations (Mitz and Wise 1987). Lateral to the SMA, microstimulation will evoke eye movements. This area is defined as SEF (Fujii et al. 2002). Several studies have shown that electrical microstimulation at low currents (<50 μA, and sometimes as

low at 10 μA) will elicit saccades in SEF (Chen and Wise 1995; Fujii et al. 1995; Mann et al. 1988; Russo and Bruce 1993; Tehovnik and Sommer 1996).

Three recent studies have explicitly connected the SEF to reward variables. Amador et al. discovered reward-predicting and reward-detecting neuronal activity in SEF (Amador et al. 2000). Schall and colleagues used the countermanding task to characterize three different types of neurons in the SEF – error, conflict, and reinforcement neurons – and suggested that these could serve a performance-monitoring function (Stuphorn et al. 2000). Roesch and Olson found modulations of neural activity in response to both reward and punishment (Roesch and Olson 2003, 2004) and concluded that these modulations during the early stages of the trials correlate with motivation and not reward expectation. In this study we present neural activity reflecting reward expectation during a later stage of the trials, specifically after the monkey performs the instructed behavior. Our findings are similar to the reports of Amador and colleagues and Stuphorn and colleagues. The reward expectancy signal we describe, however, is found in the SMA, while these other studies were recording from nearby SEF. Taken together, these results suggest that a reward expectancy signal may be present throughout the DMFC.

In this study we present evidence that a reward expectancy signal is expressed in the neural activity of the SMA during the performance of an oculomotor task. The signal is not related to the metric of the eye movement. Rather, it encodes expectation of the reward after the successful completion of the instructed behavior. The results presented here began as a discovery during a project that was originally intended to investigate the contribution of the SEF to saccades to objects. Some early recordings in the SMA

uncovered a post-saccadic bursting activity that we hypothesized might be related to the expectation of reward, and experiments devised during the course of the project confirmed this hypothesis. While future studies of reward expectancy in SMA might use tasks that are specifically designed to investigate reward variables, with the two oculomotor tasks employed here we are able to establish two novel findings. First, we show that a reward expectancy signal is present in the SMA, an area that has been thought to be concerned only with movements of the body and limbs, during an oculomotor task. Second, we show the coupling of the signal's onset time with a conditioned stimulus. These findings suggest a general learning mechanism that would reinforce all motor representations in DMFC that are active just before the animal can expect to receive a reward. A preliminary account of this study has appeared previously (Campos et al. 2003).

METHODS

Studies were performed on two behaving, male rhesus monkeys (Macaca mulatta). Each was chronically fitted with a stainless steel head post for head immobilization, and a recording chamber over a craniotomy for electrode insertions. All procedures were approved by the Caltech Institutional Animal Care and Use Committee.

Stimuli and tasks

Monkeys were seated in a dimly lit room, 42 cm from a tangent screen. Stimuli were rear-projected with 800x600 resolution and a refresh rate of 72 Hz using a custom

built software display client with OpenGL. Task logic was controlled by National Instruments real time LabView software.

Two eye movement tasks were used; a memory-guided saccade task and an object-based saccade task. In both tasks the monkey was instructed to perform a saccade from a central fixation point to one of 43 targets placed at regular intervals to cover the entire visual field out to 17 deg of visual angle in every direction from central fixation.

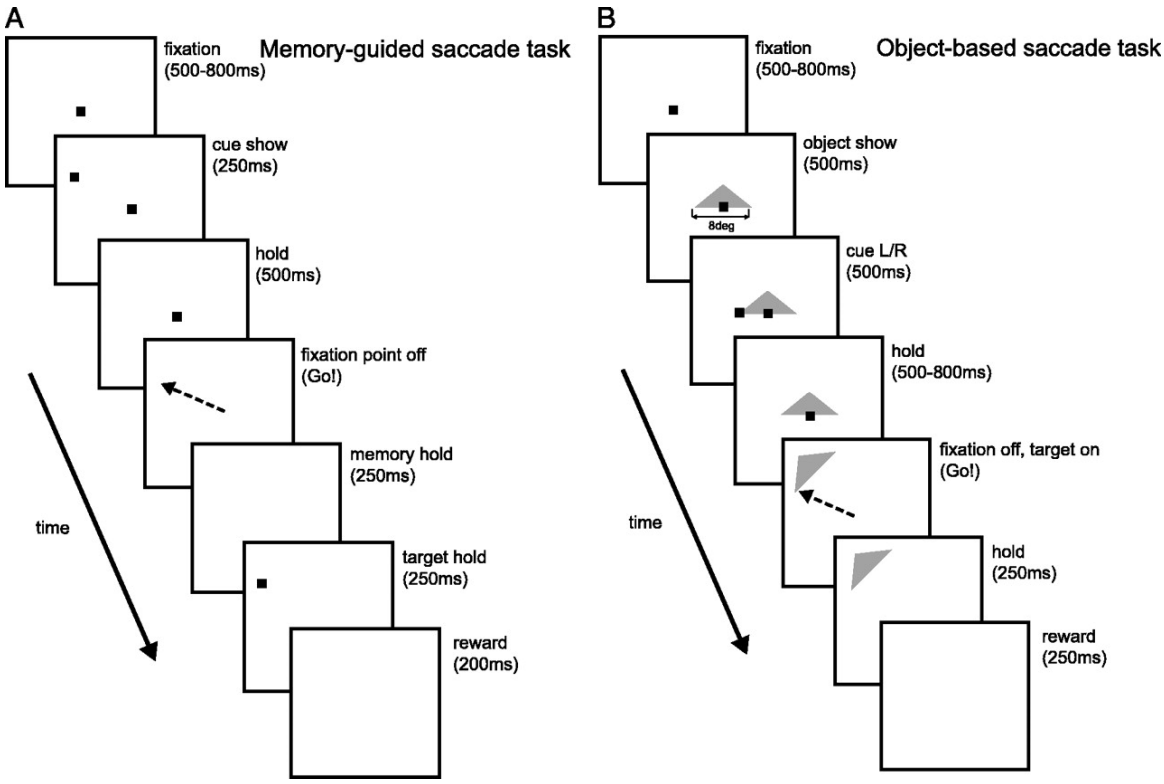

Figure 1.1 *Time course of oculomotor tasks*. Progression of tasks are shown in successive panels from the *top left to bottom right*. In the memory-guided saccade task **(a)**, the monkey is required to acquire a central fixation point at the start of the trial. After a variable delay, a cue is briefly flashed at one of 43 targets in the periphery. The possible targets cover the entire visual field out to 17 degrees. Following a hold interval, the fixation point is extinguished, and the monkey is required to saccade to the remembered target location and fixate there. After 250 ms the target reappears, and then following an additional 250 ms fixation, the animal is rewarded with a drop of juice. In the object-based saccade task **(b)**, the monkey begins the trial by acquiring a central fixation point. An object appears over the fixation point, and after a delay one side of the object is briefly cued. Following a hold period, the object is extinguished and immediately reappears in a new location. The monkey is then required to saccade to the cued portion of the object and fixate there for 250 ms before receiving a juice reward.

In the memory-guided saccade task (Figure 1.1a), monkeys were required to maintain central fixation while a peripheral target was briefly flashed, wait until the central fixation point extinguished, and then saccade to the remembered location. After successfully holding fixation at the target location, the target re-appeared to provide visual feedback of the correct eye position. The monkey then had to maintain fixation on the visible target for an additional interval of 250 ms before receiving a juice reward of about 0.2 ml.

In the object-based saccade task (Figure 1.1b), an object (isosceles triangle) was presented behind the central fixation point while the monkey fixated there. The object was cued for one of two possible locations on the object, and then, after a delay period, the object extinguished and reappeared at a peripheral location and new orientation. The monkeys were required to saccade to the previously-cued part of the object in the new location and orientation. The cued locations of the object were chosen so that the correct saccade ended in the same screen location as the targets in the memory-guided task. After maintaining fixation on the cued part of the object for 250 ms, the monkeys were rewarded with a drop (about 0.2 ml) of juice.

The memory-guided and object-based saccade tasks were designed to investigate the neural computations supporting object-based saccades; however, the important difference between the tasks for the purposes of this study was actually what happened after the saccade was completed. In the object task the target was visible at the time of the saccade, and the monkey could acquire a visible target. In the memory task the target reappeared 250 ms after the saccade to the remembered location. Thus, in the object task the animals received earlier feedback from a conditioned stimulus.

In a recording session a block of memory-guided saccades preceded a block of object based saccades. The memory-guided saccade block consisted of 3 correct saccades to each location. The object-based saccade block consisted of 12 correct saccades to each location. Control trials were performed during the memory-guided saccade block at the discretion of the experimenter.

Recording Procedure

Neurons were accessed on vertical penetrations with glass coated platinum-iridium electrodes (Fred Haer Co.). The electrodes were advanced with a Fred Haer or Narashige microdrive system through a blunt stainless steel guide tube pressed against the dura. Neurons were generally found 1-3mm beneath the exterior of the dura.

Waveforms were amplified and isolated online with a commercial hardware and software package (Plexon Inc.). Cell activity was monitored with custom built online data visualization software written in Matlab.

Data Analysis

Bursting activity was identified using a burst detection algorithm (Hanes et al. 1995; Thompson et al. 1996). Bursts were initially detected by a threshold crossing of a surprise index (SI), which is the negative of the log of a calculated significance level. The significance level describes the likelihood that the observed number of spikes would occur in a given interval, considering the average firing rate of the cell, based on the assumption that the inter-spike intervals follow a Poisson distribution. The significance level used to calculate the threshold for the SI was 0.01. The mean of the Poisson

distribution was calculated as the number of spikes in the trial divided by the duration of the trial. Since the mean can change from trial to trial, the algorithm assumes stationarity only over the duration of a single trial, and the threshold will adapt to changes in the baseline firing rate of the neuron over time. After the initial threshold crossing, the beginning and end of the burst were precisely identified, and multiple bursts could be identified in a single spike train (Thompson et al. 1996).

For ANOVA of firing activity in task intervals, the intervals were defined as follows. The baseline period was the interval between the acquisition of the fixation point and the cue appearance. The cue period was the interval that the cue was visible, and the memory period was the interval between the cue disappearance and the fixation point disappearance (the signal for the monkey to make the saccade). The saccade period was the 200 ms interval preceding the acquisition of the target, and the post-saccadic period was the interval from the target acquisition until the delivery of reward. All intervals were defined by these same events in both the memory and object-based tasks. The duration of the post-saccadic interval was 500 ms in the memory task and 250 ms in the object-based saccade task.

Electrical Stimulation

A BAK instruments stimulator was used to deliver biphasic currents at 330 Hz of typically less than 200 μA in 100-500 ms trains through the recording electrodes.

Electromyography

Electromyography (EMG) recordings were performed in one monkey with a World Precision Instruments (DAM 80) AC/DC amplifier and paired hook-wire electrodes (44 ga x 100 mm) from Viasys healthcare.

MR Imaging

Magnetic resonance (MR) imaging was performed at the Caltech Brain Imaging Center on a 3 T Siemens Trio. Anatomical images were acquired sagittally with 0.7 mm slice thickness using an in plane field of view of 168 x 168 mm on a 256 x 256 base matrix, yielding a final native voxel resolution of 0.656 x 0.656 x 0.7 mm. These images were realigned via multi-planar reformat to recording chamber landmarks using Siemens Syngo software (version MR 2003T DHHS). This rotated volume was resliced at 0.7 mm spacing along the z-axis of the chamber and visualized using the AFNI software package (Cox 1996).

RESULTS

With a series of single electrode penetrations, 173 cells were recorded in both tasks from two monkeys (monkey S: 100; R: 73). According to ANOVA of baseline firing rates versus the post-saccadic interval, 50 (S: 34; R: 16) neurons demonstrated a significant modulation in the post-saccadic interval, with 17 (S: 9; R: 8) of these modulated in the post-saccadic interval exclusively. Many of the neurons were also active during task periods. According to ANOVA of baseline firing rates versus cue, memory, and saccade

intervals 84, (S: 55; R: 29) of the recorded cells were significantly ($p < 10^{-5}$) modulated during at least one of these intervals in both tasks. A breakdown of neurons with significant modulations for the individual periods of the memory saccade task (cue: 23, memory: 51, saccade: 71), show that there was substantial activity present in all task intervals, however this activity was generally not spatially-tuned (see Table 2 and discussion below). Summary cell count information is provided in Table 1 along with results of control experiments.

TABLE 1.1. ***Total number of recorded neurons for both monkeys***

	Monkey S			***Monkey R***			Total		
	Memory	Object	Both	Memory	Object	Both	Memory	Object	Both
Total recorded neurons	103	107	100	76	77	73	179	184	173
Task related modulation	71	77	55	42	44	29	113	121	84
Reward period activity	56	59	34	31	31	16	87	90	50
Post-saccadic bursts in > 30% of trials	32	27	18	18	21	12	50	48	30
Exclusive reward period activity	29	22	9	20	21	8	49	43	17
Response to no visual feedback control	16 (26)			6 (8)			22 (34)		
Response to no reward control	10 (10)			1 (1)			11 (11)		
Response to unexpected reward	2 (22)			0 (3)			2 (25)		

All statistical tests are ANOVA ($P < 10^{-5}$). Task-related modulation indicates a modulation in one or more of cue, memory, saccade, or reward intervals relative to baseline. Reward period activity compares the baseline to reward interval; exclusive reward activity excludes neurons with significant cue or memory period activity. Control categories compare a time interval of interest (see text) associated with the control, in normal and control trials. Numbers in parentheses are the number of cells recorded while each control was run, and the numbers beside them are the number of cells with a significant modulation in firing rates according to ANOVA analyses described in the text.

TABLE 1.2. ***Cell counts for spatial tuning properties of recorded neurons***

	Cue	Memory	Saccade
Monkey S			
Active above baseline	16	37	48
Significant spatial and interval dependency	1	6	6
Monkey R			
Active above baseline	7	14	23
Significant spatial and interval dependency	0	1	0

Active above baseline refers to a significant modulation according to an ANOVA test ($P < 10^{-5}$) comparing baseline firing rates to firing rates in cue, memory, or saccade intervals. Significant spatial and interval dependency indicates significant dependence of firing rates (2-way ANOVA, $P < 10^{-3}$) on the task interval, the spatial location of the targets, and the interaction between these two factors. All tests refer to data collected in memory saccade trials.

Anatomic localization of the recording sites

The sites of all of the electrode penetrations included in this study are superimposed on axial MRI scans in Figure 1.2 (a,b). While recordings were taken on the surface of cortex, MRI sections for anatomical localization were chosen at a depth appropriate to clearly show the locations of the penetrations relative to surrounding sulci.

The sites which yielded the 50 neurons with significant (ANOVA, p<10^-5, see above) post-saccadic modulations are shown in red, and the remaining sites are shown in blue. Not all neurons recorded at the sites marked in red were modulated in the post-saccadic period. The red marker only indicates that at least one of these 50 neurons of interest was recorded at that site.

While much of SMA is in F3 on the mesial surface, there is also a portion of F3 on the dorsal surface, within about 3 mm of the midline that is also considered SMA proper (Luppino et al. 1991; Matsuzaka et al. 1992). The neurons of interest in this

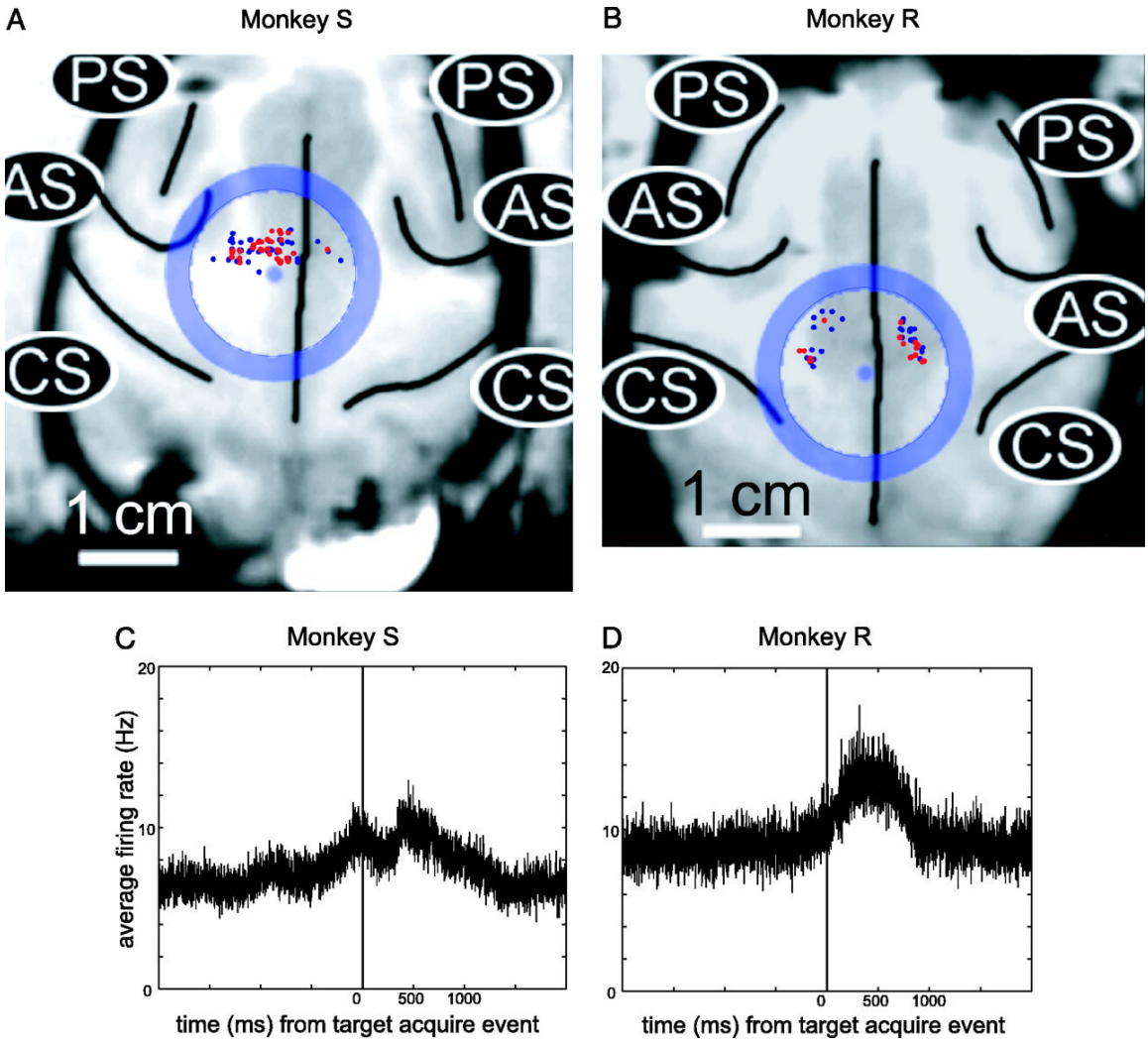

Figure 1.2. *Sites of neural recording.* Projections of chamber walls are indicated with a blue circle superimposed on axial MRI scans of Monkey S **(a)** and R **(b)**. Anatomical landmarks are of the arcuate sulci (AS), principle sulci (PS), and central sulcus (CS). Recording sites that yielded reward interval activity are shown as red dots, and the remaining recording sites are blue. Averaged output of all recorded neurons **(c, d)** shows the average firing rate for all recorded neurons for each monkey aligned on the target acquire event of memory saccade trials.

report, indicated in red on the axial slices in Figure 1.2, mostly cluster within this distance to the left (monkey's right) of the midline for monkey S, and to the right (monkey's left) of the midline for monkey R. No recordings were performed in SEF. In both monkeys some of the recordings were in area F2, lateral to SMA-proper (Luppino et al. 1991). In monkey S, the majority of the recordings were directly medial to the genu of the arcuate sulcus, while in monkey R the recordings were medial and somewhat

posterior. The SEF is medial to the arcuate sulcus and somewhat anterior, though there is some variability in the precise location of SEF as described in previous studies. See Sommer and Tehovnik (1999) for review.

Microstimulation

Electrical stimulation experiments show the progression of body movement responses typical of the SMA (Mitz and Wise 1987). Since eye movements were not observed to be elicited in either of the monkeys by stimulation of 50 μA, which is the upper limit of the low threshold criterion for eliciting eye movements in the SEF (Russo and Bruce 1993), or even currents as high as 200 μA, the recordings were not in the oculomotor area SEF.

Population characteristics

The average spike activity recorded during memory saccades from all sites for each monkey is summarized in Figure 1.2 (c,d). The average firing rate aligned to the target acquire event (end of saccade) is shown. The activity from monkey R (Figure 1.2d) is exclusively post-saccadic. In monkey S, saccadic and memory period activity was also observed (Figure 1.2c), which could be due to the more anterior placement of the chamber. In monkey S, the dominant peak of activity still occurs after a delay following the target acquire event.

While there were many neurons with modulated activity during different epochs of the task (see Table 2), very few were spatially-tuned. A 2-way ANOVA between baseline firing rates and 1) the firing rates from different task intervals and 2) the spatial

locations of the targets was used to confirm this observation. A very small number of neurons passed the significance test ($p < 10^{-3}$) for dependence of firing rate on task interval and target location (cue: 1; memory: 7; saccade: 6).

Shift in burst onset times

The post-saccadic burst in both trial types (a,b – memory, c,d – object) for one of these neurons in Figure 1.3 is illustrated with raster plots of spike traces aligned to the target acquire event (a,c) and the reward delivery (b,d). Bursts of activity identified with the burst detection algorithm (methods) are shown as horizontal blue lines beneath the spike trains. The bursts in the object task (c) begin at a time that could be related to saccade generation. However, the bursts of activity in the memory task (a) come substantially later, revealing that these bursts do not participate in the generation of a saccade, or at least not in the context of the memory saccade task. For this neuron the post-saccadic firing terminates with reward delivery. Other neurons (see Figure 1.5 for example) were also observed to terminate just before or soon after reward delivery.

In Figure 1.4a, histograms for the time to burst relative to the target acquire event in each trial type are shown for the recording presented in Figure 1.3. There is a clear separation of these two groups (ANOVA, $p << 10^{-5}$). The mean bursting times relative to the target acquire event are 105 ms in the object task and 537 ms in the memory task. The bursts in both tasks terminate with the delivery of the reward after successful completion of the task.

The difference of the mean time to burst in the memory task and the object task for the population of neurons that discharged a burst in at least 30% of the trials in both

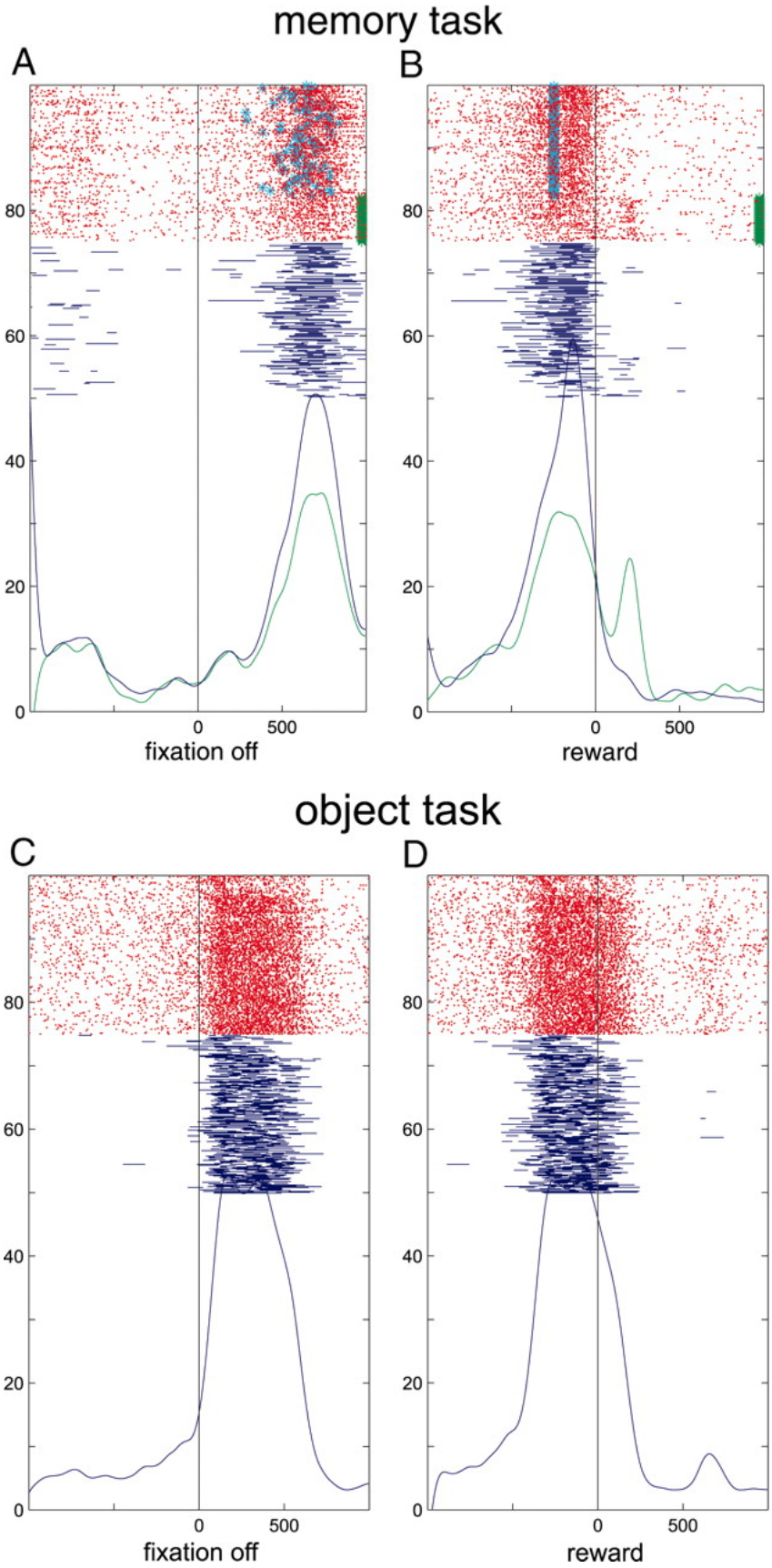

Figure 3. *Shift in burst onset times*. Peri-event time histograms in memory **(a,b)** and object **(c,d)** saccades tasks. Spikes are represented in red, aligned to the target acquire event **(a,c)** and the reward delivery event **(c,d)**. The smoothed average firing rate for normal trials is plotted as a blue curve, for no-visual feedback trials in green. Horizontal blue lines indicate periods of burst activity for the spike trains above. Green stars forming a bar on the right edge of the panels indicate trials in which visual feedback was withheld. Cyan markers indicate the reappearance of the target.

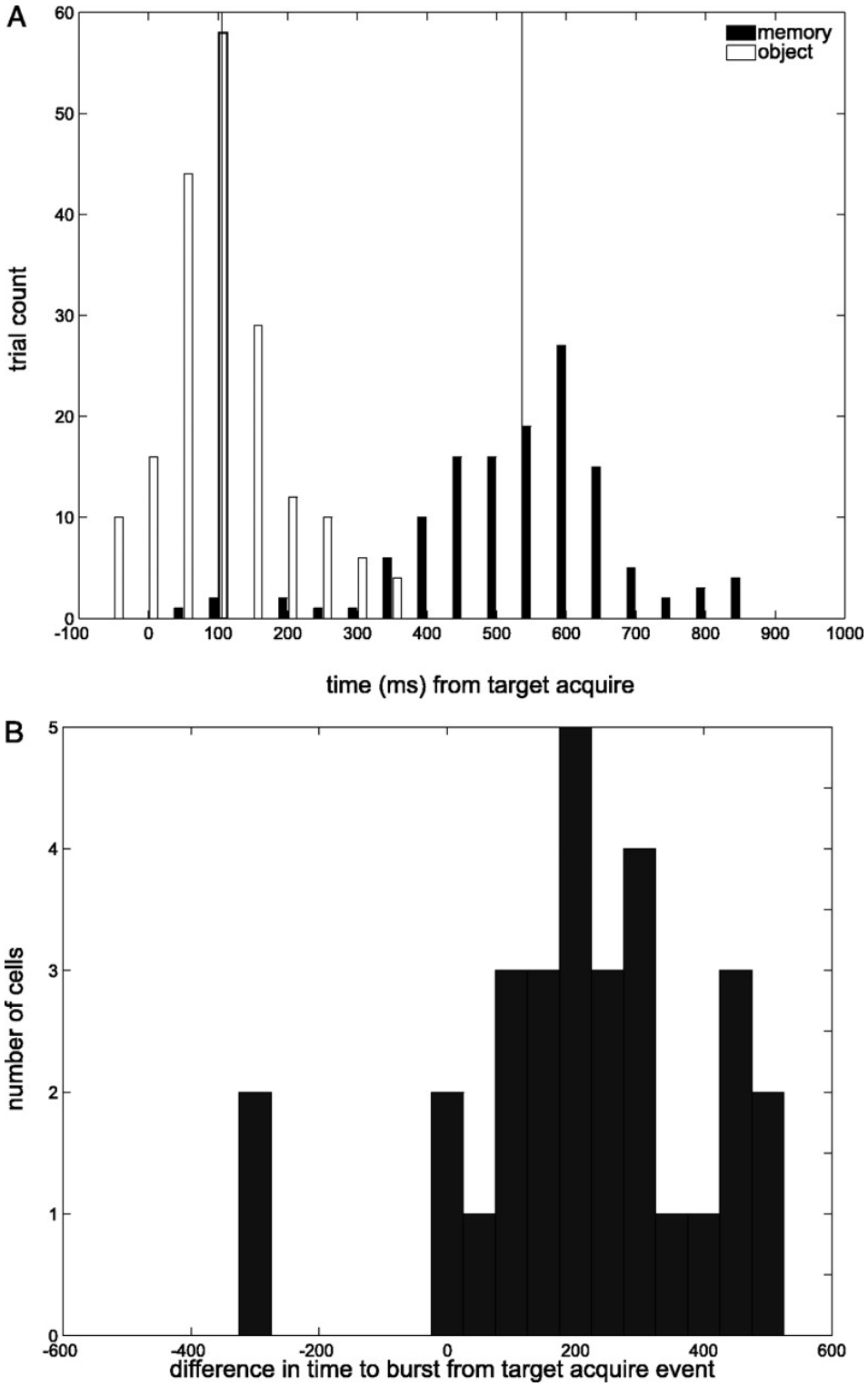

Figure 1.4. *Histograms of burst onset times*. **a)** Distribution of time to burst for each trial of the memory (filled) and object (open) saccade tasks for the cell shown in Figure 3. Mean time to burst is: memory task: 537 ms, object task: 105 ms. Memory task data clusters to the right of the object task data. **b)** Differences in time to burst onset after the target acquire event in memory vs. object tasks. Only cells with bursts in at least 30% of the trials in both tasks are shown (N=30). Mean difference: 202 ms. The population of average shift times is significantly different from 0 (t-test, $p < 10^{-5}$).

tasks (N = 30) is plotted as a histogram in Figure 1.4b. In general, the bursting activity came later, relative to the target acquire event, in the memory task compared to the object-based task. Neurons in this category showed a mean shift in the onset time of the burst of 202 ms. This number is comparable to, though slightly less than, the amount of the time the animal was required to fixate the remembered target location in the memory task before the reappearance of the target (250 ms).

The onset time of the burst corresponded to the appearance of the visual feedback, which was immediate in the object-based task, but delayed in the memory-guided saccade task. In both cases the visual feedback could serve as a predictor of a reward. The hypothesis that bursting activity reflects an expectation of reward was then tested in a series of control experiments outlined below.

Bursting does not accompany non-rewarded target acquisitions

It could be argued that the neurons simply signal the acquisition of any target, regardless of the expectation of reward. We tested this possibility by comparing the activity of the neurons after the initial acquisition of the fixation point with the activity after the reappearance of the target in the memory-guided saccade task. We used ANOVA on two intervals: the first interval was between the fixation acquire event and the appearance of the cue (250 ms), and the second interval was between the target onset and the reward delivery (250 ms). This analysis reveals that of the 50 neurons with a significant post-saccadic modulation, none were significantly active during the initial acquisition of the fixation point.

Bursting is not a visual response

Control trials of the memory-guided saccade task in which the visual feedback was withheld were run to test whether or not the bursting activity is related to the visual feedback signal. As shown in Figure 1.3 and again in Figure 1.5, removal of the visual feedback (indicated in the figures with the green bar composed of green stars) does not eliminate the onset of the bursting activity, though it may reduce the intensity or vary the onset time. Figure 1.5a shows an example in which the post-saccadic bursting activity was slightly extended by this control, though otherwise unchanged.

The bursting signal is therefore not indicating the reappearance of the target, though the visual reinforcement serves to sharpen and intensify the neural discharge. This control was run on 34 neurons, and 12 of them showed no significant difference in the mean firing rate from the time the target appeared (or should have appeared) until the end of the trial (ANOVA, $p < 10^{-5}$) in control vs. normal trials. Of the remaining neurons, many exhibited a temporal shift in their active periods or a decrease in firing, but only 1 showed an extinction of the bursting activity. This control shows that visual feedback could be dissociated from the reward delivery and the neural response remained.

Bursting properties in the absence of reward

To see if, all else being equal, the absence of reward would have an effect on the neural activity, we occasionally withheld the reward for a block of trials during the memory-guided saccade task, even for correctly performed trials. In the no reward blocks, the monkeys generally continued to correctly perform the task for about thirty trials before stopping, and this comprehension of changing task conditions was reflected

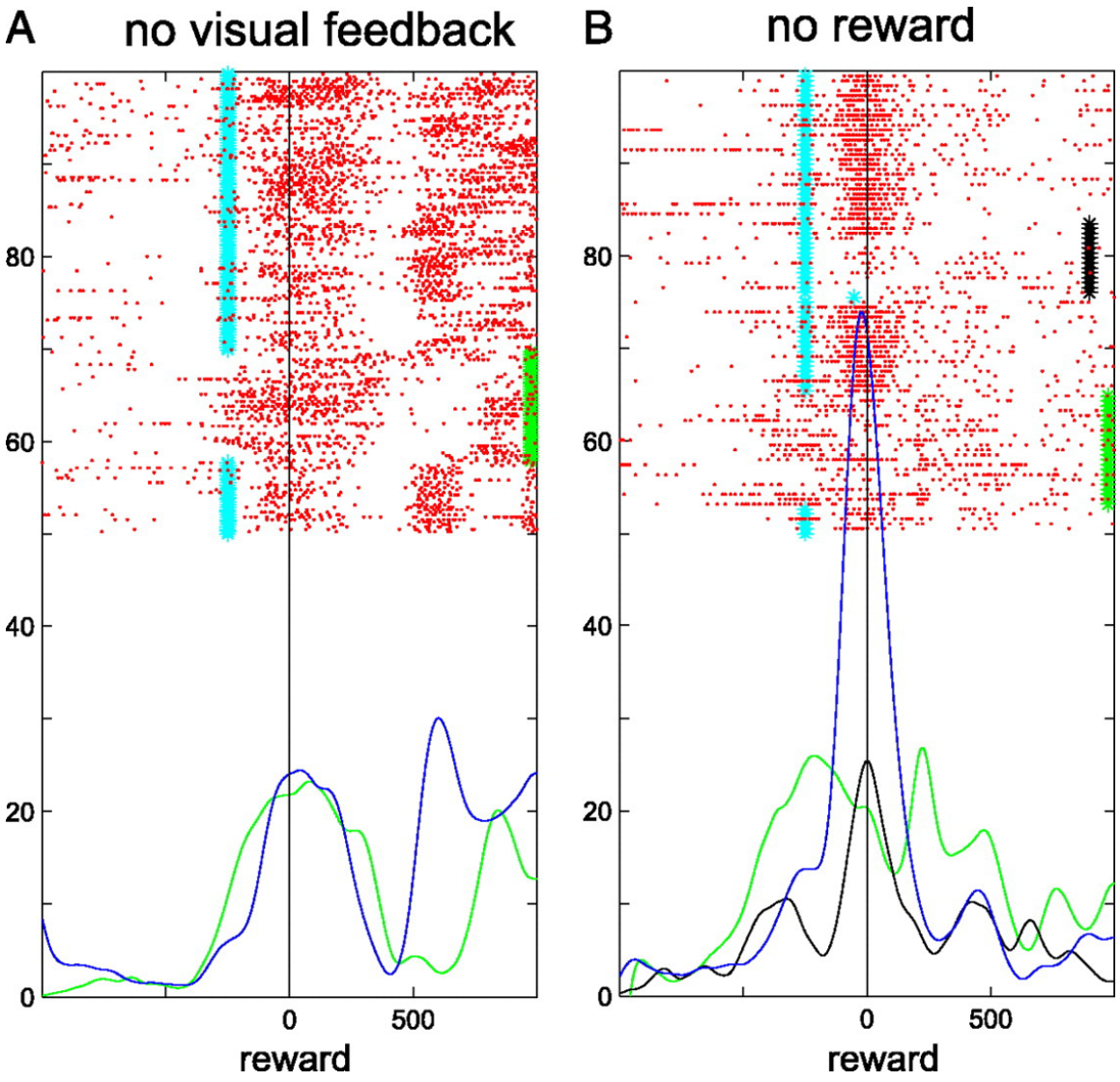

Figure 1.5. *Example response to control trials.* **(a)** Withheld visual feedback control trials. All trials shown are from the memory-saccade task. Green stars forming a bar on the edge of the panel indicate trials in which visual feedback was withheld. Smoothed average firing rates for normal trials are drawn in blue, and can be compared with the average firing rates during the withheld feedback trials drawn in green. **(b)** Withheld reward block of trials. All trials shown are from the memory-saccade task. Black stars forming a bar slightly inset from the right edge of the panel indicate the successfully completed trials in which the reward was not delivered. Green stars forming a bar on the right edge of the panel indicate trials in which visual feedback was withheld. Only the spike trains from successfully completed trials are shown. Trials are arranged chronologically from top to bottom. Smoothed average firing rates for normal trials are drawn in blue and can be compared with the average firing rates during the withheld reward trials shown in black and the withheld feedback trials drawn in green. Cyan markers indicate the reappearance of the target.

in the recorded neural activity. After a few trials, bursting activity would stop altogether. This control was run while recording 11 neurons, and all of these showed a significant difference in the mean firing rate from the target acquire event until the end of the trial

(ANOVA, $p < 10^{-5}$) in control vs. normal trials. The vast majority (10) ceased firing during the pre-reward interval in the no-reward blocks, and the remaining neuron (of the 11 that were modulated) increased its firing rate after the reward period. An example neuron is shown in Figure 1.5b. The firing activity is gradually extinguished in the no reward block (black bar). In contrast, the activity during the no-visual feedback trials (green bar) has a less precise onset time, but does not extinguish. While the no-visual feedback trials show the effect of removing a predictor of reward, the no-reward blocks reveal the dynamic effects of the monkeys coming to understand that they should no longer expect a reward.

Unexpected reward trials

By removing the reward, the possibility that the bursting activity encoded an orofacial (e.g., licking) motor response was not eliminated. Every time the monkey expected a reward, he would presumably also plan a licking movement to acquire it. The monkey would often stop licking the juice tube in the blocks of trials in which the reward was turned off, and this would correspond to the termination of the bursting activity. Of course, if the monkey no longer expected to be rewarded for the eye movements, he also had no reason to lick the juice tube.

To dissociate licking movements from the expectation of reward, control trials were run in which an unexpected reward was delivered. A bonus reward would be delivered with a 5% probability at the end of the fixation interval, just before the cue presentation. To quantify a response, an ANOVA ($p < 10^{-5}$) compared firing rates in the 200 ms interval during the bonus reward delivery with the corresponding 200 ms period

at the end of the fixation interval in normal trials. This first interval is the actual interval that the valve regulating the flow of reward was open. While running this control, 25 neurons with reward related activity were recorded, and 23 of these demonstrated no correlated activity in the unexpected juice delivery period. This control shows that the majority of the recorded neurons are not responsive to rewards when they are not expected, ruling out the possibility that the neural activity is attributable to motor commands required to obtain the reward, such as licking and swallowing.

To address the possibility that the neural activity reflected the monkey's postural responses or attempted postural responses, or preparation for either, we recorded muscle activity in three muscles active during postural adjustments. We recorded EMG (see Methods) from left and right Latissimus dorsi and right Semitendinosus of Monkey S during the performance of both tasks. We observed that these muscles were active during trunk movements and leg movements. While there was activity recorded from these muscle groups during the execution of the task, we found that it was not temporally locked to reward expectation. These negative EMG results rule out the possibility that the monkey is consistently making postural adjustments in anticipation of the reward delivery.

DISCUSSION

Bursting activity related to reward expectation was found in a cortical area that is not directly responsible for the generation of the behavior (saccade) that achieves the reward. This report separates itself from other reports by (1) investigating the reward expectation

activity in the motor area SMA and (2) showing a shift of activity in time course based on a conditioned stimulus, the visual feedback that usually predicts the upcoming reward. Below we outline and justify our findings, compare our results with the results of other studies, and suggest a functional role for the representation of reward expectancy in SMA during eye movement tasks.

Onset of reward-expectancy signal corresponds to a conditioned stimulus

The activity generally started with the conditioned stimulus and stopped with the delivery of the reward. The conditioned stimulus in this context was visual feedback that occurred before reward delivery. In the memory task, the target reappeared after 250 ms of fixation on the remembered target location. This visual feedback helped ensure accuracy in the initial learning of the task, but also became a predictor of the upcoming reward. In the object task, the saccade target was visible, and so the monkey could be sure that he made a saccade to the target because he could see it. The onset time of the reward expectancy signal corresponded to the onset of the visual feedback in the tasks, either 250 ms after the correct saccade in the memory task or immediately during the correct saccade in the object task.

As shown in control experiments, while the conditioned stimulus helped to synchronize the timing of the bursting activity, it was not necessary for the neurons to burst. This and other controls discussed below confirm that the bursting discharge carries a reward expectancy signal.

Control experiments establish the reward expectancy interpretation

In a series of control experiments, the argument was built that this activity reflects an expectation of reward. First, the bursting activity was dissociated from visual feedback, with the demonstration that visual feedback is not required for the neurons to discharge, though it regularizes the timing of the onset. Second, when the reward was removed for a block of trials, the reward expectancy activity gradually disappeared, showing that this activity represents a dynamic variable corresponding to the comprehension of a changed task condition. Finally, the possibility that the neural trace signified a licking plan or a detection of reward was ruled out since there was generally no response to unexpected reward delivery.

Reward related activity in the supplementary eye fields

Reward related neural signals have already been described in the SEF (Amador et al. 2000; Roesch and Olson 2003; Stuphorn et al. 2000). We found a reward expectancy signal in the SMA that appears very similar to types of activity found by Amador and colleagues and Stuphorn and colleagues.

Reward expectancy and reward prediction

Reward prediction (RP) neurons have been described in SEF along with a set of complementary reward-detecting (RD) neurons (Amador et al. 2000). The neural activity we are describing as reflecting reward expectation is similar to the RP neural activity. We did not find evidence of RD activity.

The firing rates of RP neurons increase before the occurrence of a reward and then abruptly cease firing at reward delivery, just as we found in the bursting activity of many of the neurons in this study. Our results, combined with the results of Amador and colleagues, are therefore evidence that reward expectation can be found in both SMA and SEF, and likely throughout the DMFC. Our study adds to the findings of RP neurons by (1) recording neural responses during the unexpected delivery of reward and (2) submitting the monkey to short blocks of no-reward trials.

We choose to use the term reward expectancy since "expectancy" captures the way the neural activity continues until reward delivery. Furthermore, this designation separates itself from reward prediction nomenclature found in the dopamine neuron literature. To predict is to foretell on the basis of experience, while to expect is to await or look forward to the coming or occurrence. The reward prediction signal found in midbrain dopamine neurons and the reward expectancy signal in the DMFC likely play different roles in learning and goal-oriented behavior (see below).

Reward expectancy and reinforcement.

Reinforcement signals have been found in SEF using a countermanding saccade task (Stuphorn et al. 2000). The reinforcement neurons were shown to increase activation while awaiting reward. The term reward expectancy describes the function of this activity. Again, the results of this study are evidence that the reward expectation signal found in the SMA is also present in the SEF.

Reward expectancy versus enhanced motivation

The post-saccadic burst cannot be a correlate of motivation (Roesch and Olson 2003, 2004) simply because it comes after the behavior it would presumably motivate. Our use of the burst detection algorithm (Hanes et al. 1995; Thompson et al. 1996) establishes that this bursting activity comes in the post-saccadic interval.

In the Roesch and Olson study, the preferred direction of a neuron was first identified, and then a memory-guided saccade task was run to and away from the preferred direction of the cell. Since we rarely found neurons to be spatially-tuned, we may have been recording from different types of neurons in the SMA.

Interestingly, the authors noted that in areas in which reward effects were common, such as the SMAr, neurons "fired more strongly than reward-insensitive neurons during the period extending from the completion of the saccade to delivery of the ingested reward." The authors did not think their paradigm capable of distinguishing between various interpretations of the significance of this effect, such as preparation and execution of liking movements or increased intensity of reward anticipation. In the present study, our control experiments show that the post-saccadic activity in SMA reflects reward expectation.

Reward expectancy versus attention

The expected value of a reward has been shown to modulate activity during the performance of a task (Ikeda and Hikosaka 2003; Platt and Glimcher 1999; Shidara and Richmond 2002; Watanabe 1996). It has been argued that so far sufficient controls for these studies have not been performed to determine whether the cognitive state being

manipulated is expected value or attention, since these two states likely occur together and can be easily confounded. Likewise, studies examining attention may have recorded the effects of expected value (Maunsell 2004).

In the current study it is unlikely that the reward expectancy signal is actually an attention signal. The signal occurs after the task and is not spatially-tuned and thus cannot reflect attention to the saccade location. It also cannot reflect attention to the reward since there was no activity when the reward was presented unexpectedly – novelty is a powerful attractor of attention.

Reward signals and reinforcement learning algorithms

A reinforcement learning algorithm (Sutton and Barto 1988) has been proposed to account for different reward-related signals that have been found in the brain, such as the error of reward prediction in midbrain dopamine neurons (Schultz et al. 1997). The prediction error signal is widely recognized as evidence for the implementation of a reinforcement learning algorithm in the brain. For example, the prediction error can serve to update action value estimates so that the animal can have accurate estimates of the reward that can be expected for an action. In this formalism, the expected value, V, is updated after every trial according to the experienced reward by the equation:

$$V^{t+1} = V^t + \alpha(R^t - V^t), \qquad (1)$$

where R^t is the amount of reward obtained at time t, V^t is the amount of reward expected at time t, α is the learning rate, and V^{t+1} is the updated estimate of expected value at time

t+1. In this formulation the time steps are individual trials, and the signal that corresponds to the error of reward prediction found in dopamine neurons (Schultz et al. 1997) is the term in the parentheses, $R^t - V^t$. The action value signal, V, that we are describing would not be used instead of a prediction error signal, R-V. Rather, both signals are supposed components of a larger reinforcement learning mechanism.

The dynamics of the reward expectancy signal in SMA corresponds to the dynamics of the expected value of the action, V. Specifically, this algorithm captures the way the post-saccadic firing activity in the SMA gradually dissipates in no-reward blocks. When the reward, R, is zero for a series of trials, the equation above will diminish the expected value of the action, V, until it reaches the new value of the reward, 0. The learning rate parameter, α, determines how quickly the estimate of the expected value approaches the new value. This equation also describes how the neural activity will return to normal firing when the reward is again delivered as usual.

Functional significance of reward expectancy in DMFC – a signal to guide learning

As in neural network models of reinforcement learning (Mazzoni et al. 1991; Suri and Schultz 1999), the reward signal found in DMFC could be used to train other parts of cortex to perform visuospatial tasks requiring arbitrary sensorimotor transformations. The reward expectancy signal found in the SEF (Amador et al. 2000; Stuphorn et al. 2000) is in position to shape future oculomotor behavior through its connections with the frontal eye fields (FEF) (Schall et al. 1993) and the superior colliculus (SC) (Fries 1984).

A reward expectancy signal is better than the detection of the reward itself for training purposes for two reasons. First, the reward expectancy signal implies that there is

an internal model with an expected sensory outcome for a behavior, in this case the conditioned stimulus. This model can be matched with a reward signal and refined as often as rewards are delivered or unexpectedly withheld. Second, the reward expectancy signal comes at a time that is more proximal to the behaviors which earned the reward, and thus may be able to reinforce the high level motor signals in DMFC related to those behaviors.

Usefulness of reward expectancy in SMA during an eye movement task

A reward expectancy signal present in DMFC could maintain and enhance the high-level representations of behaviors that earn a reward. But why would this activity be present in the SMA, which is concerned with movements of the body and limbs, during an eye movement task? It is possible that the reward expectancy signal is maintained throughout DMFC so that it can enhance any volitional motor acts that precede reward. For instance, in hand eye coordination tasks the reward signal can reinforce activity in the limb area of SMA and SEF together. Other areas of SMA which do not have a convergence of activation of the motor map activation and reward signal would not be reinforced and would not produce learning (Sutton and Barto 1988). Thus, the expectation signal may be more widely broadcast than the motor activations of a particular behavior. This broader signal may serve to learn new coordinations of different body parts for particular tasks.

REFERENCES

Amador N, Schlag-Rey M and Schlag J. Reward-Predicting and Reward-Detecting Neuronal Activity in the Primate Supplementary Eye Field. *J Neurophysiol* 84: 2166-2170, 2000.

Barraclough DJ, Conroy ML and Lee D. Prefrontal cortex and decision making in a mixed-strategy game. *Nat Neurosci* 7: 404-410, 2004.

Campos M, Breznen B and Andersen RA. Reward expectancy in dorsomedial frontal cortex of the macaque monkey. *Soc. Neurosci. Abstr* 187.183, 2003.

Chen L and Wise S. Neuronal activity in the supplementary eye field during acquisition of conditional oculomotor associations. *J Neurophysiol* 73: 1101-1121, 1995.

Cox RW. AFNI: Software for analysis and visualization of functional magnetic resonance neuroimages. Computers and Biomedical Research 29: 162-173, 1996.

Cromwell HC and Schultz W. Effects of Expectations for Different Reward Magnitudes on Neuronal Activity in Primate Striatum. *J Neurophysiol* 89: 2823-2838, 2003.

Fries W. Cortical projections to the superior colliculus in the macaque monkey: A retrograde study using horseradish peroxidase. *J. Comp. Neurol* 230: 55-76, 1984.

Fujii N, Mushiake H, Tamai M and J T. Microstimulation of the supplementary eye field during saccade preparation. *Neuroreport* 6: 2565-2568, 1995.

Fujii N, Mushiake H and Tanji J. Distribution of Eye- and Arm-Movement-Related Neuronal Activity in the SEF and in the SMA and Pre-SMA of Monkeys. *J Neurophysiol* 87: 2158-2166, 2002.

Hanes D, Thompson K and Schall J. Relationship of presaccadic activity in frontal eye field and supplementary eye field to saccade initiation in macaque: Poisson spike train analysis. *Exp Brain Res* 103: 85-96, 1995.

Hassani OK, Cromwell HC and Schultz W. Influence of Expectation of Different Rewards on Behavior-Related Neuronal Activity in the Striatum. *J Neurophysiol* 85: 2477-2489, 2001.

Hikosaka K and Watanabe M. Delay Activity of Orbital and Lateral Prefrontal Neurons of the Monkey Varying with Different Rewards. *Cereb. Cortex* 10: 263-271, 2000.

Ikeda T and Hikosaka O. Reward-dependent gain and bias of visual responses in primate superior colliculus. *Neuron* 39: 693-700, 2003.

Kobayashi S, Lauwereyns J, Koizumi M, Sakagami M and Hikosaka O. Influence of Reward Expectation on Visuospatial Processing in Macaque Lateral Prefrontal Cortex. *J Neurophysiol* 87: 1488-1498, 2002.

Luppino G, Matelli M, Camarda R and G R. Corticocortical connections of area F3 (SMA-proper) and area F6 (pre-SMA) in the macaque monkey. *J Comp Neurol* 338: 114-140, 1993.

Luppino G, Matelli M, Camarda R, Gallese V and Rizzolatti G. Multiple representations of body movements in mesial area 6 and the adjacent cingulate cortex: an intracortical microstimulation study in the macaque monkey. *J Comp Neurol* 311: 463-482, 1991.

Mann S, Thau R and Schiller P. Conditional task-related responses in monkey dorsomedial frontal cortex. *Exp Brain Res* 69: 460-468, 1988.

Matsumoto K, Suzuki W and Tanaka K. Neuronal Correlates of Goal-Based Motor Selection in the Prefrontal Cortex. *Science* 301: 229-232, 2003.

Matsuzaka Y, Aizawa H and Tanji J. A motor area rostral to the supplementary motor area (presupplementary motor area) in the monkey: neuronal activity during a learned motor task. *J Neurophysiol* 68: 653-662, 1992.

Matsuzaka Y and Tanji J. Changing directions of forthcoming arm movements: neuronal activity in the presupplementary and supplementary motor area of monkey cerebral cortex. *J Neurophysiol* 76: 2327-2342, 1996.

Maunsell JHR. Neuronal representations of cognitive state: reward or attention? *Trends in Cognitive Sciences* 8: 261-265, 2004.

Mazzoni P, Andersen RA and Jordan MI. A more biologically plausible learning rule that backpropagation applied to a network model of cortical area 7a. *Cereb. Cortex* 1: 293-307, 1991.

Mitz A and Wise S. The somatotopic organization of the supplementary motor area: intracortical microstimulation mapping. *J Neurosci* 7: 1010-1021, 1987.

Musallam S, Corneil BD, Greger B, Scherberger H and Andersen RA. Cognitive Control Signals for Neural Prosthetics. *Science* 305: 258-262, 2004.

Nakamura K, Sakai K and Hikosaka O. Neuronal Activity in Medial Frontal Cortex During Learning of Sequential Procedures. *J Neurophysiol* 80: 2671-2687, 1998.

Parthasarathy H, Schall J and Graybiel A. Distributed but convergent ordering of corticostriatal projections: analysis of the frontal eye field and the supplementary eye field in the macaque monkey. *J Neurosci* 12: 4468-4488, 1992.

Platt ML and Glimcher PW. Neural correlates of decision variables in parietal cortex. *Nature* 400: 233-238, 1999.

Roesch MR and Olson CR. Impact of Expected Reward on Neuronal Activity in Prefrontal Cortex, Frontal and Supplementary Eye Fields and Premotor Cortex. *J Neurophysiol* 90: 1766-1789, 2003.

Roesch MR and Olson CR. Neuronal Activity Related to Reward Value and Motivation in Primate Frontal Cortex. *Science* 304: 307-310, 2004.

Russo G and Bruce C. Effect of eye position within the orbit on electrically elicited saccadic eye movements: a comparison of the macaque monkey's frontal and supplementary eye fields. *J Neurophysiol* 69: 800-818, 1993.

Satoh T, Nakai S, Sato T and Kimura M. Correlated Coding of Motivation and Outcome of Decision by Dopamine Neurons. *J. Neurosci* 23: 9913-9923, 2003.

Schall JD, Morel A and Kaas JH. Topography of supplementary eye field afferents to frontal eye field in macaque: Implications for mapping between saccade coordinate systems. *Visual Neurosci* 10: 385-393, 1993.

Schlag J and Schlag-Rey M. Evidence for a supplementary eye field. *J Neurophysiol* 57: 179-200, 1987.

Schlag J and Schlag-Rey M. Unit activity related to spontaneous saccades in frontal dorsomedial cortex of monkey. *Exp Brain Res* 58: 208-211, 1985.

Schultz W, Dayan P and Montague PR. A Neural Substrate of Prediction and Reward. *Science* 275: 1593-1599, 1997.

Shidara M and Richmond BJ. Anterior Cingulate: Single Neuronal Signals Related to Degree of Reward Expectancy. *Science* 296: 1709-1711, 2002.

Shima K and Tanji J. Neuronal Activity in the Supplementary and Presupplementary Motor Areas for Temporal Organization of Multiple Movements. *J Neurophysiol* 84: 2148-2160, 2000.

Stuphorn V, Taylor T and Schall J. Performance monitoring by the supplementary eye field. *Nature* 408: 857-860, 2000.

Sugrue LP, Corrado GS and Newsome WT. Matching Behavior and the Representation of Value in the Parietal Cortex. *Science* 304: 1782-1787, 2004.

Sommer MMA, and Tehovnik EEJ. Reversible inactivation of macaque dorsomedial frontal cortex: effects on saccades and fixations. *Experimental brain research* 124: 429-446, 1999.

Suri RE and Schultz W. A neural network model with dopamine-like reinforcement signal that learns a spatial delayed response task. *Neuroscience* 91: 871-890, 1999.

Sutton RS and Barto AG. *Reinforcement Learning: An Introduction.* Cambridge, Mass: MIT Press, 1988.

Tehovnik E and Sommer M. Compensatory saccades made to remembered targets following orbital displacement by electrically stimulating the dorsomedial frontal cortex or frontal eye fields of primates. *Brain Res* 727: 221-224, 1996.

Thompson K, Hanes D, Bichot N and Schall J. Perceptual and motor processing stages identified in the activity of macaque frontal eye field neurons during visual search. *J Neurophysiol* 76: 4040-4055, 1996.

Tremblay L, Hollerman JR and Schultz W. Modifications of Reward Expectation-Related Neuronal Activity During Learning in Primate Striatum. *J Neurophysiol* 80: 964-977, 1998.

Tremblay L and Schultz W. Reward-Related Neuronal Activity During Go-Nogo Task Performance in Primate Orbitofrontal Cortex. *J Neurophysiol* 83: 1864-1876, 2000.

Watanabe K, Lauwereyns J and Hikosaka O. Neural Correlates of Rewarded and Unrewarded Eye Movements in the Primate Caudate Nucleus. *J. Neurosci* 23: 10052-10057, 2003.

Watanabe M. Reward expectancy in primate prefrontal neurons. *Nature* 382: 629-632, 1996.

CHAPTER II

NEURAL REPRESENTATION OF SEQUENTIAL STATES WITHIN AN INSTRUCTED TASK

ABSTRACT

In the study of the neural basis of sensorimotor transformations, it has become clear that the brain does not always wait to sense external events and afterwards select the appropriate responses. If there are predictable regularities in the environment, the brain begins to anticipate the timing of instructional cues and the signals to execute a response, and even the consequences of actions. An organism's ability to anticipate events reveals an internal representation of the sequential progression of behavioral states, within the context of the task being performed. Using the same eye movement tasks while recording neural data from two cortical ocuolomotor areas in the rhesus monkey, we found complementary spatial and sequential state representations of the Lateral Intraparietal Area (LIP) and the Supplementary Eye Field (SEF). While both areas encoded the position of eye movement targets, this spatial encoding was more consistently found in single neurons of LIP. In addition, the neurons of the SEF were found to collectively encode the progression of the task, with individual neurons detecting and/or anticipating different events or sets of events in the task or becoming tonically activated or depressed from one event to another and thus encoding states in an event-based manner. The

entirety of responses from SEF was used to decode the current temporal position within the context of the task. Since LIP neurons were found to respond similarly when encoding an eye movement plan (saccade period) or the location of brightly flashed stimulus (cue period), the temporal information provided from SEF could be used to imply the significance of the spatial representation found in LIP.

INTRODUCTION

In the context of a wide range of experimental paradigms, task performance improves if a subject can anticipate when and where an instructional cue will become available, and expert performance is frequently accompanied by anticipatory or short-latency movements (Miyashita et al., 1996) which optimize the rate of reward (Glimcher, 2004). Anticipatory neural activity, characterized by increases or decreases in firing rate activity prior to external events, which can support this behavior has been found in a variety of brain structures including the striatum (Apicella et al., 1992); caudate (Hikosaka et al., 1989; Lauwereyns et al., 2002b; Lauwereyns et al., 2002a; Watanabe and Hikosaka, 2005); frontal eye fields (Bruce and Goldberg, 1985; Coe et al., 2002); dorsal premotor cortex (Mauritz and Wise, 1986; Vaadia et al., 1988); cingulate motor area (Niki and Watanabe, 1979); supplementary motor area; pre-supplementary motor area (Akkal, 2004); as well the two areas under study in this report, the supplementary eye fields (Coe et al., 2002) and the lateral intraparietal area (Colby et al., 1996; Coe et al., 2002; Maimon and Assad, 2006). Anticipatory neural activity has been supposed to support the expectation of predictable sensory events (Apicella et al., 1992) that are linked to reward

(Lauwereyns et al., 2002b); expectation of reward itself (Amador et al., 2000; Stuphorn et al., 2000; Campos et al., 2005); behavioral biases for a particular movement (Mauritz and Wise, 1986; Hikosaka et al., 1989; Coe et al., 2002; Takikawa et al., 2002; Watanabe and Hikosaka, 2005) to attenuate reaction-time delays (MacKay and Crammond, 1987); the readiness to produce or cancel a movement (Libet et al., 1983) which has similarly been described as the beginnings of a proactive triggering process (Maimon and Assad, 2006); the inhibition of reflexive movements (Guitton et al., 1985); and tracking behavior, as in smooth pursuit (Heinen and Liu, 1997).

Anticipatory, or climbing, neural activity is the hallmark of one of the two prevailing views on how behavioral timing is accomplished in the brain (Macar et al., 1999; Brody et al., 2003; Reutimann et al., 2004). The competing model posits that timing is encoded as particular groupings of activated neurons in a network (Mauk and Buonomano, 2004; Lucchetti et al., 2005). The two models are not mutually exclusive. The anticipation of events posited by accumulator models, and the detection that those events required for network models, are complementary processes and have long been observed within the firing of single neurons (Fuster and Alexander, 1971). In support of both models, Niki and Watanabe first discussed timing units, which included neurons with anticipatory rises before perceptual events and during motor preparation, as well as tonic activations extending through the delay period (Niki and Watanabe, 1979). More recently, there have been studies presenting neural activations not related to spatial parameters that provide further evidence for the network-based representation of behavioral timing, including state-encoding responses in rCMA before, during, and after every event in a trial, thereby reflecting each step of the behavioral task (Hoshi et al.,

2005), and event-detecting activity in the claustrum preceeding all movements in a non-selective manner (Shima et al., 1996). Results such as these have been the basis of the controversial hypothesis that the prefrontal cortex is primarily engaged in the temporal structuring of behavior (Fuster, 1989).

The two cortical oculomotor areas of interest in this report, LIP and SEF, have both been shown to participate in the representation of behavioral timing. Anatomical connections suggest that SEF is directly involved in specifying when a saccade should occur (Shook et al., 1990), and SEF microstimulation can trigger an already planned movement to any direction (Missal and Heinen, 2004). Neurons in SEF without an apparent directional preference have been termed omni-directional (Chen and Wise, 1996), and such a signal may be required to trigger eye movements without regard for their direction. The timing of the microstimulation, however, has to be in the appropriate interval, otherwise it will delay the reaction time and instead facilitate fixation (Isoda, 2005), which cautions that the temporal responsibilities of SEF are not limited to providing a trigger for movement, but may also enhance fixation behavior when that is appropriate. Further evidence for the representation of time in SEF includes the effect of cooling of premotor cortex in monkeys, including SEF, which renders monkeys unable to perform a movement at the instructed time (Sasaki and Gemba, 1986), and disruptive stimulation in SEF that leads to temporal re-ordering of eye movements of a sequence, even though target endpoints remain accurate (Histed and Miller, 2006).

LIP neurons are generally thought to be involved in specifying the spatial location of salient cues and eye movement targets (Andersen et al., 1985; Andersen, 1995; Andersen et al., 1997; Gottlieb et al., 1998), and in contrast to the behavioral ordering

disruptions resulting from SEF inactivation, temporary LIP inactivation results in deficits of saccade metrics (Li and Andersen, 2001). LIP activity, however, has been shown to correlate with eye movement start times (Ipata et al., 2006) and exhibits a slight anticipatory rise before predictable visual cue presentations (Colby et al., 1996), revealing access to timing information. Recent studies have further proposed that LIP neurons might themselves represent the passage of time during motor planning by gradually enhancing or suppressing the motor plans for which elapsed time is an instructive cue (Leon and Shadlen, 2003; Janssen and Shadlen, 2005).

In this study we characterize the encoding of populations of neurons in LIP and SEF with respect to spatial and behavioral state representations, while the monkeys performed a memory-guided saccade task. To assess and compare the contribution each area makes to the spatial representation of the target, as well as to the representation of the current behavioral state within the context of the task sequence, we then characterize the performance of a decoding algorithm on the spatial position of the target, or separately for the temporal interval. Recording from these two oculomotor structures during the performance of the same task, we are able to better understand the ways in which the different areas are specialized and complementary.

METHODS

Studies were performed with two behaving male rhesus monkeys (Macaca mulatta). Each was chronically fitted with a stainless steel head post for head immobilization and two recording chambers over small craniotomies for electrode insertions. Experimental

procedures were in accordance with the California Institute of Technology Institutional Animal Care and Use Committee.

Monkeys were seated in a dimly lit room, 34 cm from a tangent LCD monitor. Stimuli were presented with 800x600 resolution and a refresh rate of 75 Hz using a custom built software display client with OpenGL. Task logic was controlled by National Instruments real time LabView software.

Eye movement monitoring

Eye movements were monitored with an infrared oculometer (ISCAN Inc.). A high-speed camera was mounted on a wooden frame above the monkey's head and, along with an infra-red source, directed into an infra-red reflective hot-mirror held fixed at a 45 degree angle just in front of the monkey's eyes. A trapezoidal notch was cut from the mirror so that it could be placed close around the monkey's nose. For both monkeys the left eye was monitored. Facial whiskers and brow hairs around the left eye were clipped regularly to improve the quality of the eye-tracking image.

Training methods

The monkeys then began eye movement training after fixation behavior was well trained. First monkeys were trained to saccade to a new target that appeared at the same moment that the centrally presented fixation cue extinguished. Modifications to this task were then introduced to train the monkeys to perform memory-guided saccades. Shortly after the monkey began central fixation, a spatial cue was briefly (~50ms) flashed in the periphery. When the fixation point extinguished 300-500ms later, the target appeared in

the same location as the cue, and the monkey was rewarded if he made a saccade to the target in a short period of time (within ~700 ms). If the monkey broke fixation during the briefly flashed cue, the trial was aborted, and the monkey had to wait 1.5-2 sec until the next trial started. In this way, the monkey learned to withhold any eye movements until the fixation point extinguished. Over the course of 2-3 weeks, the cue flash duration was extended in small increments to 250 ms and was presented 500 – 800 ms after the start of fixation. Finally, the target stimulus was not presented immediately after the fixation point extinguished, but was instead presented just after the monkey had moved his eyes to where the target would appear. The monkeys had learned this final step easily, indicating to us that they had made the association that the cue stimulus instructed the future eye movement. The timing of the target reappearance was extended to occur 250 ms after successfully fixating the remembered cue location. The monkey continued training until task performance reliably reached about 85%, at which point the chamber placement surgery was performed.

MR Imaging

Magnetic resonance (MR) imaging was performed at the Caltech Brain Imaging Center on a 3 T Siemens Trio. For monkey M, an anatomical MRI scan was performed prior to the chamber surgery to confirm the stereotaxic coordinates of the cortical areas of interest. These areas are typically found in the same positions relative to the ear canal (zero in the anterior-posterior axis of stereotaxic coordinates) of different monkeys. The lateral intraparietal area (LIP) is found generally at 6 mm posterior and 12 mm lateral. The supplementary eye fields are found at 22-26 mm anterior and 4 mm lateral. The

recordable area of a chamber is 14 mm in diameter, and each area of interest is typically 4 mm in diameter, so there is some room for error. Further, the SEF of both hemispheres is sometimes accessible from one chamber placed directly over the midline (0mm, 24mm), and we placed the frontal chamber as such. The anatomical MRI images of monkey M confirmed that these typical stereotaxic positions would be suitable for the chamber placement surgery.

The MRI scan was performed after the chamber placement surgery of monkey L, and the standard sterotaxic coordinates were used to locate the areas of interest during the surgery. During the post-operative MRI, a high-contrast agent (gallidium) was inserted into the chamber, which appeared brightly just above the dura in the MR image, with clearly defined chamber walls. With these images the satisfactory placement of the chambers could be verified and the precise locations of subsequent electrode penetrations could be planned.

Following the chamber placement surgery, exploratory electrode penetrations were performed to map out the cortical areas accessible to the chambers. For monkey M, for whom the MRI was performed prior to the chamber surgery, we had only a rough estimate of the cortical structures beneath the exposed dura.

Chamber Mapping and Electrical Stimulation

For monkey M, two weeks were required to map the parietal chamber using a combination of passive recording and somatosensory examinations to determine the response properties of the encountered neurons until we were satisfied that the eye movement area, LIP, was located. In the frontal chamber, electrical microstimulation was

added to the exploratory recording and somatosensory examination techniques. A BAK instruments stimulator was used to deliver biphasic currents at 330 Hz of typically less than 200 μA in 100-500 ms trains through the recording electrodes. In the SEF, but not in adjacent regions, eye movements can be elicited at a low threshold (<50 uA). In addition, there are body movement representations just medial to the SEF (in the supplementary and pre-supplemntary motor areas) in which electrical microstimulation will evoke stereotyped movements on the limb, torso, and face. The left SEF of monkey M was found readily within a couple of days. Guided by the post-operative MRIs of monkey L, we were able to find both areas of interest in just two penetrations for each chamber. We did not confirm the location of SEF with electrical microstimulation, since the signals that we recorded we convincing and the location was corroborated by the MR images.

Behavioral task

A memory-guided saccade task was used. The monkey was instructed to perform a saccade from a central fixation point to one of 43 targets placed at regular intervals to cover the entire visual field out to 15 deg of visual angle in every direction from central fixation. Monkeys were required to maintain central fixation while a peripheral target was briefly flashed, wait until the central fixation point extinguished, and then saccade to the remembered location. After successfully holding fixation at the target location, the target re-appeared to provide visual feedback of the correct eye position. The monkey was then required to maintain fixation on the visible target for an additional interval of 250 ms before receiving a juice reward of about 0.2 ml.

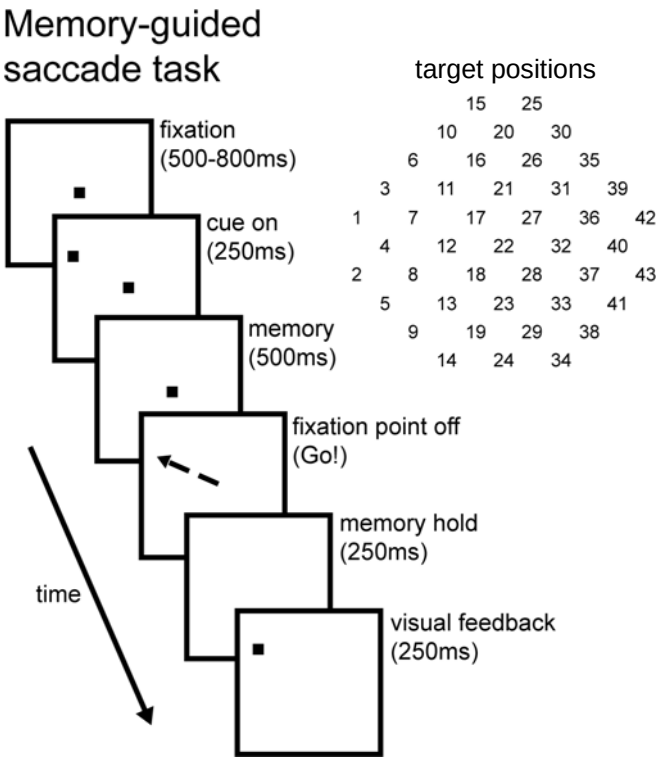

Figure 2.1. *Time course of oculomotor task.* The temporal progression is shown in successive panels from top left to bottom right. The monkey is required to acquire a central fixation point at the start of the trial. After a variable delay (500-800 ms), a cue is briefly flashed (250 ms) at one of 43 targets in the periphery. The possible targets cover the entire visual field out to 15 degrees (inset). Following a hold interval the fixation point is extinguished and the monkey is required to saccade to the remembered target location and fixate there. After 250 ms the target reappears, and then following an additional 250 ms fixation, the animal is rewarded with a drop of juice.

Recording Procedure

Neurons were accessed on vertical penetrations with glass coated platinum-iridium electrodes (Fred Haer Co.) or Thomas Recording electrodes (ThomasRecording Gmbh). The electrodes were advanced with a Narishige or Thomas microdrive system through a blunt stainless steel guide tube pressed against the dura for SEF recordings or a sharp stainless steel guidetube puncturing the dura and driven down 1 mm for LIP recordings. Neurons were generally found 1-3mm beneath the exterior of the dura for SEF recordings and 5-9 mm beneath the level of the dura for LIP recordings.

Waveforms were amplified and isolated online with a commercial hardware and software package (Plexon Inc.). Cell activity was monitored with custom built online data visualization software written in Matlab.

Neuron classification analysis

To standardize the spike trains for each trial, spike trains were aligned to four different events that occurred at varying intervals, and these four spike trains were then merged around the time of the shortest interval between each event. These events were fixation appearance, cue appearance, fixation point disappearance (go signal), and the visual feedback signal. The spike trains extended 400 ms before the fixation point on event until 350 ms afterwards. This was followed by the spike train data from the period 225 ms before the cue appearance event until 575 ms afterwards, then 350 ms before the fixation off event until 400 afterwards, and finally, 200 ms before the target reappearance until 500 ms afterwards.

Using these merged spike trains, firing activity during different states and events were then compared to baseline firing levels to determine if there were significant activations or depressions. The baseline firing rate was defined as the total number of spikes in the merged spike trains divided by the total duration. This calculation of the baseline firing rate does not include inter-trial intervals, and importantly, does not assume that any particular interval is a common resting interval for all of the neurons. The definitions of all of the state and event intervals incorporated the known latencies of responses in LIP and SEF, which are both greater than 40 ms (Schall, 1991; Bisley et al., 2004), and all of the state and event definitions cover the entire duration of the time-standardized trials, with short (40 ms) gaps between each state and subsequent event, to allow for variability in onset latencies. The *pre-trial state* was defined as the 400 ms prior to the appearance of the central fixation point at the start of the trial until 30 ms afterwards. The *fixation point on event* was defined as the 150 ms interval starting 70 ms

after the appearance of the fixation point. The *pre-cue state* was defined as the interval from the end of the fixation point on event until 30 ms after the cue presentation. The *cue on event* was defined as the 150 ms interval starting 70 ms after the presentation of the cue. The *memory state* was defined as the interval from the end of the cue on event until 30 ms after the fixation point disappearance (the signal for the monkey to make the saccade). The *saccade event* was defined as the 300 ms interval starting 70 ms after the fixation point disappearance (allowing time for the execution of the saccade). The *post-saccade state* was defined as the interval from the end of the saccade event until 30 ms after reappearance of the target. The *visual feedback event* was defined as the 150 ms starting 70 ms after the reappearance of the target. Finally, the *reward state* was defined as the time from the end of the visual feedback event until 50 ms after the end of the delivery of reward. Significant increases or decreases in any of these intervals was defined as the likelihood of the firing rate in that interval, assuming a Poisson distribution and taking the baseline firing rate as the mean ($p < 0.05$). In addition to calculating activations and suppressions in entire event or state intervals, tests were performed on smoothed firing rates at 10 ms intervals to provide a continuous measure of significant activations.

Anticipatory activity was defined as a significant rise or decrease in firing rate in the 200 ms at the end of the following states: pre-trial, pre-cue, memory, and post-saccadic. Significant changes refers to non-overlapping mean firing rates +/- the standard error of the mean for the 100 ms prior to the end of the state versus the 100 ms preceeding the first interval. State encoding activations or deactivations are defined as significant deviations from the baseline firing rate for at least 25% of the duration of the

same intervals, such that the activity at the end is not characterized as anticipatory. Event detection activity was defined the same as state encoding activity, but limited to the four previously defined event intervals, and anticipatory activity was not tested in the event periods. Spatially-tuned activity was defined with respect to the goodness-of-fit of the firing rates to a two dimensional Gaussian model of the response field, as described below.

Regression analysis to model contributions of target or distractor location to neuronal activity

We used standard quantitative models implemented with MATLAB to evaluate the dependence of firing rate on cue or distractor position (Campos et al. 2006; Draper and Smith, 1981; Press et al.; 2002, Zar, 1974). The spikes trains were smoothed by convolving with a Gaussian (sigma = 50 ms) to estimate the instantaneous firing rate for individual trials. An initial estimate of the center of the response field (b_3, b_4) was calculated as the vector average of all of trials with associated firing rates that were >50% of the maximum firing rate. Initial estimates of the remaining parameters were chosen arbitrarily: $b_0 = 100$, $b_1 = 4$, $b_2 = 3$. The firing rates were then regressed on a two-dimensional Gaussian using the following equation:

$$F = b_0 + b_1 \cdot \exp\left(-\frac{(x-b_3)^2 + (y-b_4)^2}{b_2^{\,2}}\right) \qquad \textbf{Eq. \#1}$$

where (x,y) is the position of the target. The regression was computed, and the values for the parameters were stored along with the p and r^2 values describing the goodness-of-fit for the regressions.

Nearest neighbor decode algorithm

The following method is adapted from a recent study, and the following description closely resembles the method previously published (Quiroga et al. 2006). Each data set contained at least 129 trials (43 targets x 3 repetitions). From these merged spike trains of 3000 ms duration, varying window sizes were used to count spiking events to then be used as input into the decoding algorithm. The 75 ms time window performed better than window sizes that were slightly larger or smaller, and so 75 ms window sizes are used in all of the temporal decode results presented. Alternately, spiking events from each of the 9 states and events was used as input for spatial position decoding.

Cells were considered simultaneously recorded in the sense that, for each of three trials to each of the 43 target positions, the responses of all cells were grouped together as a single trial with *m* values (in which *m* is the number of cells). Trials were considered as points in an *m*-dimensional space, each coordinate representing the mean firing rate for each of the *m* cells. One at a time, each of these 129 trials was decoded based on the distribution of all other trials (leave-one-out decoding) and was assigned to the class of its nearest neighbor in the m-dimensional space using Euclidean distance (Duda et al. 2001, Quiroga et al 2006). In the event that there were less than three trials recorded for a given direction, the third trial was randomly chosen from the recorded trials. When only one

trial was recorded, the neuron contributed to the decode of other directions, but not to decodes of the directions with only one recorded trial.

For the temporal decode, each trial was decoded at every 75 ms from the beginning to the end of the trial. Firing rates from the left out trial were compared with mean firing rates collapsed across all directions in the same interval and all other intervals. The time interval of the nearest neighbor was assigned as the decoded time interval of the left-out trial. For the spatial decode, the left-out trial was compared with the 128 other "simultaneously" recorded trials using the same temporal window in the other trials, and the mean firing rate was calculated individually for each cue or distractor position. The nearest neighbor was identified, and the decoded target was assigned as the same as that of the nearest neighbor.

RESULTS

The neuronal sample presented in this report consists of 444 neurons recorded from two monkeys while the monkeys performed memory-guided saccades (Figure 2.1). There were 289 neurons recorded from SEF and 155 recorded from LIP (see Table 2.1 for further details).

	Monkey M LIP	Monkey M SEF	Monkey L LIP	Monkey L SEF	Total LIP	Total SEF	Total
Total Recorded	58	177	97	112	155	289	444
Task Related	42	124	39	60	81	184	265

Table 2.1. *Cell counts for the neuronal database.* Detail of the number of recorded and task related neurons, broken down by monkey and cortical area as well as combined.

Non-spatial and spatially-tuned neural activations

We observed that many of the task-related neurons in our database of SEF neurons exhibited robust responses that were not spatially-tuned for any particular range of directions or amplitudes. In Figure 2.2 there are examples of three general types of non-spatial neuronal activity, which adequately cover the range of non-spatial responses we observed. The three types are event detection, anticipation, and state encoding activity. For the purposes of cell categorization, we defined event detection activity as a phasic (~150 ms) non-spatial activation or suppression at one or multiple events within the trial. The neuron shown in Figure 2.2a detected the following events with non-spatial increases in firing activity: fixation point on, cue on, fixation point off, and visual feedback. From this single neuron an observer could judge that one of these relevant events had occurred. We defined anticipatory activity as a smooth buildup or suppression of activity, which may or may not be spatially-tuned, before perceptual or motor events. The neuron shown in Figure 2.2b exhibited a gradual firing rate increase leading up to the cue presentation (cue on), and then went silent. From this single neuron an observer could judge that the monkey was currently in the pre-cue state and, based on the firing rate, have an idea of how long the monkey expected to wait until the presentation of the cue. We defined state encoding activity as a non-spatial tonic activation stretching from one event to another in the task sequence. The neuron shown in Figure 2.2c was active from the fixation point on event until the cue appearance and again from the target acquisition to the visual feedback event. From this single neuron, an observer could deduce that the monkey was currently in either the pre-cue or post-saccade states. The prevalence of these types of activity is shown graphically in Supplementary Figure 2.S2.

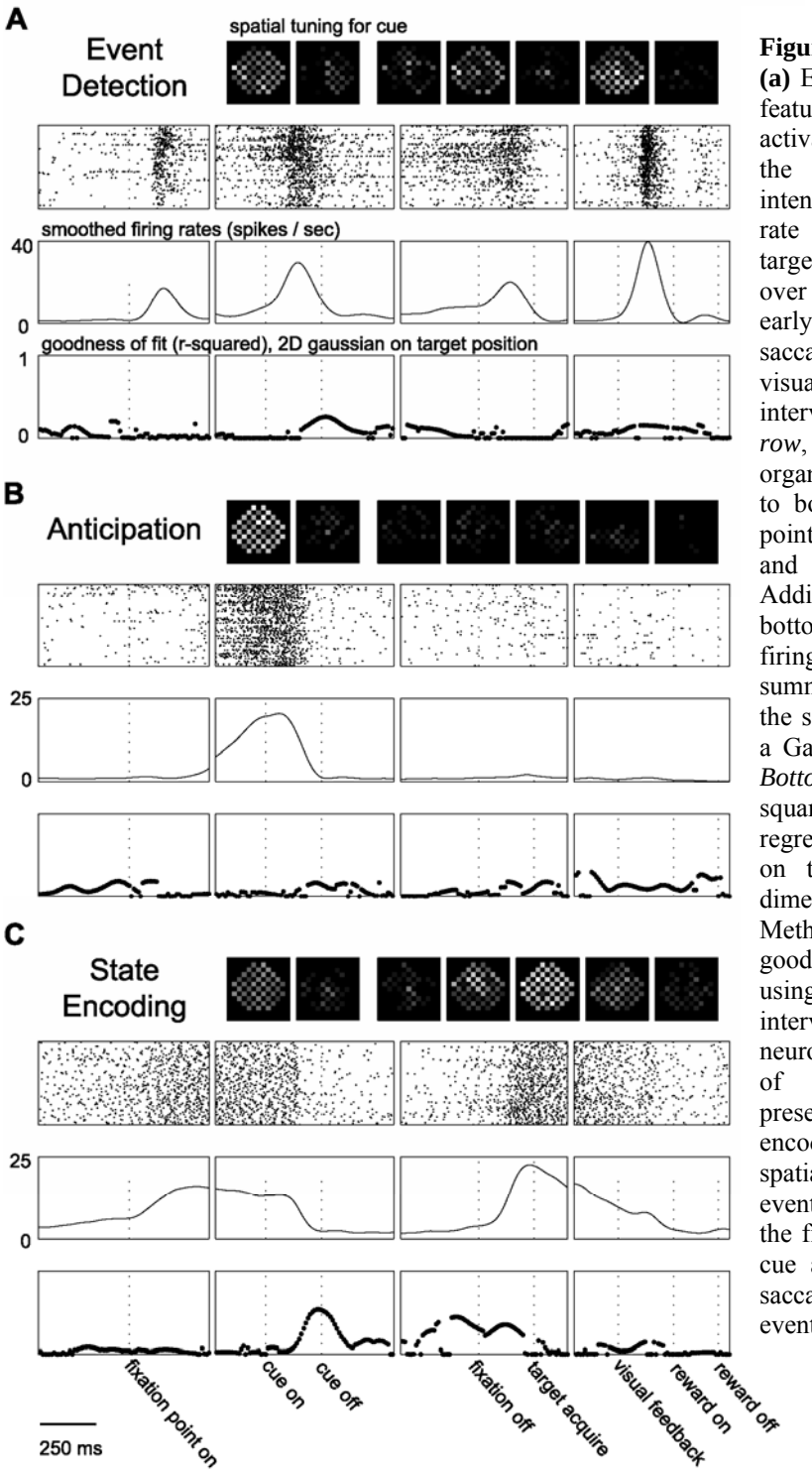

Figure 2.2. *Example SEF neurons.* **(a)** Example event detection neuron featuring non-spatial transient activations at many events within the trial. *Top row*, firing rate intensity plots showing mean firing rate for all correct trials to each target position, arranged spatially, over 200 ms intervals in the cue on, early memory, late memory, pre-saccadic, saccadic, post-saccadic, visual feedback, and reward intervals, from left to right. *Second row*, spike trains for each trial, organized chronologically from top to bottom, aligned on the fixation point on, cue on, fixation point off, and visual feedback events. Additional event times are labeled at bottom. *Third row*, smoothed spike firing rates in time, estimated by summing the spike train rasters in the second row and smoothing with a Gaussian filter (sigma = 50 ms). *Bottom row*, goodness-of-fit (r-squared) values for non-linear regressions of smoothed firing rates on target position using a two-dimensional Gaussian model (see Methods). Each point represents the goodness-of-fit for a regression using firing rates taken at 10 ms intervals. **(b)** Example anticipation neuron featuring non-spatial buildup of activity before the cue presentation. **(c)** Example state encoding neuron featuring a non-spatial tonic activation from one event to another, in this case from the fixation point on event until the cue appearance and also from the saccade until the visual feedback event.

In addition to the three types of non-spatial activations just discussed, many SEF neurons exhibited spatially-tuned responses at various points in the trial following the cue

presentation. These responses were qualitatively similar to the responses of LIP neurons, and so for brevity we only show examples of spatial tuning from the LIP database (see Supplementary Figure 2.S1).

The numbers of recorded neurons that were spatially-tuned or activated or suppressed in a non-spatial manner at each point in time are shown graphically in Figure 2.3 and broken down into state and movement period classifications in Supplementary Figure 2.S2. The neurons in LIP were more likely to be spatially-tuned during the trial, compared to active but non-spatial, as in SEF. The spatially-tuned activity exhibited by SEF neurons tended to occur early in the trail and then taper off, whereas in LIP more neurons were spatially-tuned around the time of the movement versus the cue presentation. The LIP population also contained a substantial number of neurons spatially-tuned in the post-saccadic time periods. Finally, note that the SEF population contained several significantly active or suppressed neurons that were not spatially-tuned at all points in time within the trial.

Decoding the current temporal interval or state

Based on the observation that certain SEF neurons that are not spatially-tuned are in fact temporally tuned, we next tested whether the responses of a large population of SEF neurons could be used to decode the current temporal interval of a trial within the context of the task. We adapted a model-free decode method developed in our lab and originally applied to the spatial decode of eye and arm movements (Quiroga et al 2006) and quantified its performance in decoding the specific time interval within the task to which a set of firing rates belonged (see Methods). In Figure 2.4a-c are the results of the

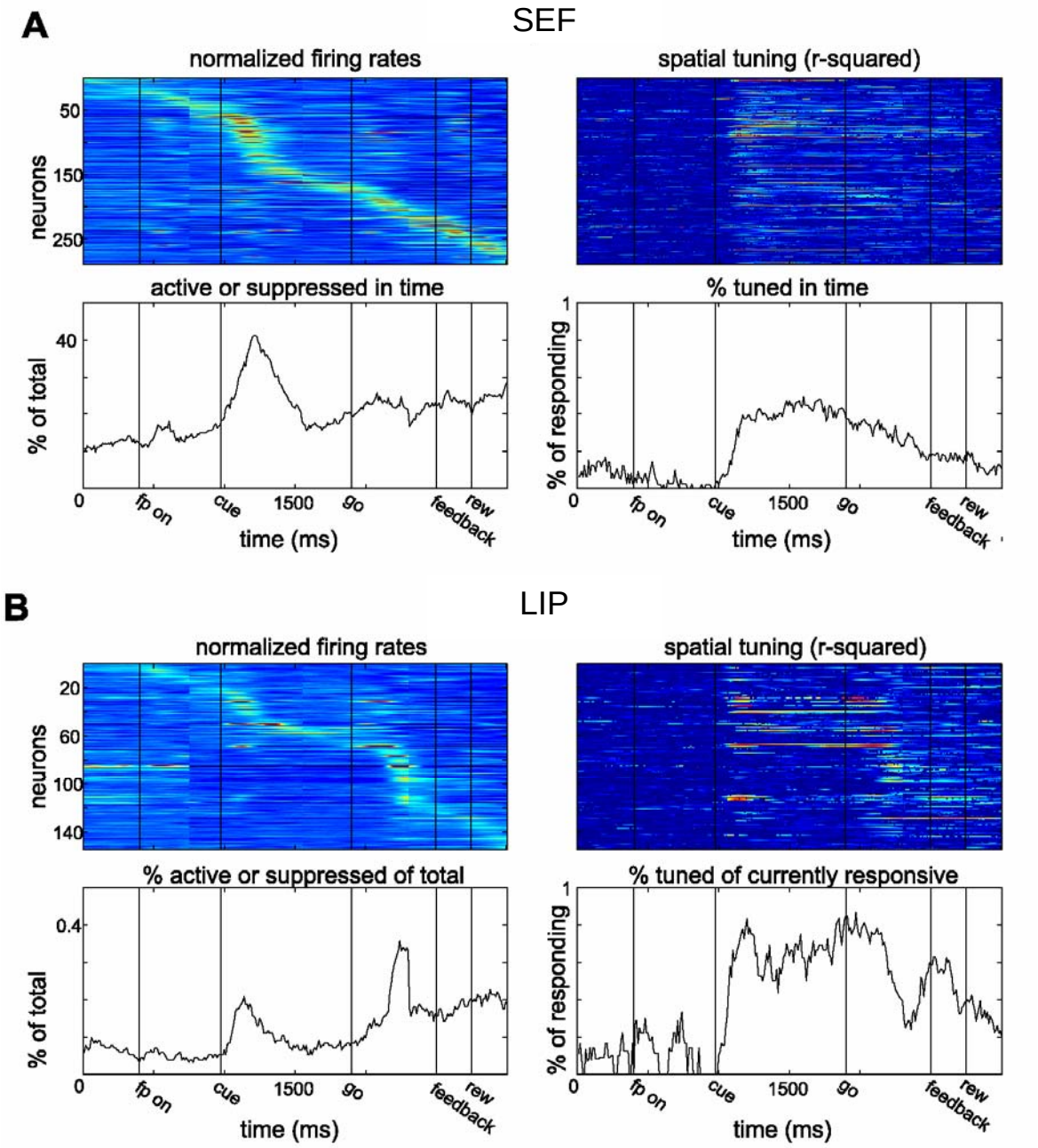

Figure 2.3. *Continuous measures of activation, suppression, and spatial tuning*. Continuous measures of spatial tuning and firing rate increases and decreases for all recorded neurons in the **(a)** SEF databases, data from both monkeys combined. *Top row, left column*, normalized firing rates, each row corresponding to one neuron. The color scale ranges from no firing activity (blue) to 5 times the baseline firing rate (red). Neurons are sorted according to the occurrence of their maximum firing rates. The time progression corresponds to merging the four histograms shown in Figure 2.2. *Top row, right column*, r-squared values (goodness-of-fit) for non-linear regressions on a two-dimensional Gaussian, using smoothed firing rates at every 10 ms and the positions of the saccade targets. Each row corresponds to the neuron from the same row in the left column. Color scale ranges from 0 (blue) to 1 (red). *Bottom row, left column*, total number of significantly active or suppressed neurons at all points in time, shown as the percentage of the total number of recorded neurons in the sample. *Bottom row, right column*, percentage of neurons that are spatially tuned, of the neurons that are responsive at that point in time (spatially tuned and/or significantly active or suppressed). **(b)** Continuous measures of spatial tuning and firing rate increases and decreases for all recorded neurons in the LIP databases, data from both monkeys combined.

method using the full database of SEF neurons collected in monkey M. The performance of the monkey M SEF database was higher than that of monkey L, mainly on account of a larger sample size, though the results were qualitatively similar. In the summary subsection below we illustrate the decode performance as a function of sample sizes via bootstrapping.

The decode algorithm works by calculating the Euclidean distance between all of the observed firing rates of a given pseudo-simultaneously recorded test trial (in which all neurons are considered as recorded simultaneously – see Methods) in a short time window and comparing these to the average firing rates of all of the neurons calculated without including this test trial. The interval with the shortest Euclidean distance is then declared the decoded temporal interval. Temporal intervals of 75 ms duration were tested for the temporal extent of the trial. This process was repeated for 129 trials, which is three repetitions to each of 43 targets. Figure 2.4a shows the confusion matrix for the temporal decode for this database. High intensity along the diagonal indicates that time intervals were decoded correctly. The decode algorithm frequently decoded the exact temporal interval. Figure 2.4b shows the percentage of exactly correct decodes (dotted line) for all points in time in the trial. The algorithm tended to have peaks of performance around the fixation point on, cue on, fixation point off, and reward events.

Though the algorithm was less able to decode the exact temporal interval at times removed from the four events listed above, it frequently did succeed in decoding a temporal interval that was nearby. Furthermore, between events, the decoded temporal interval tended to be another temporal interval within the same state (e.g., pre-cue). The boxes in the confusion matrix in Figure 2.4a outline the temporal extent of the different

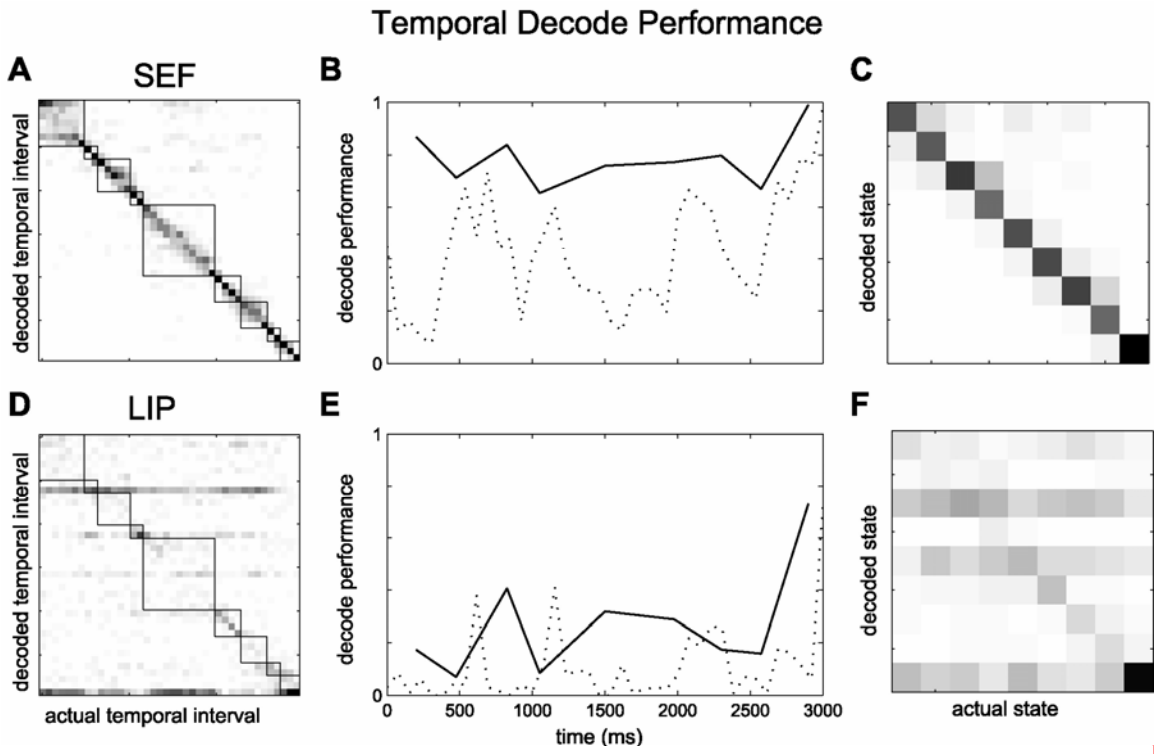

Figure 2.4. *Temporal decode performance.* Temporal decode results from monkey M, SEF and LIP databases. **(a)** Confusion matrix for the 40 actual temporal intervals (horizontal axis – each interval is 75 ms) and 40 decoded temporal intervals (vertical axis). Intensity indicates the percentage of trials decoded as each time interval, at each point in time (range 0 to 50%). Span of the different event periods and states are boxed. **(b)** Temporal decode performance across the trial, calculated as the percentage of trials correctly decoded in the exact same temporal interval (dotted line) or a temporal interval within the same event period or state (solid line). **(c)** Confusion matrix for the temporal decode by state. Intensity indicates the percentage of trials within each event period or state (horizontal axis) decoded as a temporal interval in each of the nine possible states (vertical axis). Range is 0 – 100%. **(d)** Confusion matrix for temporal decode, as in (a), for the monkey M, LIP database. **(e)** Temporal decode performance across the trial using the LIP database, same conventions as in (b). **(f)** Confusion matrix for the temporal decode by state for LIP database, same conventions as in (c).

states and event period in the trial. Figure 2.4c averages over these periods and shows the confusion matrix of the temporal decode given state by state. Intensity along the diagonal indicates that firing rates for each temporal interval were almost always decoded as the same or another temporal interval within the same state. The performance of the temporal decode within the same state is shown as a solid line in Figure 2.4b. Notice that while the dotted line (exact) dips between events, the solid line (within state) maintains high performance.

The database from area LIP of the same monkey did not perform well when using the same temporal decode algorithm. The confusion matrix for the LIP database is shown in Figure 2.4d. There were substantially fewer LIP neurons recorded, and so the comparison with the SEF database is not fair. We deal with the issue of sample size below, and for similar numbers of cells, the LIP population performs considerably poorer in decoding temporal intervals. The exact and within-state temporal decode performance is shown in Figure 2.4e, and finally the within state confusion matrix is shown in Figure 2.4f.

Despite the inability to decode temporal intervals across the trial, the LIP databases did manage to decode the reward state quite clearly. The SEF decode performance is high for all of the states and is exceptionally high at the reward state. Apparently, the neural signals present around the time of reward are quite distinct from the signals present at other periods in both LIP and SEF.

Decoding the target location

The LIP database achieved a much better performance when attempting to use a spatial decode. Unlike the activity of the example SEF neurons shown in Figure 2.2, LIP neurons tended to be spatially-tuned (see Supplementary Figures 2.S1 and 2.S2) and therefore exhibited increased firing rates for only a small number of the target locations, remaining inactive for the other directions. Because of this dependence of the firing activity on target position, the majority of task-related LIP neurons contributed reliable information to the spatial decode.

Since spatial decode performance in previous literature has included spiking data from the entire memory or saccadic periods (Shenoy, 2003; Musallam et al., 2004), the spatial decode was implemented in which firing rates were calculated from an entire state, such as cue, memory, or saccade states. To compute the performance of the spatial decode with a higher error tolerance, all decoded target positions within a given angular span of the actual target direction were counted as correct.

Summary temporal and spatial decode results

The temporal and spatial decode performance of each area is shown in Figures 2.5, which compare performances using randomly chosen subsets of neurons, so that data from the two areas can be directly compared, even though the original numbers of recorded neurons were unequal. SEF performed better in decoding the current temporal interval, and LIP performed better in decoding the location of the target. The temporal decode results shown in Figure 2.5 show the correct state decode performance for increasing population sizes. The mean of the solid line in Figure 2.4b would be plotted as a single point at the far right side of Figure 2.5a, since the results shown in Figure 2.4 are from the entire SEF dataset of monkey M. As shown in Figure 2.4, SEF achieves better performance for the temporal decode, and since the red line rises earlier and higher than the blue line, it is clear that SEF achieves better performance even when the neuron sample sizes are comparable. The mean values correspond to the performance that one could hope to achieve with a random sampling of neurons in each area, such as would be encountered with an unmovable electrode array.

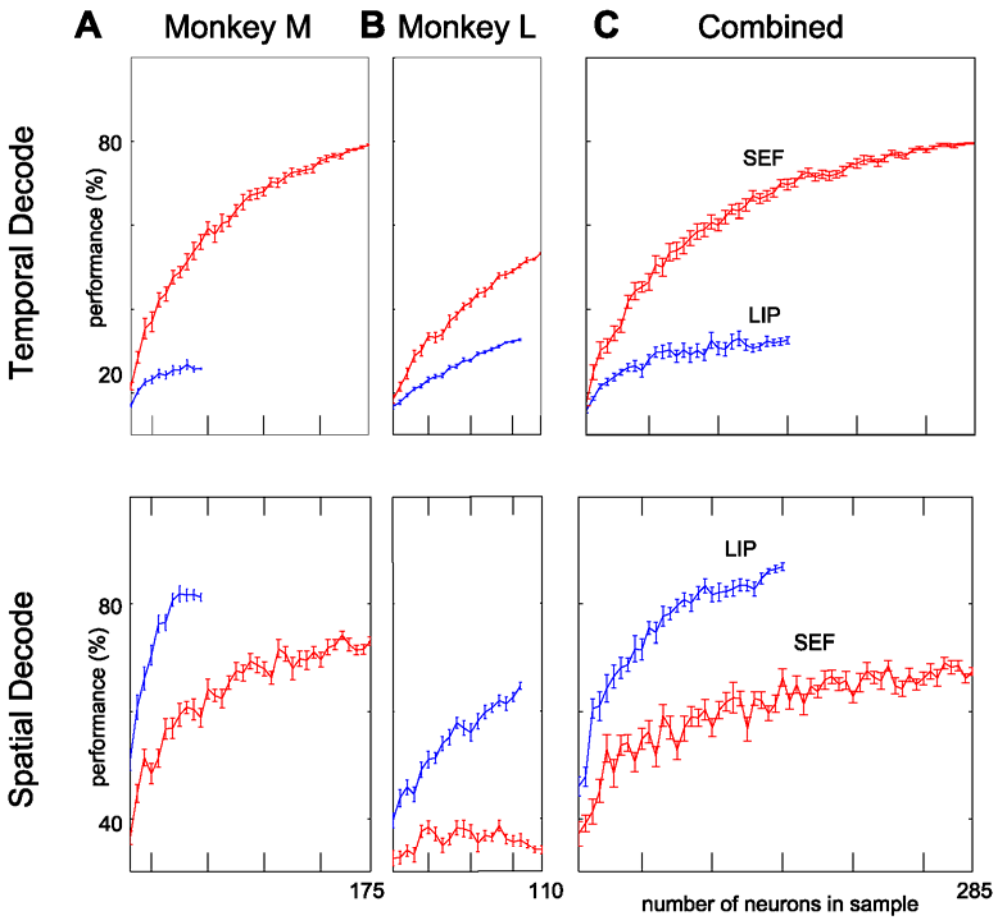

Figure 2.5. *Summary temporal and spatial decode results.* **(a)** Monkey M. *Top row*, Temporal decode results using different neuron population sizes. Mean temporal decode performance for correct state classifications (vertical axis) using random samplings (without replacement) of different neuron population sizes (horizontal axis) with a 75 msec time window for spike train inputs. Error bars are standard error of the mean for the different samples. Red lines are SEF results. Blue lines are LIP results. *Bottom row*, saccade period spatial decode performance for position classifications within 45 degrees of the actual target position (vertical axis) using random samplings (without replacement) of different neuron population sizes (horizontal axis). Error bars are standard error of the mean. Red lines are SEF results. Blue lines are LIP results. **(b)** Monkey L, same conventions as in (a). **(c)** Data from both monkeys combined, same conventions as in (a).

The results for the spatial decode are shown in Figure 2.5d-f, which shows the mean performance for a given sample size in decoding the target position in the saccadic interval. Area LIP outperforms SEF in the movement (saccadic) period. The relative performance in the cue period was not consistent for the two monkeys, which is attributable to the paucity of LIP neurons with cue period activations in the monkey L

database. LIP and SEF performed equally well for both monkeys in the memory period (not shown) when comparing neuron populations of equal size.

DISCUSSION

In this report we have shown that SEF contains neurons that support the representation of sequential states within the context of an oculomotor task. LIP neurons tended to respond spatially and were not found to assist in the sequential state representation, despite previous reports that elapsed time influences LIP activity when it is integral to the eye movement instruction (Leon and Shadlen, 2003; Janssen and Shadlen, 2005). To substantiate these findings, we ran spatial and temporal decodes. SEF, with a variety of temporally tuned cell types, was much better able to provide a readout of the current temporal interval, or state, within the context of the task. LIP, with mainly spatially-tuned activations, was not able to provide an accurate readout of the current state, but outperformed SEF in regards to reading out the intended eye movement location. SEF also contained spatially-tuned neurons, and the target location was decodeable from SEF as well, though not as clearly. Overall, the prevalence of SEF neurons with activity that was not spatially-tuned made it a better predictor of the current behavioral state.

The three general non-spatial cell types identified in SEF support both the accumulator (Macar et al., 1999; Brody et al., 2003; Reutimann et al., 2004) and state-dependent network (Mauk and Buonomano, 2004; Lucchetti et al., 2005) models of the neural representation of behavioral timing. Event detecting neurons could serve to transition the local network of temporal units into a new state, which would be in turn

stably maintained by the activity of state-encoding neurons. Anticipatory neurons could also accumulate inputs from the tonic state encoding neurons, providing high-resolution estimates of the elapsed time since the previous event. These three types of units can therefore work together to provide temporal information on multiple time-scales, suggesting that state-dependent network and accumulator models describe the representation of time within SEF at different levels of temporal resolution.

The non-spatial activations we described may serve other functions as well. Individually, event-detecting neurons, for example responding to the cue presentation, might serve to inhibit a reflexive saccade to the cue stimulus. The variety of circumstances under which event-detecting neurons fired, however, implies no single functional explanation for that type of activity would be sufficient. Note that the example event-detecting neuron in Figure 2.2a responded to visual stimuli onsets or offsets in central or peripheral locations. Anticipatory activity has been described previously in SEF neurons and was considered as a bias for a particular movement (Coe et al., 2002). Such a bias does not seem a reasonable explanation for the pre-cue anticipatory activity reported in our study, since there were 43 potential targets, chosen randomly, and it would be a highly inefficient strategy if the monkey tried to predict the upcoming saccade target. In our study we found examples of anticipatory activity after the cued instruction that was either spatially-tuned or not. In the cases in which anticipatory activations were spatially-tuned, as happened frequently in the memory period, this activity is likely to reflect the preparation for an upcoming movement, perhaps in conjunction with similar neurons in LIP. For the neurons exhibiting pre-saccadic climbing activations that were not spatially-tuned, these could not contribute to the motor preparation for the particular

saccade that would be executed on any given trial. Instead, such neurons may have contributed to the timing of the executed saccade on every trial, and the buildup of activity at this final stage may have contributed to a growing readiness of move the eyes. Similarly, the anticipatory activity in the pre-cue period may have contributed to a readiness to perceive relevant information. State encoding neurons, in addition to representing the current state of the trial, may also serve behavioral purposes such as facilitating fixation in the pre-saccadic intervals via inhibitory connections to omnipause neurons (Shook et al., 1990); withholding reflexive movements (Everling and Munoz, 2000); preparing for any movement in general, termed "preparatory set" (Shima et al., 1996; Everling and Munoz, 2000; Hoshi et al., 2005); integrating task rules for the selection of task-appropriate motor plans (Miller et al., 2005); and stimulus encoding in a manner that is dissociated from the spatial location of the stimuli.

We used a simple model-free nearest-neighbor decode that usually leads to error rates greater than the minimum possible, the Bayesian rate (Duda, 2001). Other decode algorithms that make use of the inherent structure of spatial and temporal receptive fields will likely outperform the results presented here.

The spatial tuning for saccade targets found in abundance in area LIP provides a basis from which to decode eye movement intentions. The same responsiveness, however, to the visual cue and also to distractor stimuli indicates a challenge to the implementation of neuroprosthetic devices in parietal cortex. Also in PRR, the neighboring area that encodes arm movement intentions, a visual transient can be observed when a new stimulus is flashed in the neuron's response field (Snyder et al., 1997). Though the argument that sensory and attention-related activations in LIP would

confound movement planning signals (Bisley and Goldberg, 2003) is avoided when eye and arm movements are made in isolation or to different targets (Quian Quiroga et al., 2006), there still remains the problem that movement signals are only properly decodable when the decoder interprets data from the appropriate interval of the task sequence, and further, that in natural circumstances eye and arm movements are frequently made together. In order to properly decode the movement intentions from parietal neurons, it is necessary to know if the current representation formed by the firing activity of the neurons is a transient for a visual stimulus, or indeed represents the upcoming motor intention. There have been some efforts to get around this problem, including a state machine decoding design in which the movement encoding state necessarily follows the visual onset state (Shenoy, 2003), or through the use of spectral analysis of local field potentials to identify state transitions (Bokil et al., 2006). In controlled experimental situations, the regularities within the task help in choosing the appropriate interval for movement intention decoding, though in natural situations there are not fixed duration planning periods, and so these approaches may not be satisfactory. It may instead be simpler to look to SEF for state sequence information. While SEF does not provide as clear of a spatial representation, it does have abundant information regarding the sequential progression of the task.

With access to SEF and LIP neural activity, one could decode the current state from SEF and use that information to collect firing activity from LIP spanning an entire relevant state to achieve the most accurate spatial decode possible. Additionally, SEF could provide the important signal of when to execute the movement. As the functions of frontal cortex become more apparent, we can continue to find higher levels of

computation already performed in the brain for dealing with complex natural environments and situations that are not well approximated by experimental paradigms.

REFERENCES

Akkal D (2004) Time predictability modulates pre-supplementary motor area neuronal activity. Neuroreport 15:1283.

Amador N, Schlag-Rey M, Schlag J (2000) Reward-Predicting and Reward-Detecting Neuronal Activity in the Primate Supplementary Eye Field. J Neurophysiol 84:2166-2170.

Andersen RA (1995) Encoding of Intention and Spatial Location in the Posterior Parietal Cortex. Cereb Cortex 5:457-469.

Andersen RA, Essick GK, Siegel RM (1985) Encoding of spatial location by posterior parietal neurons. Science 230:456-458.

Andersen RA, Snyder LH, Bradley DC, Xing J (1997) Multimodal representation of space in the posterior parietal cortex and its use in planning movements. Annual Review of Neuroscience 20:303-330.

Apicella P, Scarnati E, Ljungberg T, Schultz W (1992) Neuronal activity in monkey striatum related to the expectation of predictable environmental events. J Neurophysiol 68:945-960.

Bisley JW, Goldberg ME (2003) Neuronal Activity in the Lateral Intraparietal Area and Spatial Attention. Science 299:81-86.

Bisley JW, Krishna BS, Goldberg ME (2004) A Rapid and Precise On-Response in Posterior Parietal Cortex. J Neurosci 24:1833-1838.

Bokil HSHS, Pesaran BB, Andersen RARA, Mitra PPPP (2006) A method for detection and classification of events in neural activity. IEEE transactions on bio-medical engineering 53:1678-1687.

Brody CD, Hernandez A, Zainos A, Romo R (2003) Timing and Neural Encoding of Somatosensory Parametric Working Memory in Macaque Prefrontal Cortex. Cereb Cortex 13:1196-1207.

Bruce CJ, Goldberg ME (1985) Primate frontal eye fields. I. Single neurons discharging before saccades. J Neurophysiol 53:603-635.

Campos M, Breznen B, Bernheim K, Andersen RA (2005) Supplementary Motor Area Encodes Reward Expectancy in Eye-Movement Tasks. J Neurophysiol 94:1325-1335.

Campos M, Cherian A, Segraves MA (2006) Effects of Eye Position upon Activity of Neurons in Macaque Superior Colliculus. J Neurophysiol 95:505-526.

Chen LL, Wise SP (1996) Evolution of Directional Preferences in the Supplementary Eye Field during Acquisition of Conditional Oculomotor Associations. J Neurosci 16:3067-3081.

Coe B, Tomihara K, Matsuzawa M, Hikosaka O (2002) Visual and Anticipatory Bias in Three Cortical Eye Fields of the Monkey during an Adaptive Decision-Making Task. J Neurosci 22:5081-5090.

Colby CL, Duhamel JR, Goldberg ME (1996) Visual, presaccadic, and cognitive activation of single neurons in monkey lateral intraparietal area. J Neurophysiol 76:2841-2852.

Draper NR, Smith H (1981) Applied Regression Analysis. New York: Wiley.

Duda ROF (2001) Pattern classification.

Everling S, Munoz DP (2000) Neuronal Correlates for Preparatory Set Associated with Pro-Saccades and Anti-Saccades in the Primate Frontal Eye Field. J Neurosci 20:387-400.

Fuster JM, Alexander GE (1971) Neuron Activity Related to Short-Term Memory. Science 173:652-654.

Fuster JMF (1989) The prefrontal cortex: anatomy, physiology, and neuropsychology of the frontal lobe.

Glimcher PW (2004) Decisions, Uncertainty, and the Brain: The Science of Neuroeconomics.

Gottlieb JP, Kusunoki M, Goldberg ME (1998) The representation of visual salience in monkey parietal cortex. Nature 391:481-484.

Guitton D, Buchtel HA, Douglas RM (1985) Frontal lobe lesions in man cause difficulties in suppressing reflexive glances and in generating goal-directed saccades. Experimental Brain Research 58:455-472.

Heinen SSJ, Liu MM (1997) Single-neuron activity in the dorsomedial frontal cortex during smooth-pursuit eye movements to predictable target motion. Visual neuroscience 14:853-865.

Hikosaka O, Sakamoto M, Usui S (1989) Functional properties of monkey caudate neurons. III. Activities related to expectation of target and reward. J Neurophysiol 61:814-832.

Histed MH, Miller EK (2006) Microstimulation of Frontal Cortex Can Reorder a Remembered Spatial Sequence. PLoS Biology 4.

Hoshi E, Sawamura H, Tanji J (2005) Neurons in the Rostral Cingulate Motor Area Monitor Multiple Phases of Visuomotor Behavior With Modest Parametric Selectivity. J Neurophysiol 94:640-656.

Ipata AE, Gee AL, Goldberg ME, Bisley JW (2006) Activity in the Lateral Intraparietal Area Predicts the Goal and Latency of Saccades in a Free-Viewing Visual Search Task. J Neurosci 26:3656-3661.

Isoda M (2005) Context-Dependent Stimulation Effects on Saccade Initiation in the Presupplementary Motor Area of the Monkey. J Neurophysiol 93:3016-3022.

Janssen P, Shadlen MN (2005) A representation of the hazard rate of elapsed time in macaque area LIP. Nat Neurosci 8:234-241.

Lauwereyns J, Watanabe K, Coe B, Hikosaka O (2002a) A neural correlate of response bias in monkey caudate nucleus. Nature 418:413-417.

Lauwereyns J, Takikawa Y, Kawagoe R, Kobayashi S, Koizumi M, Coe B, Sakagami M, Hikosaka O (2002b) Feature-Based Anticipation of Cues that Predict Reward in Monkey Caudate Nucleus. Neuron 33:463-473.

Leon MI, Shadlen MN (2003) Representation of Time by Neurons in the Posterior Parietal Cortex of the Macaque. Neuron 38:317-327.

Li C-SR, Andersen RA (2001) Inactivation of macaque lateral intraparietal area delays initiation of the second saccade predominantly from contralesional eye positions in a double-saccade task. Experimental Brain Research 137:45-57.

Libet BB, Wright EEW, Gleason CCA (1983) Preparation- or intention-to-act, in relation to pre-event potentials recorded at the vertex. Electroencephalography and clinical neurophysiology 56:367-372.

Lucchetti C, Ulrici A, Bon L (2005) Dorsal premotor areas of nonhuman primate: functional flexibility in time domain. European Journal of Applied Physiology 95:121-130.

Macar Fo, Vidal F, Casini L (1999) The supplementary motor area in motor and sensory timing: evidence from slow brain potential changes. Experimental Brain Research 125:271-280.

MacKay WWA, Crammond DDJ (1987) Neuronal correlates in posterior parietal lobe of the expectation of events. Behavioural brain research 24:167-179.

Maimon G, Assad JA (2006) A cognitive signal for the proactive timing of action in macaque LIP. Nat Neurosci advanced online publication.

Mauk MD, Buonomano DV (2004) The neural basis of temporal processing. Annual Review of Neuroscience 27:307-340.

Mauritz KH, Wise SP (1986) Premotor cortex of the rhesus monkey: neuronal activity in anticipation of predictable environmental events. Experimental Brain Research 61:229-244.

Miller LM, Sun FT, Curtis CE, D'Esposito M (2005) Functional interactions between oculomotor regions during prosaccades and antisaccades. Human Brain Mapping 26:119-127.

Missal M, Heinen SJ (2004) Supplementary Eye Fields Stimulation Facilitates Anticipatory Pursuit. J Neurophysiol 92:1257-1262.

Miyashita K, Rand MK, Miyachi S, Hikosaka O (1996) Anticipatory saccades in sequential procedural learning in monkeys. J Neurophysiol 76:1361-1366.

Musallam S, Corneil BD, Greger B, Scherberger H, Andersen RA (2004) Cognitive Control Signals for Neural Prosthetics. Science 305:258-262.

Niki H, Watanabe M (1979) Prefrontal and cingulate unit activity during timing behavior in the monkey. Brain Research 171:213-224.

Press WH, Teukolsky SA, Vetterling WT, Flannery BP (2002) Numerical Recipes in C++: The Art of Scientific Computing. Cambridge: Cambridge University Press..

Quian Quiroga R, Snyder LH, Batista AP, Cui H, Andersen RA (2006) Movement Intention Is Better Predicted than Attention in the Posterior Parietal Cortex. J Neurosci 26:3615-3620.

Reutimann J, Yakovlev V, Fusi S, Senn W (2004) Climbing Neuronal Activity as an Event-Based Cortical Representation of Time. J Neurosci 24:3295-3303.

Sasaki K, Gemba H (1986) Effects of premotor cortex cooling upon visually initiated hand movements in the monkey. Brain Research 374:278-286.

Schall JD (1991) Neuronal activity related to visually guided saccadic eye movements in the supplementary motor area of rhesus monkeys. J Neurophysiol 66:530-558.

Shenoy KV (2003) Neural prosthetic control signals from plan activity. Neuroreport 14:591.

Shima K, Hoshi E, Tanji J (1996) Neuronal activity in the claustrum of the monkey during performance of multiple movements. J Neurophysiol 76:2115-2119.

Shook BL, Schlag-Rey M, Schlag J (1990) Primate supplementary eye field: I. Comparative aspects of mesencephalic and pontine connections. The Journal of Comparative Neurology 301:618-642.

Snyder LH, Batista AP, Andersen RA (1997) Coding of intention in the posterior parietal cortex. Nature 386:167-170.

Stuphorn V, Taylor TL, Schall JD (2000) Performance monitoring by the supplementary eye field. Nature 408:857-860.

Takikawa Y, Kawagoe R, Hikosaka O (2002) Reward-Dependent Spatial Selectivity of Anticipatory Activity in Monkey Caudate Neurons. J Neurophysiol 87:508-515.

Vaadia EE, Kurata KK, Wise SSP (1988) Neuronal activity preceding directional and nondirectional cues in the premotor cortex of rhesus monkeys. Somatosensory & motor research 6:207-230.

Watanabe K, Hikosaka O (2005) Immediate Changes in Anticipatory Activity of Caudate Neurons Associated With Reversal of Position-Reward Contingency. J Neurophysiol 94:1879-1887.

Zar JH (1974). Biostatistical analysis. Englewood Cliffs, N.J.,: Prentice-Hall.

SUPPLEMENTARY MATERIALS

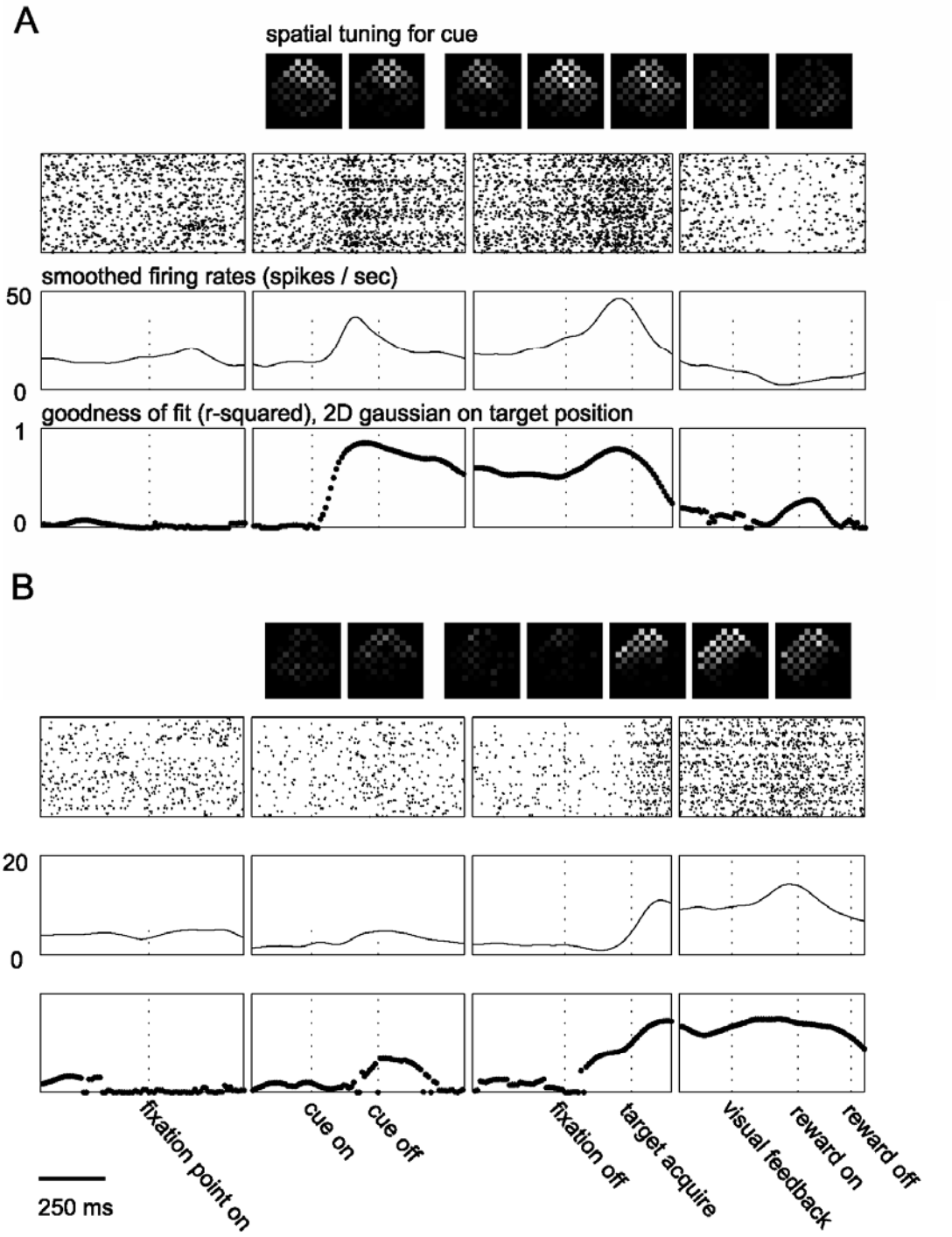

Supplementary Figure 2.S1. *Example LIP neurons.* Same plotting conventions as in Figure 2.1. **(a)** Example neuron with spatially tuned firing activity in the cue, memory, and saccade intervals. **(b)** Example neuron tuned after the completion of the instructed saccade in the post-saccadic, visual feedback, and reward intervals.

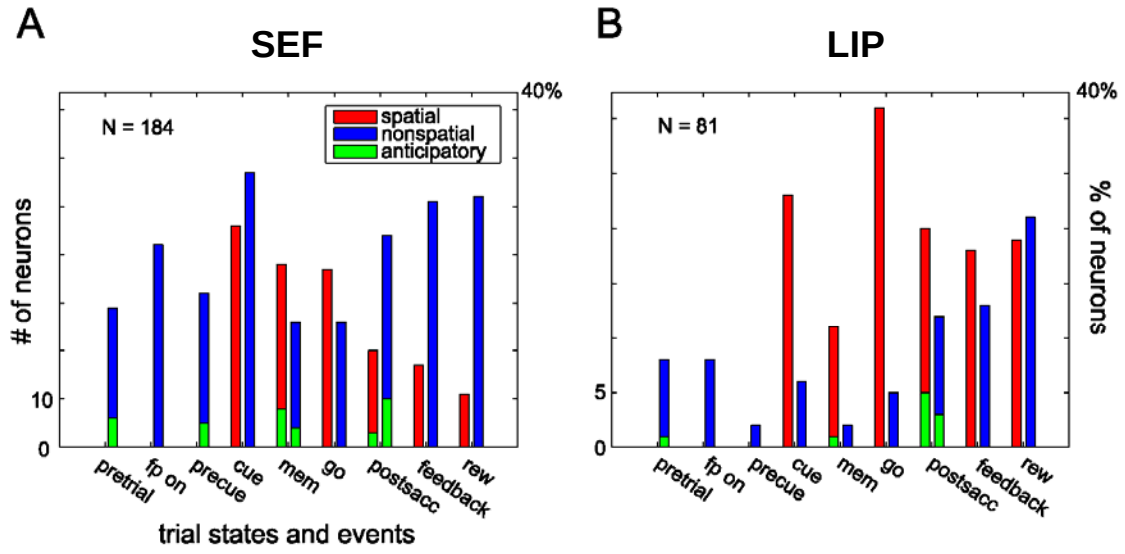

Supplementary Figure 2.S2. *Activity types exhibited by individual neurons.* Prevalence of activity types in the **(a)** SEF databases, data from both monkeys combined. The labels on the horizontal axis are the four events and five states during which each neuron was tested for spatially-tuned neural activity (red) or non-spatially-tuned activations or suppressions (blue). The states are pretrial, pre-cue, memory, post-saccade, and reward, which span the intervals before and after the four events: fixation point on, cue presentation, fixation point off (go), and visual feedback. Neurons were further tested for anticipatory activations or suppressions (green) at the end of the first four states. Event detection activity as shown in Figure 2.2a is included in the blue bars above the four event labels. Anticipation activity as shown in Figure 2.2b is included in the green bars above the first four state interval labels. State encoding activity as shown in Figure 2.2c is included in the blue portions of the bars above the state interval labels. Both bar graphs are scaled so that the top of the vertical axis corresponds to 40% of the task related neurons in the database. **(b)** Prevalence of activity types in the LIP databases, data from both monkeys combined.

Event-based representation of time

A group of neurons temporally tuned to different events could in principle indicate which event the monkey is experiencing at any point in time. Several examples of event detection activity are shown in Supplementary Figure 2.S3. The first three example neurons responded to only one event. The first responded to the fixation point on event with an activation, the second to the cue on event with a brief depression, and the third to the target acquisition with an activation. By interpreting the activity of these three neurons, the most recent event can be known by noting which neuron was recently modulated, and a confident estimate of the current state of the monkey can be

extrapolated. For example, on a given trial, if the neuron depicted in green was recently active, but the neuron depicted in cyan had not yet been depressed, then an observer could deduce that the monkey was in the pre-cue state. The remaining examples shown in Supplementary Figure 2.S3 respond to multiple events. These neurons do not themselves definitively tell us which event has just occurred. For example, if the neuron depicted in black is active, we can only

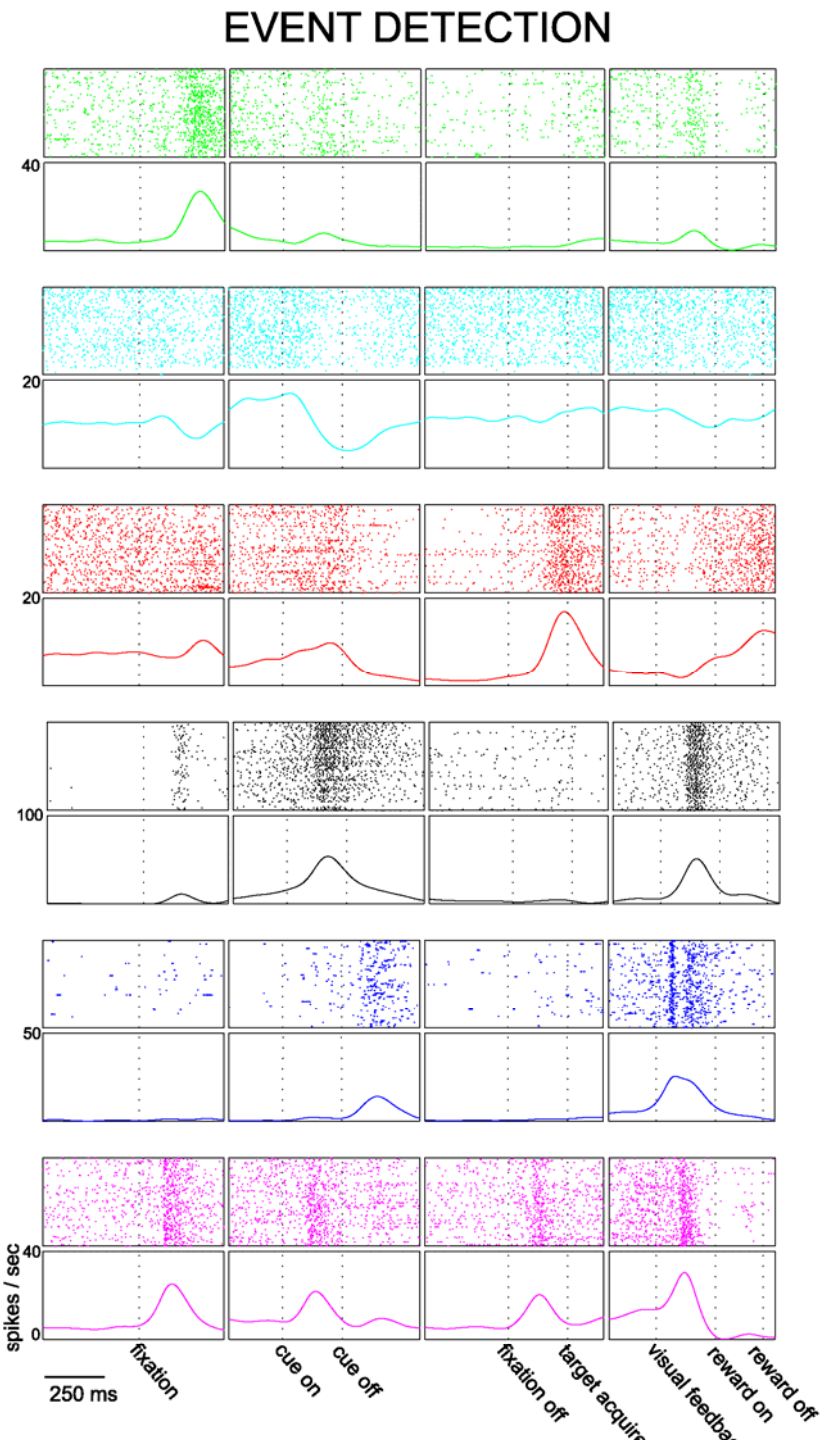

Supplementary Figure 2.S3. *Variety of event detection activity in SEF.* Six example neurons with event detection activity. Same alignment and smoothing conventions as in Figure 2.1, but only the spike train rasters and smoothed firing rates are shown. None of these example neurons exhibited spatial tuning in any interval. Each neuron is depicted with a unique marker and line color. Green, fixation point on activation. Cyan, cue on deactivation. Red, fixation point off activation. Black, visual feedback activation, as well as cue appearance activation, and smaller fixation point on activation. Blue, cue off and target reappear activations. Magenta, fixation point on, cue on, fixation point off, and visual feedback activations.

deduce that either the cue on *or* the visual feedback event has just occurred. However, if we combine this information with the information from the neuron depicted in cyan, which tells us that the cue on period has just occurred or that it has not, then we can reliably state with very basic logic that either the cue is on (black neuron active, cyan neuron depressed) or the visual feedback is on (black neuron active, cyan neuron at baseline). Combinations of additional neurons can encode the most recent event with increasing precision and coverage of the temporal intervals in the trial.

While it may be satisfactory to know which event happened most recently, it may also be helpful to know how much time has elapsed since the previous event. For this function, neurons with anticipatory activity are very well suited (Brody et al., 2003). For example, a neuron may increase its firing rate by one spike per second over the course of sixty seconds. It might start with a baseline firing rate of 10 Hz, and then 1 second after a triggering event rise to 11Hz, rise to 12Hz after 2 seconds, and so on. If the neuron is known to steadily increase in this manner, and later on we measure the firing rate at 34 Hz, we can then infer that 24 seconds have passed since the triggering event. The equation that yields the current time would be: (current firing rate – baseline) / (increase in firing rate per second). The example neurons shown in Supplementary Figure 2.S4 rise in anticipation of certain events, and then reset once those events occur. As shown in that figure, a single neuron can rise before just one event in the trial, or several. In the case that the neuron exhibits anticipatory activity prior to multiple events, knowledge of the current state of the monkey is required to make sense of each anticipatory buildup.

The final piece of the event-based representation of time in SEF is the population of neurons that represent different states. As the monkey moves through the tasks, he

goes from one state to another, first waiting for the fixation point to appear, then fixating that point while awaiting the movement instruction, then continuing to fixate while planning the instructed eye movement, then executing the movement, re-establishing fixation at the target, perceiving the visual feedback, and finally achieving a reward. The example neurons in Supplementary Figure 2.S5 show

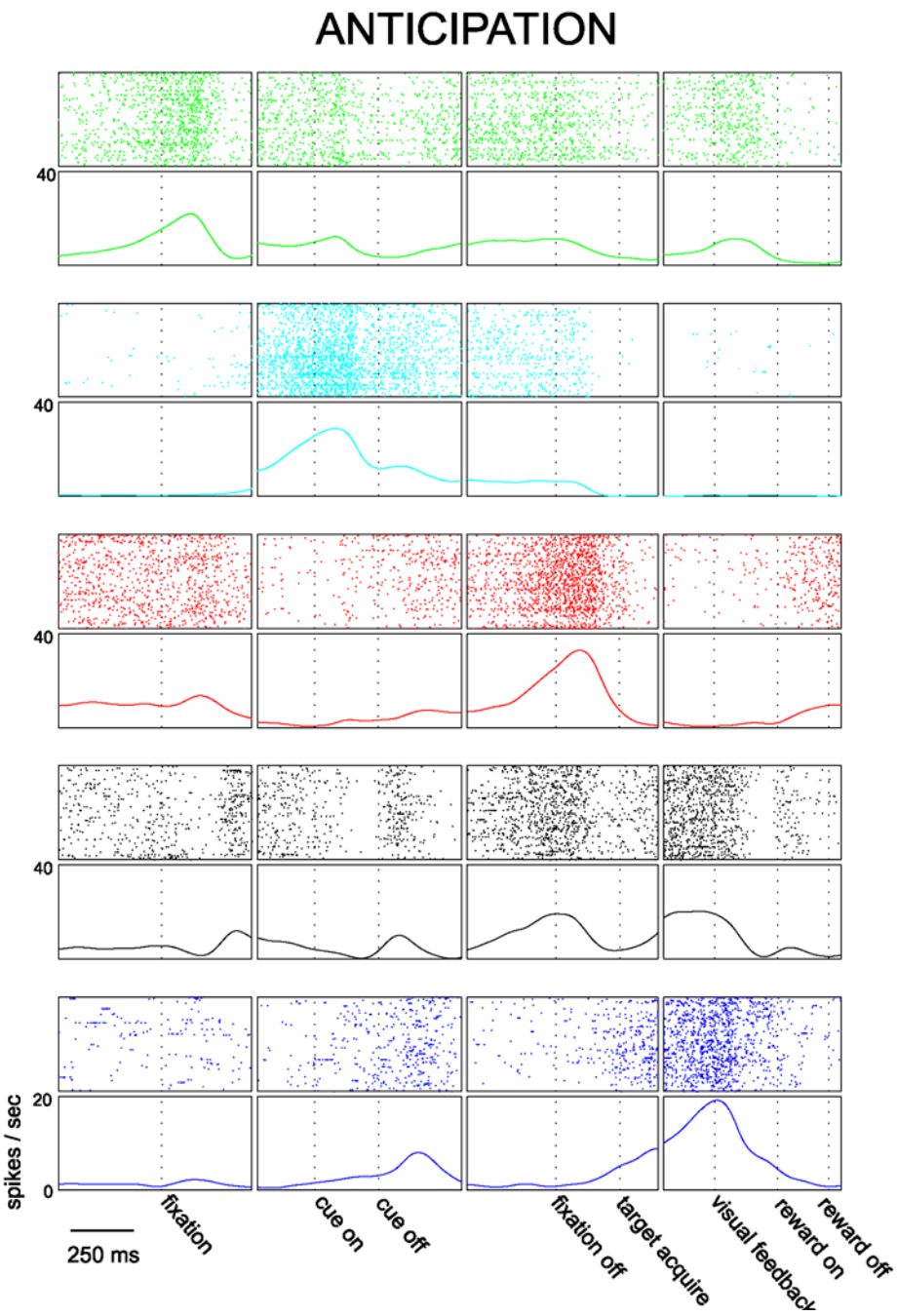

Supplementary Figure 2.S4. *Variety of anticipation activity in SEF.* Five example neurons with anticipatory activity for different events. Same plotting conventions as in Supplementary Figure 2.S3. Green, anticipates fixation point on event at the start of the trial. Cyan, anticipates cue on event. Red, anticipates fixation off event. Black, anticipates fixation off and visual feedback events. Blue, anticipates visual feedback event.

a variety of neurons that are tonically active during one or more of these states. None of these responses are spatially-tuned, and like event-detection activity, can be used together to decode the state in which the monkey is currently engaged.

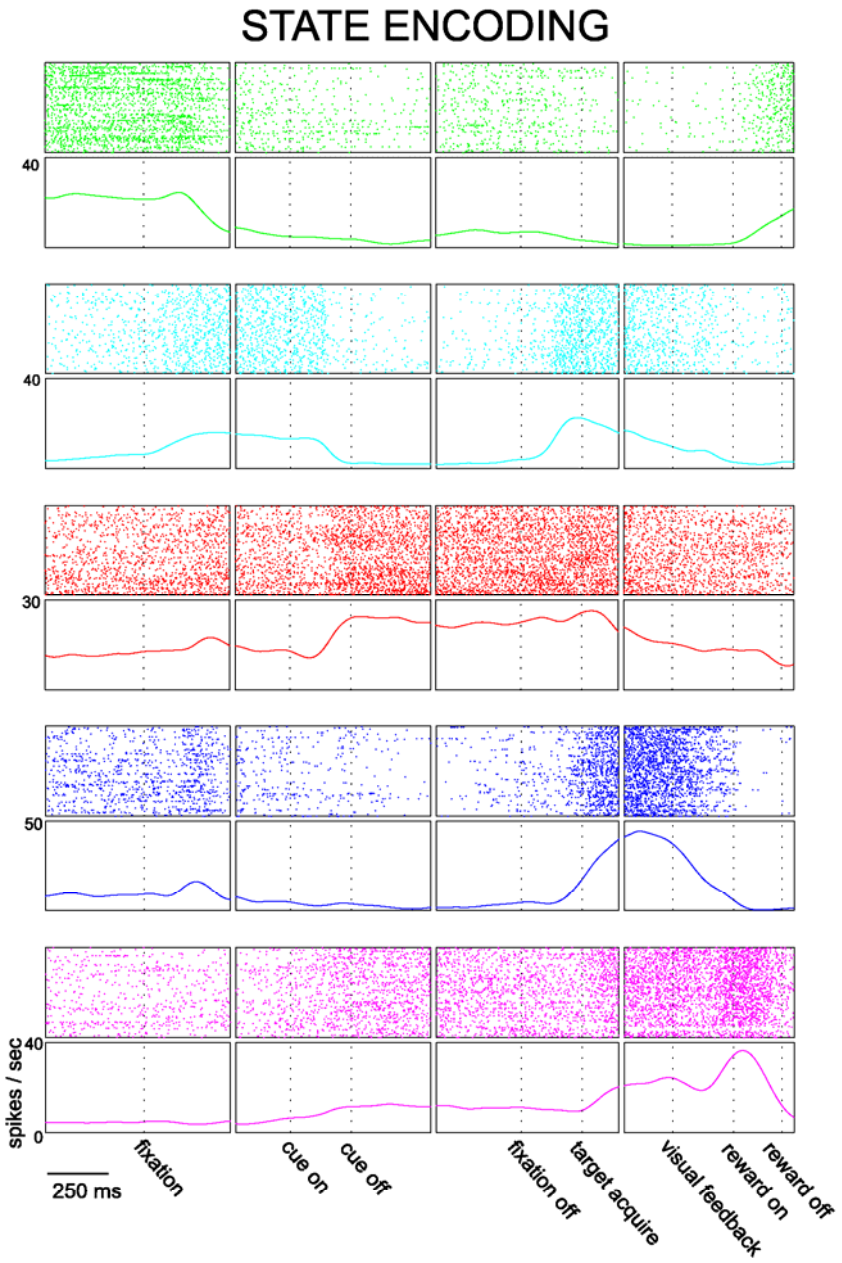

Supplementary Figure 2.S5. *Variety of state encoders in SEF.* Five example neurons with state encoding activity spanning intervals between different events. Same plotting conventions as in Supplementary Figure 2.S3. Green, encodes pre-trial state, active from the end of the reward (right side) until just after the fixation on event. Cyan, encodes pre-cue and post-saccadic states, active from the fixation point on event until just after the cue on event (same neuron as in Figure 2.1c). Red, encodes memory or planning state, active from the cue off event until the fixation point off event. Blue, encodes post-saccadic event, active from the end of saccade until the visual feedback event. Magenta, encodes multiple states in a step-wise fashion, with increasing tonic activations for memory, post-saccadic, and reward states.

CHAPTER III

SELECTION OF TARGETS AND DISREGARD OF IRRELEVANT STIMULI IN MONKEY LIP AND SEF

ABSTRACT

When faced with a task situation involving a target and one or several distractors, the brain areas involved in oculomotor control must selectively represent the target and ignore or suppress the distractors. We recorded single unit activity from cortical areas LIP and SEF in two monkeys performing a variant on the memory-guided saccade task, in which a distractor stimulus (1 of 2 green polygonal objects) was presented prior to the cue stimulus (small while dot), which was briefly flashed. The distractor persisted until 200 ms before the signal for the monkey to saccade to the remembered location of the spatial cue. Neither of the monkeys had previous exposure to any task in which the distractor stimuli (objects) were relevant. We found that most LIP neurons serially encoded the location of the distractor, then the cue, and that many LIP neurons then encoded the distractor position again in the middle of the memory period. The cue response dominated in the late memory period and around the time of the saccade. Thus, LIP responded to both cue and distractor stimuli, but selectively maintained the representation of intended eye movement targets. Most spatially-tuned SEF neurons responded in a still more selective manner, most responding only to the cue and ignoring

the distractor. A smaller group of SEF neurons responded only to the distractor, and were silent during the presentation of the cue. These SEF responses could be thought to label the task relevance of the target and distractor stimuli. Another class of SEF neurons responded at various times in the trial, but without spatial tuning, perhaps marking the passage of time in an event-based manner and suggesting a mechanism for the category specific tuned responses. Taken together, we find that, first, SEF in the frontal cortex labels relevant and irrelevant stimuli, and second, parietal cortex, after encoding the locations of multiple stimuli, selectively maintains the spatial representations required for planning behavior. These are important components of target selection when various stimuli are presented at different times.

INTRODUCTION

When faced with an eye movement task situation involving a target and one or several distractors, the brain areas involved in oculomotor control must selectively represent the target of the subsequent eye movement for motor preparation, and ignore or suppress the distractors. Since muscimol inactivation of LIP disrupts the selection of the correct target from an array of distractors (Wardak et al., 2002), and human patients with bilateral parietal lesions have trouble filtering out distractors and selecting appropriate targets (Friedman-Hill et al., 2003), LIP is supposed to be an active participant in the target selection processes, which involves other brain areas as well. Neural activity in the caudate rises in anticipation of a target cue, but not the same stimulus if the task context dictates that it will serve as a distractor (Hikosaka et al., 1989), which may bias

perceptual processing. When the task is not predicatable, prefrontal cortex neurons represent the target location amongst distractors in sustained activity around 140 ms after the stimulus presentation, though the initial response is non-selective (Rainer et al., 1998), which is a similar timecourse as observed in FEF (Schall et al., 1995), and IT neurons can discriminate between targets and distractors even more quickly (Chelazzi et al., 1993). Concurrently with enhanced representations of the target locations, PFC neurons also respond to the location of where not to look, which suggests the active disregard of irrelevant information and the suppression of unwanted movements (Hasegawa et al., 2004), and prefrontal neurons do not fully ignore irrelevant and distracting stimulus dimensions when they are relevant in other task contexts (Lauwereyns et al., 2001). Furthermore, ventrolateral PFC neurons appear to be mainly concerned with inhibiting unwanted responses, not facilitating wanted ones (Sakagami et al., 2001).

Studies on the role of LIP in representing irrelevant information have produced conflicting results. LIP neurons were found to automatically encode irrelevant salient stimuli, even in a passive fixation task (Constantinidis and Steinmetz, 2005), though other studies have found that LIP only represents stimulus features that are relevant (Assad, 2003). LIP neurons initially respond almost equally to a distractor stimulus or a target, but exhibit selective instruction-dependent activity in the delay-period (Sereno and Amador, 2006), suggesting that there may be two co-existing modes of representation in LIP, the first responding to all salient sudden onset stimuli, and the second which exhibits movement command specificity (Snyder et al., 1997; Gottlieb et al., 2005). The initial response to a distractor can also be attenuated if it is predictable (Ipata et al., 2006b),

reflecting the effect of top-down influences on the response to sudden-onset stimuli (Jonides and Yantis, 1988).

In the context of learned sequential eye movements, SEF neurons will respond differentially to the same visual array in which the assignment of each stimulus to the category of target or distractor is reversed, which can be used to identify which stimulus is the appropriate target at this stage in the learned sequence (Lu et al., 2002). SEF is also an important contributor in the execution of anti-saccades, which require internally driven eye-movement plans away from the location of the visual stimulus (Schlag-Rey et al., 1997).

The timing of the presentation of a target and a distractor is of critical importance to subsequent processing. FEF initially responds to both targets and distractors when presented simultaneously in a search array (Bichot and Schall, 1999). In contrast, when a pop-out distractor is presented in the receptive field of an LIP neuron at the same time that a target is presented elsewhere, the LIP neuron does not respond (Gottlieb, 2002), revealing that LIP neurons can be highly selective immediately upon the stimulus presentations. When the saccade target and distractor are presented asynchronously, LIP can represent the spatial location of more than one stimulus at the same time (Gottlieb et al., 2005), even when an eye movement plan has been formed (Powell and Goldberg, 2000), though at the time of the saccade LIP always represents the eye movement goal alone (Andersen et al., 1985; Ipata et al., 2006a). These timing effects are in contrast to findings from inferotemporal cortex, where a target and distractor presented synchronously then compete for the same "representational substrate," but when the two

stimuli are presented in series this competition is abolished, and the second stimulus simply overwrites the first (Desimone and Duncan, 1995).

In this study we characterize the encoding of populations of neurons in LIP and SEF with respect to spatial representations in a target selection paradigm, in which the monkeys performed a memory-guided saccade task with and without an asynchronously presented distractor stimulus. To understand the dynamics of these representations, we then computed the performance of a decoding algorithm on the spatial position of the target or distractor.

METHODS

Studies were performed with two behaving, male rhesus monkeys (Macaca mulatta). Each was chronically fitted with a stainless steel head post for head immobilization and two recording chambers over small craniotomies for electrode insertions. Experimental procedures were in accordance with the California Institute of Technology Institutional Animal Care and Use Committee.

The same monkeys were used in a previous study (Chapter 2) of the same brain areas, and the methods regarding training, chamber mapping, recording procedure, and data analysis are largely the same. See Chapter 2 for elaborated methodological descriptions. Important points will be repeated here, but only methods not employed in the previous study will be described in detail.

Behavioral tasks

Two eye movement tasks were used, a memory-guided saccade task and a distractor task. In both tasks the monkey was instructed to perform a saccade from a central fixation point to one of 43 targets placed at regular intervals to cover the entire visual field out to 15 deg of visual angle in every direction from central fixation.

In the memory-guided saccade task (Figure 3.1a), monkeys were required to maintain central fixation while a peripheral target was briefly flashed, wait until the central fixation point extinguished, and then saccade to the remembered location. In the distractor task (Figure 3.1b), the monkeys performed a memory-guided saccade task as described above, but a distractor stimulus (green isosceles triangle or semicircle) was presented peripherally while the monkey fixated at the start of the trial. After a fixed interval following the distractor presentation (500 ms), the cue (small white dot) was briefly flashed, and the trial proceeded just as above. The distractor stimulus remained visible while the spatial cue was flashed and remained until 200 ms before the central fixation off event, which was the "go signal." At the go signal, the monkeys were required to saccade to the remembered location of the cue.

The distractor and cue locations were chosen randomly with replacement from the possible 43 target locations. The orientation of the distractor (+/- 45, +/- 135 degrees) and the identity of the object (triangle or semi-circle) were also chosen randomly at the start of each trial. Distractor task and memory-guided saccade task trials were interleaved, and the distractor trails were performed 8 times more frequently than memory trials to cover the variety of orientation and identity combinations of the distractor. A typical recording

session included 400 - 1000 correct trials depending on the isolation quality as monitored by the experimenter.

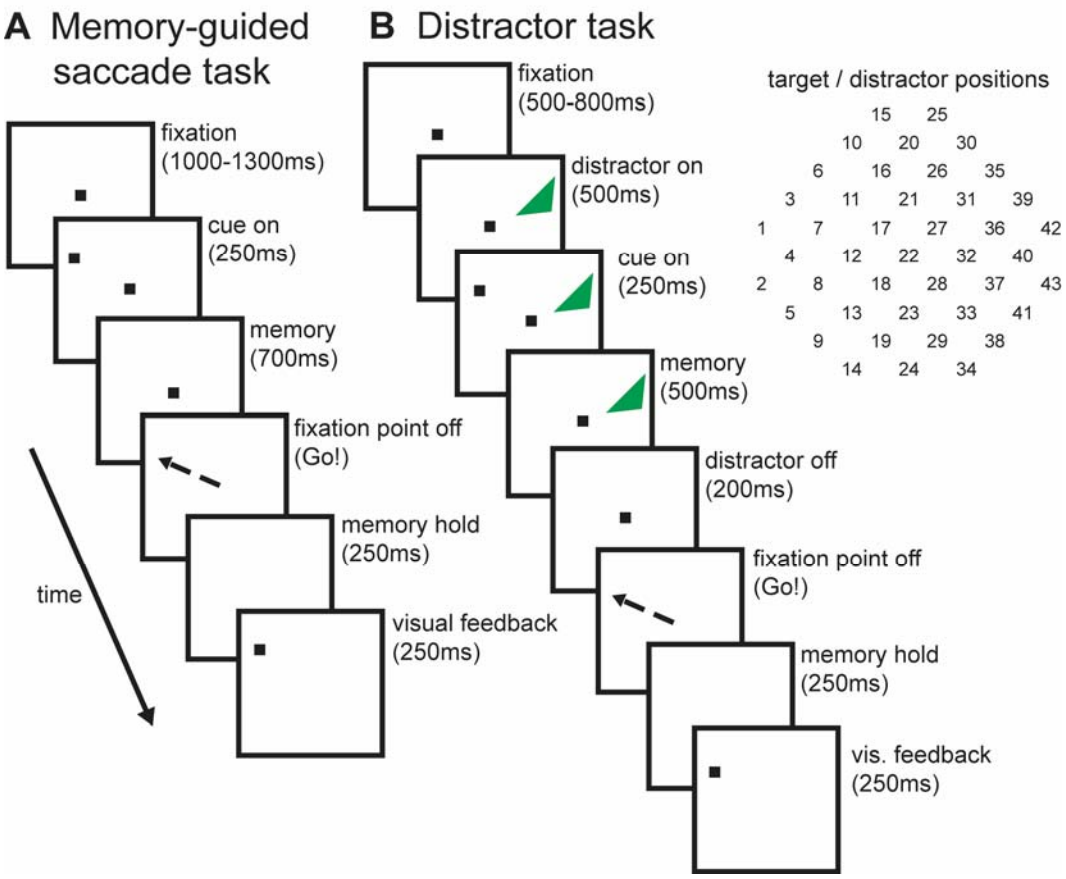

Figure 3.1. *Time course of oculomotor tasks.* The temporal progression of each task is shown in successive panels from top left to bottom right. In the memory-guided saccade task **(a)**, the monkey is required to acquire a central fixation point at the start of the trial. After a variable delay (1000-1300 ms), a cue is briefly flashed (250 ms) at one of 43 targets in the periphery. The possible targets cover the entire visual field out to 15 degrees. Following a hold interval, the fixation point is extinguished, and the monkey is required to saccade to the remembered target location and fixate there. After 250 ms, the target reappears, and then following an additional 250 ms fixation, the animal is rewarded with a drop of juice. In the distractor task **(b)**, the monkey begins the trial by acquiring a central fixation point. After a variable delay (500-800 ms), an object appears at one of the same 43 peripheral locations that are used as possible targets. The cue appears 500 ms later at a randomly chosen peripheral target location, possibly the same as the distractor, and then the trial proceeds as in the memory-saccade task. The distractor remains illuminated until 200 ms before the fixation point is extinguished.

Recording Procedure

Neurons were accessed with between three and six independently-controlled Thomas Recording electrodes (ThomasRecording Gmbh),from one or two head-mounted micromanipulators. With this arrangement, up to 10 neurons could be recorded simultaneously.

Neuron classification analysis

To standardize the spike trains for each trial, spike trains were aligned to four different events that occurred at varying intervals, and these four spike trains were then merged around the time of the shortest interval between each event. The spike trains were merged in the same manner as was detailed in the previous study (Chapter 2), except that the second alignment event was the distractor presentation, and the merged spike trains included the additional 500 ms between the distractor and cue presentations. Using these merged spike trains, firing activity during different states and events were then compared to baseline firing levels to determine if there were significant activations or depressions. All intervals were defined by these same events in both the memory and distractor tasks, though in distractor tasks there was the additional *distractor on event* (150 ms interval starting 70 ms after the distractor presentation) and *pre-distractor state* (from fixation point on event until 30 ms after distractor presentation). Also, the *pre-cue state* started after the distractor on event, instead of the fixation point on event.

Regressions of firing rates using a two-dimensional Gaussian were performed separately on cue or distractor target locations.

Nearest neighbor decode algorithm

For the nearest-neighbor decode (Chapter 2), only 129 trials were used from each dataset and were taken from the distractor trials. A full recorded data set included many more than 129 trials, but many datasets were not recorded to completion because of the difficulty in maintaining acceptable isolation quality for two hours, as required for a full data set. Therefore, the use of only 129 trials ensured that each dataset contributed the same number of trials.

The distractor stimulus was a green isosceles triangle or semi-circle, rotated to one of 4 different orientations. For the purposes of this report, we collapsed the different object types and orientations sampled at each target location and consider each object as presented at the location of the center of its base. The subtle effects of object type and orientation will be presented in a future report.

The 129 trials chosen for the decode analysis were the first three trials for which the cue (or distractor) was presented in each of the 43 target locations. A 150 ms time window was used for the spatial decodes in order to track how the spatial decode performances for the cue versus the distractor varied in time.

RESULTS

The neuronal sample presented in this report consists of 420 neurons recorded from two monkeys during the performance of interleaved memory and distractor task trials (Figure 3.1). There were 203 neurons recorded from SEF and 217 neurons recorded from LIP (see Table 3.1 for further details).

	Monkey M LIP	Monkey M SEF	Monkey L LIP	Monkey L SEF	Total LIP	Total SEF	Total
Total Recorded	119	98	98	105	217	203	420
Task Related	48	70	48	50	96	120	216

Table 3.1. *Cell counts for the neuronal database.* Detail of the number of recorded and task related neurons, broken down by monkey and cortical area and combined.

Spatially-tuned responses to a distractor stimulus

The spatial representations differed in qualitatively significant ways between the two areas. Whereas visually-responsive LIP neurons would almost always respond in a spatially specific manner to the cue and the distractor, several SEF neurons would respond to only one or the other. The activity of LIP neurons was correlated with the cue or distractor positions to differing degrees at different times in the trials. To visualize these dynamics, the bottom row of the example neuron panels of Figure 3.2 shows the goodness-of-fit to a two-dimensional Gaussian model of the firing rate on the target (red) or distractor (black) positions. When there is a good fit for only one of the stimuli, only that regression has a high r-squared value. When the r-squared value is high for both models, the neuron is responding to both stimuli in a spatially-tuned manner. The example neurons shown in Figure panels 3.2a and b selectively maintain the cue representation after a short and long "competition," respectively, meaning that the goodness-of-fit for the distractor position model decays soon or long after the presentation of the cue. The example neuron shown in Figure 3.2a exhibits a brief response to the distractor, but the response to the cue is larger in magnitude and longer lasting. It appears that this neuron also loses the cue tuning briefly when the distractor disappears, but overall this movement plan is maintained throughout the memory and saccadic periods. The example neuron shown in Figure 3.2b responds

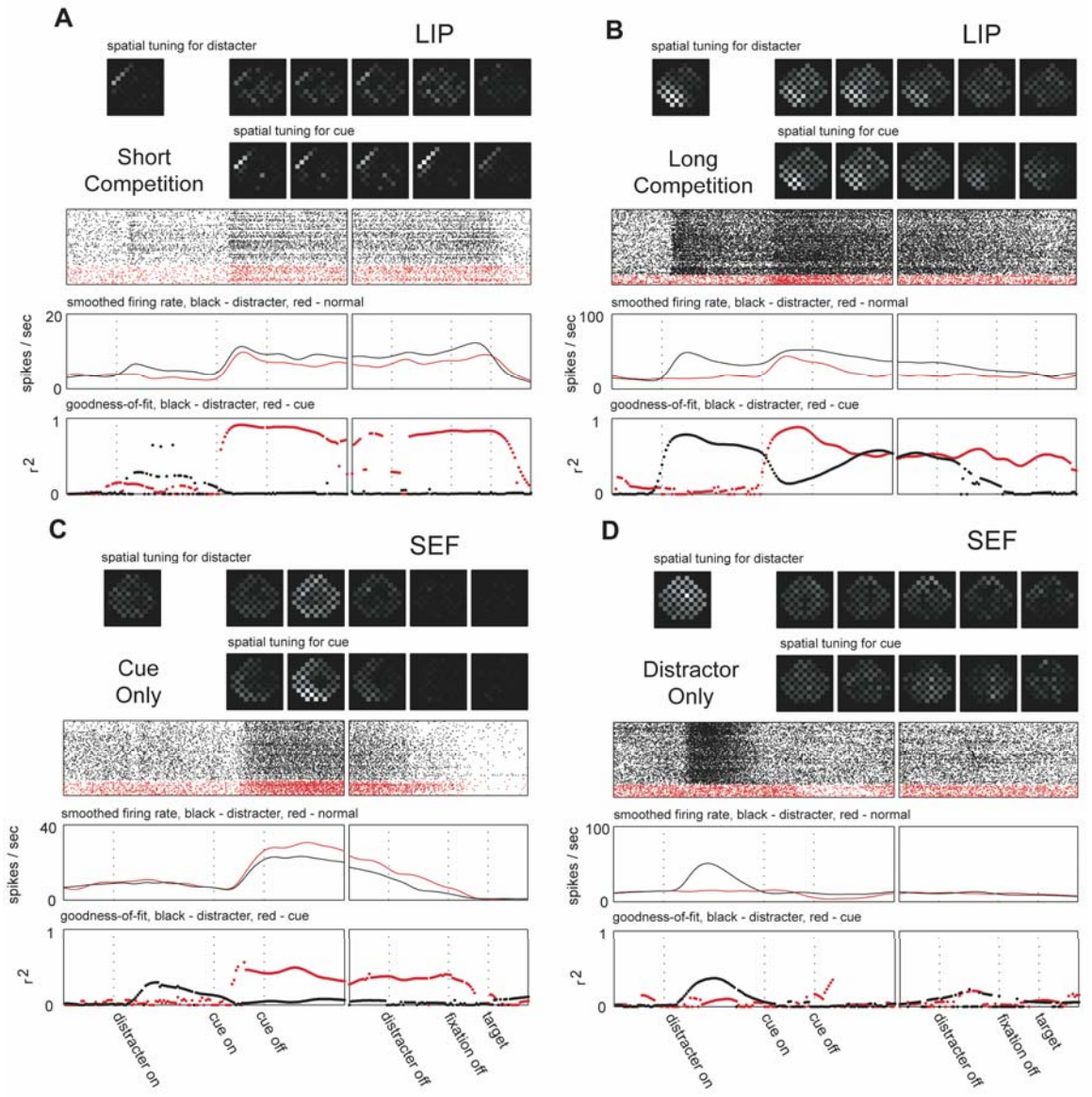

Figure 3.2. *Responses to a distractor.* **(a)** Example LIP neuron with spatial responses to the distractor and cue that selectively maintains the representation of the target after a short interval. *Top row*, firing rate intensity plots showing mean firing rate for all correct trials involving each possible distractor position over 200 ms intervals in the distractor on, cue on, early memory, distractor off, saccadic and post-saccadic intervals, from left to right. *Second row*, firing rate intensity plots showing mean firing rates for all correct trials to each target position. *Third row*, spike trains for each trial, organized chronologically from top to bottom, aligned on the cue on and fixation point off events. Additional event times are labeled at bottom. Trials depicted with black dots are distractor trials, and red dots are memory trials with no distractor. *Fourth row*, smoothed spike firing rates in time. Black and red lines refer to distractor and memory trials, respectively. *Bottom row*, goodness-of-fit (r-squared) values of non-linear regressions of smoothed firing rates on target (red) or distractor (black) position using a two-dimensional Gaussian model. Each point represents a regression using firing rates taken at 10 ms intervals. **(b)** Example LIP neuron with spatial responses to the distractor and cue, but which selectively maintains the representation of the target after a long non-discriminative interval. **(c)** Example SEF neuron that only responds to the cue and ignores the distractor stimulus. **(d)** Example SEF neuron that only responds to the distractor and ignores the cue stimulus.

with similar intensity to the distractor and the cue, and the increased firing activity is sustained in both cases. As can be seen in the intensity plots and also in the progression of r-squared values, the distractor model does not describe the data well after the cue is presented and into the early memory period. This tuning for the distractor, however, then rebounds, and based on the goodness-of-fit values, it appears that the neuron is representing both stimuli locations. After the distractor disappears, the representation of the target again dominates and continues into the post-saccade interval. These two types of neurons strongly affect the dynamics of the spatial decode, as is shown below in Figure 3.5.

Figure panels 3.2c and d show two typical examples of spatially-tuned neurons from SEF. The first example neuron exhibits strong spatial tuning after the presentation of the cue. The salient features of this neuron's firing pattern are the moderate baseline firing rate that is unchanged by the presentation of the distractor, followed by the large sustained response with a moderately long latency after the cue presentation. The cue response is also spatially-tuned, responding more strongly to cue presentations in the bottom left. The second example SEF neuron responds with a transient increase in activity following the presentation of the distractor, and then ignores the presentation of the cue. This response is also spatially-tuned, preferring distractor presentations up and to the right. These are both examples of neurons that respond to visual stimuli in particular locations, but only when the stimuli are members of a preferred category. In the SEF database there were more neurons responding in a spatially-tuned manner to the cue than to the distractor, as is shown below in Figure 3.3.

The numbers of recorded neurons that were spatially-tuned or activated or suppressed in a non-spatial manner at each point in time are shown graphically in Figure 3.3, panels a and b, and broken down into state and movement period classifications in panels c and d. The initial response to the distractor was markedly different in the LIP

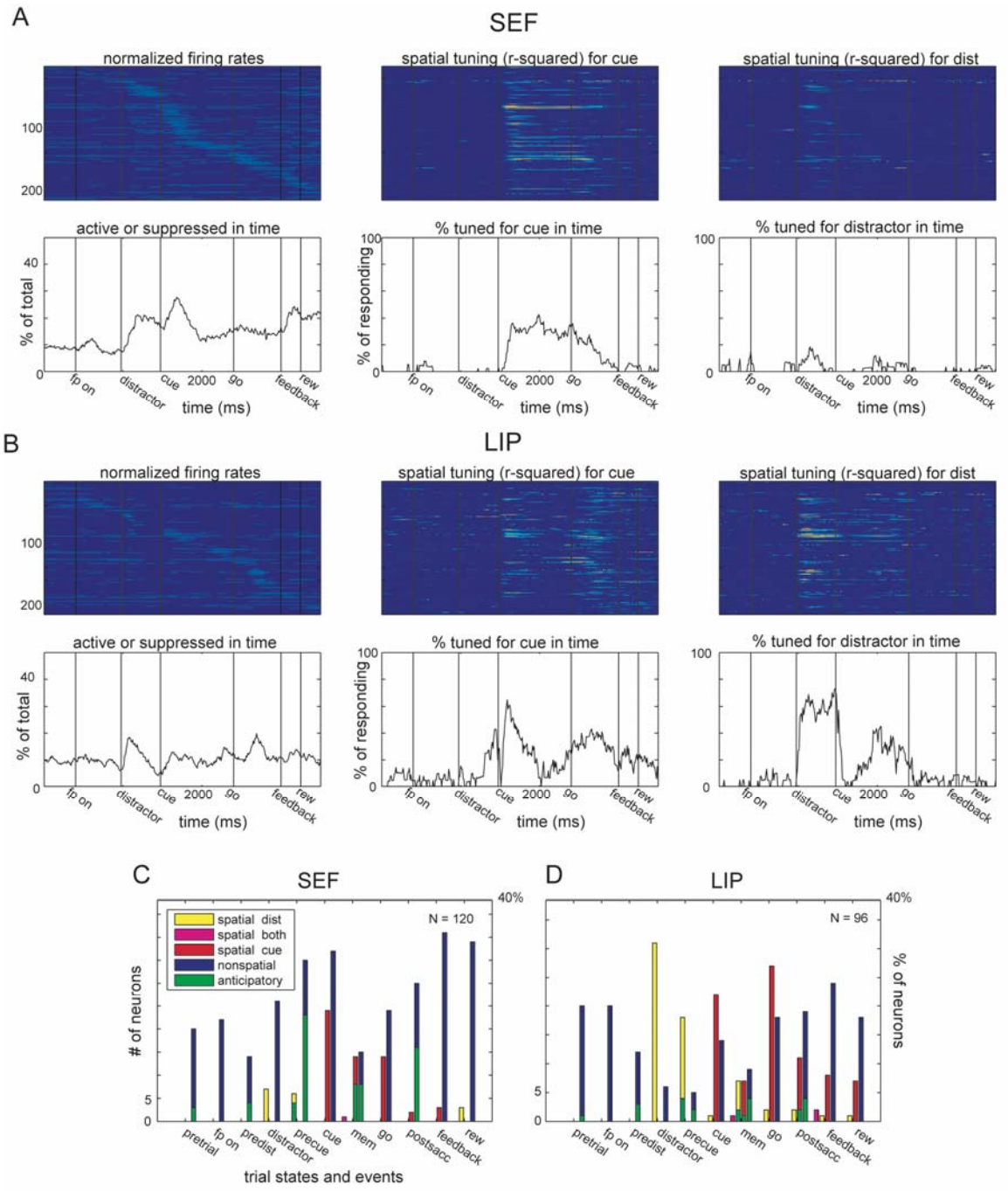

and SEF populations. As can be seen in the right column of panels a and b, around 60% of the task-related LIP neurons encoded the distractor postion, whereas less than 20% of the SEF neurons encoded the distractor position at this point in the trial. In the middle of the memory period, the distinction is more severe, with approximately 40% of the task-related LIP neurons encoding the distractor positon, compared to effectively none in SEF. Comparing the middle and right columns of the LIP results, it is clear that the population as a whole tends to encode the distractor position first, followed by the cue position, then encodes the distractor position again, until the cue position encoding again dominates just prior to the eye movement go signal. In panels c and d, the yellow bars echo the finding that LIP neurons tend to encode the distractor position, while SEF neurons tend to ignore the location of this irrelevant stimulus.

Similar to the findings discussed in Chapter 2, we additionally found that the

Figure 3.3. (previous page) *Continuous measures of activation, suppression, and spatial tuning.* Continuous measures of spatial tuning and firing rate increases and decreases for all recorded neurons in the **(a)** SEF databases, data from both monkeys combined. *Top row, left*, normalized firing rates, each row corresponding to one neuron. The color scale ranges from no firing activity (blue) to 5 times the baseline firing rate (red). Neurons are sorted according to the occurrence of their maximum firing rates. The time progression corresponds to merging the four histograms shown in Figure 3.2. *Top row, middle*, r-squared values (goodness-of-fit) for non-linear regressions of target position (or, *right:* distractor position) on a two-dimensional Gaussian using smoothed firing rates at every 10 ms and the positions of the saccade targets. Each row corresponds to the neuron from the same row in the left column. Color scale ranges from 0 (blue) to 1 (red). *Bottom row, left*, total number of significantly active or suppressed neurons at all points in time, shown as the percentage of the total number of recorded neurons in the sample. *Bottom row, middle*, percentage of neurons that are spatially tuned with respect to the target position (or, *right:* distractor position) of the neurons that are responsive at that point in time (spatially-tuned and/or significantly active or suppressed). **(b)** Continuous measures of spatial tuning and firing rate increases and decreases for all recorded neurons in the LIP databases, data from both monkeys combined. **(c, d)** Activity types exhibited by individual neurons. The labels on the horizontal axis are the five events and six states during which each neuron was tested for spatially-tuned neural activity (red), or non-spatially-tuned activations or suppressions (blue). The states are pretrial, pre-distractor, pre-cue, memory, post-saccade, and reward, which span the intervals before and after the five events: fixation point on, distractor presentation, cue presentation, fixation point off (go), and visual feedback. Neurons were further tested for anticipatory activations or suppressions (green) at the end of the first five states. Both bar graphs are scaled so that the top of the vertical axis corresponds to 40% of the task related neurons in the database. Prevalence of activity types in different event or states in the **(c)** SEF and **(d)** LIP databases, data from both monkeys combined.

neurons in LIP were more likely to be spatially-tuned during the trial, compared to active but non-spatial, as was commonly observed for SEF neurons. Furthermore, the LIP neurons were more likely to be active and to carry spatially-tuned information around the time of the instructed saccade.

Temporally tuned responses to a distractor stimulus

Many SEF neurons encoded states or events in a non-spatial but temporally tuned manner (Chapter 2), which may explain the ability of SEF neurons to selectively represent either the cue or distractor stimuli. The three neurons shown in Figure 3.4 encode for successive states of the task. The first is active from the beginning of the trial until the cue extinguishes, though there is

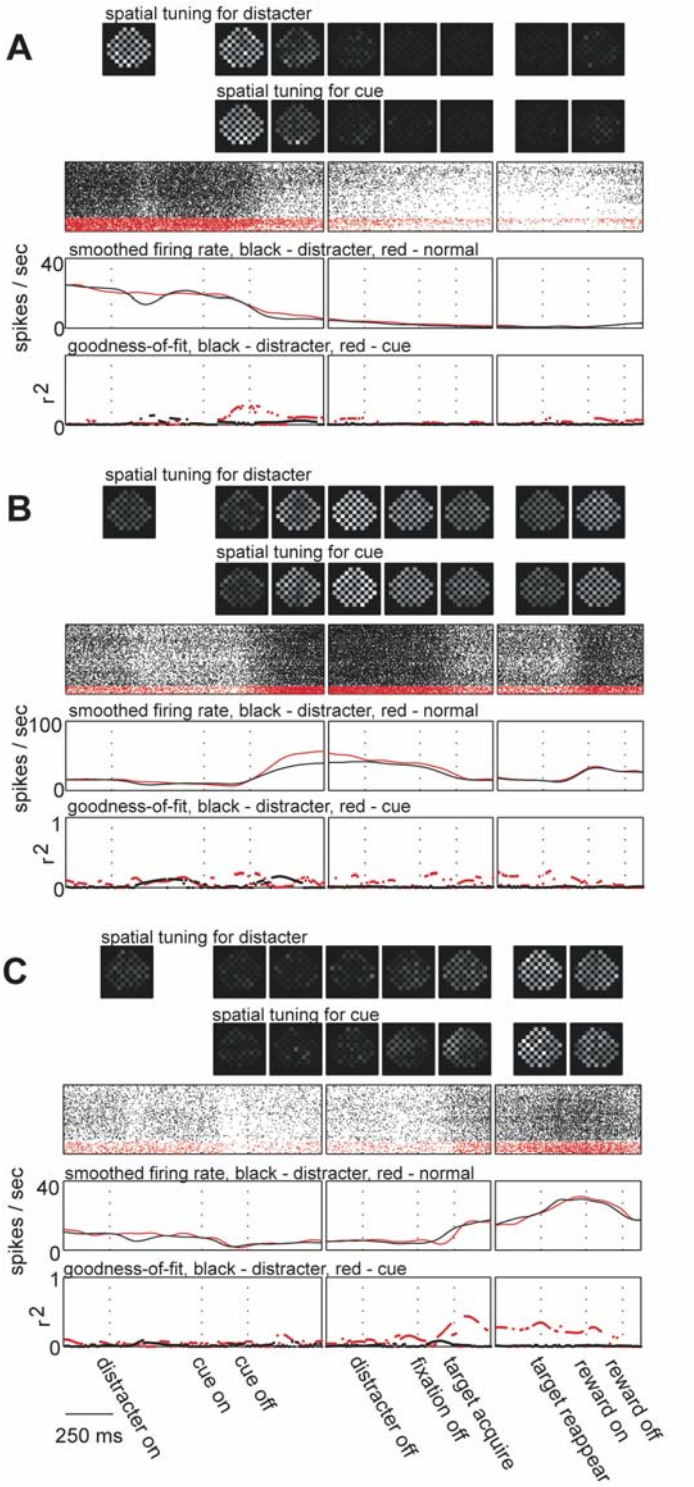

Figure 3.4. *Variety of state encoding neurons in SEF.* Same plotting conventions as in Figure 3.2. **(a)** Example neuron tonically active from the pre-trial interval until the memory period. Cell also exhibits a slight suppression in response to the distractor presentation. **(b)** Example neuron tonically active in the memory and reward intervals. **(c)** Example neuron tonically active in the post-saccadic period, with additionally increased activation after the visual feedback event.

a brief and slight suppression when the distractor is presented. The second neuron encodes the memory period, and the third neuron encodes the interval from the saccade until the end of the trial. The prevalence of each of these types of neurons is shown in Figure 3.3.

Dynamics of cue and distractor representations

The dynamics of the decode performance are shown in Figure 3.5. When taking a large population (N=200) of LIP neurons, the distractor location is decodeable while it is presented, soon after, and again in the middle portion of the memory period while the distractor is still illuminated and until it extinguishes. The cue location is

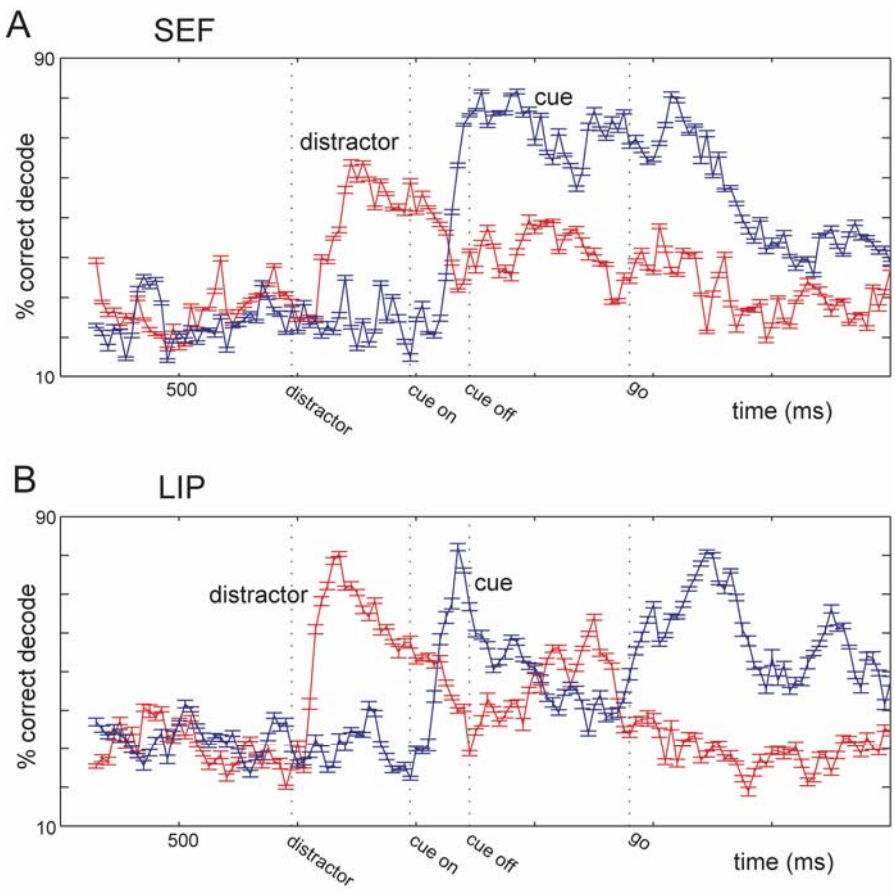

Figure 3.5. *Spatial decode performance for cue and distractor positions*. Mean spatial decode performance (+/- standard error of the mean) for randomly sampled neuron populations of 200 neurons from the phase II SEF **(a)** and LIP **(b)** databases. The distractor on, cue on, cue off, and fixation point off (go) events are labeled on the horiztontal axis, and with vertical dotted lines. Decodes were computed at 25 ms intervals, and include 150 ms of spiking data prior to the point at which the performance is plotted. The decode of the distractor position is shown in red, and the cue position is shown in blue.

decodeable when it is presented and soon afterwards. It is then obfuscated somewhat during the middle portion of the memory period, and then is strongly decodable again just before and during the instructed saccade.

According to the decode results, a large population (N=200) of SEF neurons largely ignored the location of the distractor, and instead represented the location of the cue in the memory and saccade periods.

DISCUSSION

In this report we have shown that SEF neurons frequently encode the position of either the cue or the distractor in a distractor task, but that LIP neurons usually represented both stimuli. The small number of SEF neurons tuned to the location of the distractor led to poor decodeability of the distractor location when it was presented and soon afterwards. During the memory period, in contrast to the results for LIP, the target position remained decodeable and the distractor position was not. It appears that SEF as a whole selectively maintains the representation of the stimuli that are relevant for task completion. SEF therefore might label the significance of a stimulus and help to selectively maintain only those representations that are relevant, holding the representation of the relevant cue in order to bias the target selection process occurring in LIP.

The temporally tuned neurons shown in Figure 3.4 could provide the mechanism whereby other SEF neurons selectively encode the location of the cue or distractor stimuli. For example, the neuron shown in Figure 3.4a, active from the beginning of the trial until the presentation of the cue, could inhibit other neurons during the presentation

of the distractor stimulus, effectively gating the flow of information into a neuron such as the one shown in Figure 3.2c, which selectively encodes the cue location. Temporally tuned SEF responses could also serve a dual purpose: to help LIP neurons favor the relevant cue and suppress the representation of the distractor in the course of the target selection process.

The long competition examples in LIP indicate that LIP participates in the target selection process and considers all salient stimuli. On a single trial, the cue and distractor are only rarely in close proximity and do not therefore compete for the same response field. The existence of activity tuned for the distractor location during the memory period indicates that there is a long competition between the representation of the cue and distractor locations on the population level. The second example LIP neuron (Figure 3.2b) seems to participate in this competition more so than the first (Figure 3.2a). LIP, therefore, actively maintains representations of multiple stimuli until it eventually represents the intended movement alone.

Despite the poor cue position decode performance in the memory period for the entire population of LIP neurons, there were single neurons, such as the one presented in Figure 3.2a, that did maintain a clear representation of the intended eye movement target throughout the memory period. Using our decode method, we found that the LIP neurons that encoded the distractor position obfuscated the cue position information. This result, however, does not preclude the possibility that a well chosen subset of LIP neurons could provide an accurate readout of the intended eye movement throughout the memory period. There are known functional differences between LIP neurons that project to mid-brain eye movement centers, being more likely to encode the final eye movement goal,

and neurons that project to other cortical areas, being more likely to encode the locations of visual stimuli (Ferraina et al., 2002). While our neuron recording procedure did not identify the cortical layer to which each recorded neuron belonged, this functional distinction may account for the differences observed in the example LIP neurons shown in Figure 3.2. The neurons that engage in a long competition may be the same neurons that project to other cortical areas, while the neurons that immediately represent the intended eye movement target may be the ones that project downstream to the superior colliculus to prepare for a specific eye movement. If so, this could be exploited in order to read-out eye movement intentions from parietal cortex in the presence of distractor stimuli, or alternatively to read-out all suddenly appearing potential eye movement targets, if that is of interest.

The data from LIP and SEF offer insights into the mechanisms of target selection of eye movement targets in the distributed cortical oculomotor network. To accomplish the task utilized in our study, the distractor needs to be ignored and the cue remembered. We found that most LIP neurons responded to both the distractor and cue stimuli in a spatially-tuned manner, while SEF neurons responded to one or the other. The dynamics of the spatial representations in the two areas suggest that LIP is involved in target selection, while SEF selectively maintains a representation of relevant stimuli, perhaps so that it can influence the target selection process occurring in LIP and other areas.

REFERENCES

Andersen RA, Essick GK, Siegel RM (1985) Encoding of spatial location by posterior parietal neurons. Science 230:456-458.

Assad JA (2003) Neural coding of behavioral relevance in parietal cortex. Current Opinion in Neurobiology 13:194-197.

Bichot NP, Schall JD (1999) Effects of similarity and history on neural mechanisms of visual selection. Nat Neurosci 2:549-554.

Chelazzi L, Miller EK, Duncan J, Desimone R (1993) A neural basis for visual search in inferior temporal cortex. Nature 363:345-347.

Constantinidis C, Steinmetz MA (2005) Posterior Parietal Cortex Automatically Encodes the Location of Salient Stimuli. J Neurosci 25:233-238.

Desimone R, Duncan J (1995) Neural Mechanisms of Selective Visual Attention. Annual Review of Neuroscience 18:193-222.

Ferraina S, Pare M, Wurtz RH (2002) Comparison of Cortico-Cortical and Cortico-Collicular Signals for the Generation of Saccadic Eye Movements. J Neurophysiol 87:845-858.

Friedman-Hill SR, Robertson LC, Desimone R, Ungerleider LG (2003) Posterior parietal cortex and the filtering of distractors. PNAS 100:4263-4268.

Gottlieb J (2002) Parietal mechanisms of target representation. Current Opinion in Neurobiology 12:134-140.

Gottlieb J, Kusunoki M, Goldberg ME (2005) Simultaneous Representation of Saccade Targets and Visual Onsets in Monkey Lateral Intraparietal Area. Cereb Cortex 15:1198-1206.

Hasegawa RP, Peterson BW, Goldberg ME (2004) Prefrontal Neurons Coding Suppression of Specific Saccades. Neuron 43:415-425.

Hikosaka O, Sakamoto M, Usui S (1989) Functional properties of monkey caudate neurons. III. Activities related to expectation of target and reward. J Neurophysiol 61:814-832.

Ipata AE, Gee AL, Goldberg ME, Bisley JW (2006a) Activity in the Lateral Intraparietal Area Predicts the Goal and Latency of Saccades in a Free-Viewing Visual Search Task. J Neurosci 26:3656-3661.

Ipata AE, Gee AL, Gottlieb J, Bisley JW, Goldberg ME (2006b) LIP responses to a popout stimulus are reduced if it is overtly ignored. Nat Neurosci 9:1071-1076.

Jonides JJ, Yantis SS (1988) Uniqueness of abrupt visual onset in capturing attention. Perception & psychophysics 43:346-354.

Lauwereyns J, Sakagami M, Tsutsui K-I, Kobayashi S, Koizumi M, Hikosaka O (2001) Responses to Task-Irrelevant Visual Features by Primate Prefrontal Neurons. J Neurophysiol 86:2001-2010.

Lu X, Matsuzawa M, Hikosaka O (2002) A Neural Correlate of Oculomotor Sequences in Supplementary Eye Field. Neuron 34:317-325.

Powell KD, Goldberg ME (2000) Response of Neurons in the Lateral Intraparietal Area to a Distractor Flashed During the Delay Period of a Memory-Guided Saccade. J Neurophysiol 84:301-310.

Rainer G, Asaad WF, Miller EK (1998) Selective representation of relevant information by neurons in the primate prefrontal cortex. Nature 393:577-579.

Sakagami M, Tsutsui K-i, Lauwereyns J, Koizumi M, Kobayashi S, Hikosaka O (2001) A Code for Behavioral Inhibition on the Basis of Color, But Not Motion, in Ventrolateral Prefrontal Cortex of Macaque Monkey. J Neurosci 21:4801-4808.

Schall JD, Hanes DP, Thompson KG, King DJ (1995) Saccade target selection in frontal eye field of macaque. I. Visual and premovement activation. J Neurosci 15:6905-6918.

Schlag-Rey M, Amador N, Sanchez H, Schlag J (1997) Antisaccade performance predicted by neuronal activity in the supplementary eye field. Nature 390:398-401.

Sereno AB, Amador SC (2006) Attention and Memory-Related Responses of Neurons in the Lateral Intraparietal Area During Spatial and Shape-Delayed Match-to-Sample Tasks. J Neurophysiol 95:1078-1098.

Snyder LH, Batista AP, Andersen RA (1997) Coding of intention in the posterior parietal cortex. Nature 386:167-170.

Wardak C, Olivier E, Duhamel J-R (2002) Saccadic Target Selection Deficits after Lateral Intraparietal Area Inactivation in Monkeys. J Neurosci 22:9877-9884.

CHAPTER IV

INDIVIDUAL LIP NEURONS REMAP DIRECTIONAL TUNING PREFERENCES IN DIFFERENT TASK CONTEXTS

ABSTRACT

To investigate the spatial tuning of parietal neurons of macaque monkeys in more natural circumstances, we compared their activity in two eye movement tasks. In both tasks the spatial locations of the eye movement targets were the same. The movements, however, were instructed differently. In one case, the monkeys made saccades towards remembered locations of briefly flashed dots of light. In the other case, monkeys targeted vertices of a triangular object that was shown in the periphery. We found that parietal neurons encoded the spatial location of saccade targets in both tasks, but the tuning of individual cells changed substantially between the tasks. The cells often either lost their tuning or changed their preferred direction in different contexts of the task. On the population level it was possible to decode the direction of the upcoming saccade using the tuning within the task itself, but not using the tuning of the cells from the complement task. In addition to spatial tuning, parietal cells also encoded the orientation of the object on the screen and the object-based location of the target. Our results suggest that the tuning of the cells in parietal cortex is task dependent and can change dramatically under different cognitive demands.

INTRODUCTION

Visual information entering the retina is thought to be processed in two functionally distinct and anatomically segregated cortical streams. The ventral stream facilitates perception, or is concerned with identifying 'what' is in the visual scene, while the dorsal stream facilitates action planning, or is concerned with 'where' and 'how' to interact with the environment (Goodale and Milner, 1992). Neurophysiological evidence largely supports this view, though there are studies demonstrating that object identity-related (what) signals are present in the lateral intraparietal area, LIP (Sereno and Maunsell, 1998, Amador and Sereno, 2006) in the dorsal stream. According to the what/where framework, LIP representations would only be concerned with 'where' to direct the eyes, and not be influenced by "what" is to be found at that location. The presence of object-feature information in the dorsal stream thus demands modifications to the what/where framework.

A different line of evidence for the presence of object-based representations in the dorsal pathway comes from the study of hemi-field neglect patients. Neglect is a spatial representation disorder following parietal damage, in which patients are unaware of portions of their visual field and do not generate eye movements to inspect the neglected area. Case studies suggest that neglect can affect judgment in multiple reference frames, including an object-based representation. In a well-known case study, a neglect patient was given the task of copying a picture of flowers (Halligan & Marshall, 1993), first presented with a picture of one flower with two stems branching out of a flowerpot. The subject reproduced only the right side of the right branch, neglecting the entire left

branch. In the second experiment only the top half of the picture was presented to the subject and the subject reproduced the right side of both branches. This can be interpreted as a deficit in the ability to reproduce a portion of the image in an object-based reference frame. When information was provided to the patient that would allow the picture to be considered a single object, there was a global deficit to the reproduction, but when the subject was presented with two objects, the deficit occured on each object individually. Because of this and similar deficits of hemi-field neglect patients, parietal cortex is thought to support object-based representations of space, though the mechanism remains unknown.

The study of eye movements, and in particular the way they are encoded when generated with respect to objects, has been used to investigate the neural mechanism of an object-based representation in LIP (Sereno and Maunsell, 1998) as well as the supplementary eye fields, SEF (Olson and Gettner, 1995). These data suggest at least two possible mechanisms of object-based eye movement control, which should resemble the object-based representations of space, in these areas known to participate in oculomotor behavior. While the Olson and Gettner (1995) study of SEF concluded that information about target position is encoded in an explicit object-based reference frame (Olson and Gettner, 1995), theoretical work has shown that the same results could be generated by neurons encoding eye movements in an eye-centered reference frame, but with a gain modulation by object-centered variables (Deneve and Pouget, 2003). Deneve and Pouget argue that a gain mechanism may appear as a purely object-based encoding if the space of possible eye movements is insufficiently sampled, as in the case of Olson and Gettner (1995). A preliminary report, with a more complete sampling of space, suggests that the

gain-field model can account for some but not all object-centered activity in the SEF (Moorman & Olson, 2003). The gain-modulated alternative is more computationally efficient, since an eye-centered encoding of eye movements can directly code the motor error for moving the eye, while an eye movement encoded in an object-based reference frame would need to take into account the orientation and retinal position of the object and the location of the target on the object in order to generate the proper eye movement vector. Multiple intentional maps in parietal cortex are encoded in an eye-centered reference frame that is gain-modulated by other variables (Andersen and Buneo, 2002). The gain modulation of these cells by eye, head, body, and limb position signals enables the population of parietal neurons to be read out in any of a variety of spatial representations by down-stream motor structures (Andersen et al., 1993).

A new object-based saccade paradigm has been developed in our lab to resolve issues of object-based encoding in area LIP. Since an object-based encoding would be apparent during object rotation, translation, and scaling, in our new paradigm we investigate both rotation and translation. We recorded neural activity while monkeys performed eye movements to instructed sides of a displaced isosceles triangle and compared this activity with that found while the monkeys performed the same eye movements in a standard memory-guided saccade task. In addition, noting that a sufficient sampling of the visual field is essential to appreciate the possible effects of gain modulation in the neural signals (Olson & Gettner, 1995; Deneve & Pouget, 2003), the new paradigm uses a dense mapping of 43 target points spaced at regular intervals out to 17 degrees of visual angle in every direction. The new task is thus designed to investigate possible neural selectivity for the conventionally-appreciated retinal representations as

well as three object-based variables: object orientation, retinotopic location of the object, and object-based target position.

METHODS

The experiments were conducted with two male macaque monkeys (*Macaca mulatta)*, monkey R and monkey S, the same two animals that were used in our previous study (Campos et al. 2005 – Chapter 1). Each was chronically fitted with a stainless steel head post for head immobilization and a recording chamber over a craniotomy for electrode insertions. The stereotaxic coordinates for chamber placement were posterior 6mm lateral 12mm. The chamber on monkey R was over the right hemisphere; in monkey S it was over the left hemisphere. All procedures were approved by the Caltech Institutional Animal Care and Use Committee.

Behavioral Tasks

The two behavioral tasks in this study are shown in Figure 4.1. The tasks were identical to the tasks used in our previous study (Campos et al. 2005 – Chapter 1). Monkeys were seated in a dimly lit room, 42 cm from a tangent screen. Stimuli were rear-projected with 800x600 pixels resolution and a refresh rate of 72 Hz using a custom-built software display client utilizing OpenGL API. Task logic was controlled by National Instruments real-time LabView software. Two eye-movement tasks were used: a memory-guided saccade task (MEM-SACC) and an object-based saccade task (OBJ-SACC). In both tasks, the monkey was instructed to perform a saccade from a central

fixation point to 1 of 43 targets placed at regular intervals to cover the entire visual field out to 17° of visual angle in every direction from central fixation. In the MEM-SACC task (Figure 4.1*A*), monkeys were required to maintain central fixation while a peripheral target was briefly flashed, and then wait until the central fixation point was extinguished, which was the signal to saccade to the remembered location. After successfully holding fixation at the target location, the target re-appeared to provide visual feedback. The monkey then had to maintain fixation on the visible target for an additional interval of 250 ms before receiving a liquid reward. The screen locations of the 43 targets are shown in Figure 4.1B.

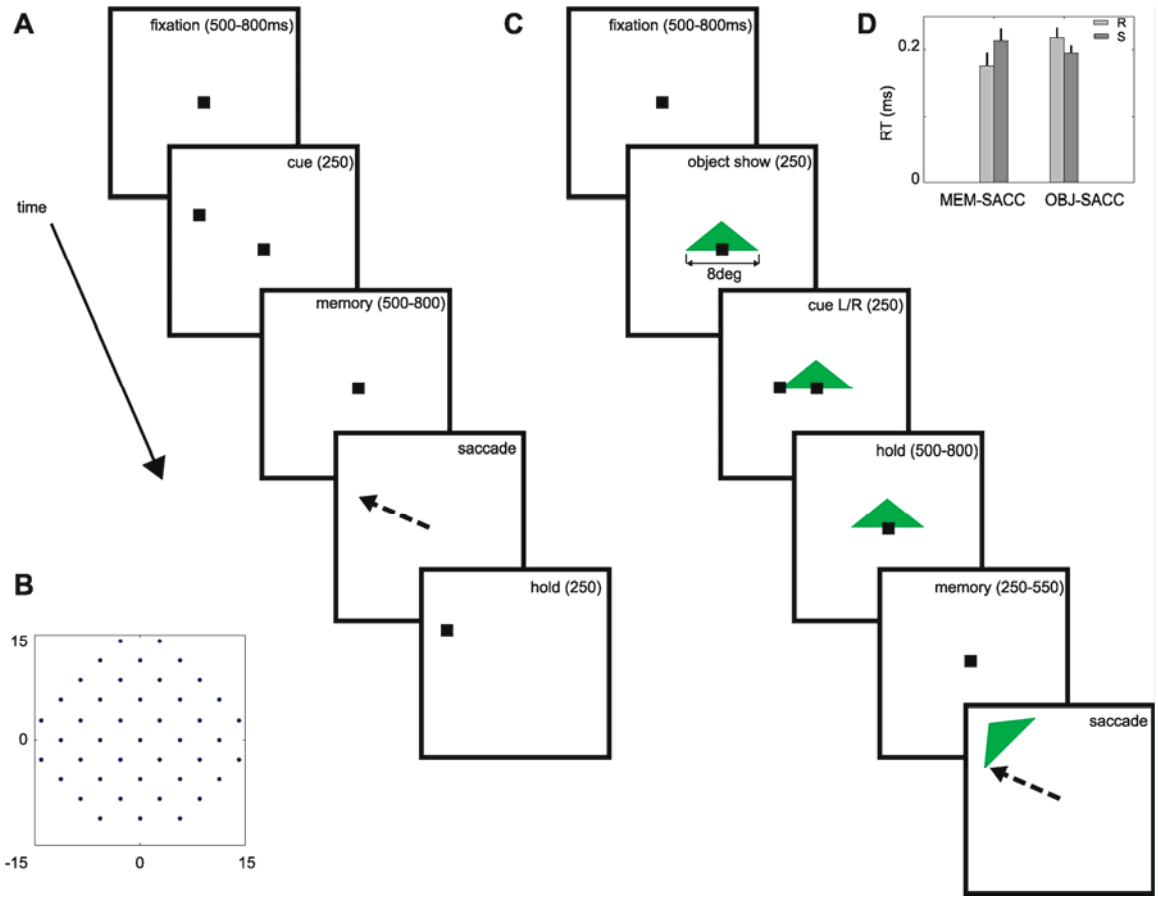

Figure 4.1. *Behavioral tasks used in the experiment.* **A** Timeline for the MEM-SACC task. **B** Saccade targets used in both tasks. Scale on the axes is in degrees of visual angle. **C** Timeline for the OBJ-SACC task. **D** Mean reaction times of the two monkeys in each task. Error bars are standard deviations. The differences are significant in all comparisons across monkeys and tasks (two-tailed t-test $p<0.05$).

The same set of targets was used in the OBJ-SACC task, the timeline of which is shown in Figure 4.1C. This task started with a fixation period identical to the one in the MEM-SACC task. Then, after 500-800 ms of fixation, an isosceles green triangle was displayed foveaIy behind the fixation point, leaving the fixation point visible. The triangle was displayed always in the same position, with the base aligned horizontally, centered on the fixation point and pointing upwards. After 250 ms, one of the two vertices at the base ends was cued by a 250 ms flash of a white dot. This cue labeled the side of the triangle that was later to become the target of a saccade. The object stayed visible for another 500-800 ms with no cues displayed. Then the object was extinguished, and a memory period of 250-550 ms followed in which the monkey continued to maintain the fixation of the central dot. Then, simultaneously, the central fixation point was extinguished, and the triangle was displayed in a peripheral location. This was the signal to saccade to the previously-cued side of the triangle. After fixating the side of the triangle for additional 250ms, monkeys were rewarded by a drop of liquid. The final positions and orientations of the triangle were selected so that the target vertices always aligned with one of the 43 targets, as shown in Figure 4.1B. This was achieved by placing the triangle on one of the points of the grid and rotating it by plus or minus 45 degrees. Throughout the experiment only these two orientations were used. The size of the triangle was 8 degrees, double the spacing between the points of the grid along the alignment lines. Thus, when the triangle was placed with its base center aligned with one of the grid points and rotated, the two vertices on both symmetrical sides of the object lined up with two targets on the grid. The two tasks were run in blocks, starting with the MEM-SACC

task and followed by the OBJ-SACC task. We collected three repetitions per target and condition, which resulted in 129 MEM-SACC trials and 516 OBJ-SACC trials per cell, although for some cells the data set was not complete. Cells with too few recorded data were excluded from the analysis.

Recording procedure

Neurons were accessed on vertical penetrations with glass-coated platinum-iridium electrodes (Fred Haer). The electrodes were advanced with a Fred Haer or Narashige microdrive system through a blunt stainless steel guide tube pressed against the dura. Neurons were generally found 1–7 mm beneath the exterior of the dura. Waveforms were amplified and isolated on-line with a commercial hardware and software package (Plexon). Cell activity was monitored with custom built on-line data visualization software written in Matlab.

Data Analysis

To establish the spatial tuning of neurons, we used three models. First we fitted the data, using nonlinear regression, with a two-dimensional Gaussian, given by the equation:

$$fr(x,y) = a_0 * \exp\left(-\frac{(x-x_0)^2 + (y-y_0)^2}{\sigma^2}\right) + a_1 . \qquad (1)$$

Here the firing rate *fr* of a neuron is regressed against the independent spatial variables *x*,*y*, with parameter a_0 signifying the amplitude, a_1 the background firing rate, x_0, y_0 the

coordinates of the center of the receptive field, and σ corresponding to the width of the receptive field.

We also calculated tuning of the cells using two circular measures, one being the circular VonMises distribution and the other preferred angle (Bartschelet 1981). For the purpose of these calculations, each target was characterized by its polar angle measured with respect to the line starting at the fixation point and extending horizontally to the right. Thus, the two targets directly to the right of the fixation point had angles of 0 degrees, and the two targets directly to the left had angles of 180 degrees. The VonMises distribution is a unimodal circular distribution equivalent to the normal distribution in linear space. One of the parameters of this model is the mean angle of the distribution. We used non-linear regression to fit the VonMises distribution to the data and extracted the mean angle of the fit and considered it to be the preferred angle of the cell. The other way of calculating the preferred angle was to calculate the angle of the mean vector. The mean vector was calculated as a vectorial sum of weighted unity vectors associated with each target's angle. The weights of the unity vectors were set as the mean firing rate of the corresponding neuron in a given task and condition. Vectorial sum of the weighted unity vectors yielded the mean vector, and the angle of this vector was the preferred angle of the cell.

In order to decode the spatial information carried by the entire population of neurons, we used the population vector analysis (Georgopoulos et al. 1989). The population vector was calculated as the vector sum of base vectors, one base vector per cell, each vector weighted by the activity of the cell in the given task. Each cell's base

vector is a unity vector in 2D, pointing in the direction of that cell's preferred direction. The population vector is given by the formula:

$$\mathbf{P} = \sum_i y_i \mathbf{b}_i \,. \qquad (2)$$

Here **P** is the population vector, y_i is the weighting factor based on the firing rate of the *i*-th cell in the given time interval, and $\mathbf{b}_i$ is the base vector of the *i*-th cell. The base vectors were unity vectors with their angles corresponding to the preferred angle of each cell. The sum in this equation is over all tuned cells. The weighting factor was calculated as $y_i = \dfrac{fr_i^t - \langle fr_i \rangle}{std(fr_i)}$, where fr_i^t is the mean firing rate in the given interval, $\langle fr_i \rangle$ is the overall mean firing rate of the neuron in the recording session, and $std(fr_i)$ is the overall standard deviation of the firing rate. We recalculated the population vectors using several weighting factors, including raw firing rate and firing rate normalized by subtracting the background firing rate. The results of these calculations were very similar to the results reported in the paper.

To assess how well the individual neurons represented the information about the object orientation and object-centered location of the saccade target, we calculated receiver operating characteristics (ROC) for each neuron. This measure was originally developed in signal detection theory to reflect the probability that an ideal observer could accurately report the value of a binary variable under observation, and has been successfully applied to neurophysiology data (Britten et al. 1992). The probability of correct recognition is a single number between 0.5 and 1, 0.5 corresponding to a chance performance and 1 corresponding to the absolute certainty. This probability corresponds to the area below the ROC curve, which is constructed by moving the classification

threshold across the two distributions, counting the number of hits and false alarms, and plotting them against each other in a graph. We calculated the ROC characteristics for discrimination between the left and right side of the triangle and for discrimination of the two object orientations used in the task, i.e., +45 and -45 degrees. For the purpose of tracking the discriminability throughout the trial, we calculated the mean firing rate of the response to each of the two possible values of the variable being discriminated in 100ms time windows. The two sets of responses formed the two distributions that were then used to calculate the ROC curve. We then calculated the area under the curve for each time window and plotted it. This calculation included all neurons that had significantly different mean firing rates (two-tailed t-test $p<0.05$) in the memory period for the object left/right discrimination and in the 300ms following the go signal in the object orientation discrimination.

RESULTS

We recorded a total of 87 cells in area LIP in two monkeys, 40 in monkey R and 47 in monkey S. The most consistent feature in the cells' responses was a change in the firing characteristics between the two tasks. An example of a recorded cell is shown in Figure 4.2. The activity of the cell in the MEM-SACC task is shown in Figure 4.2A, and the activity of the same cell in the OBJ-SACC task is shown in Figure 4.2B. First we describe the activity in the MEM-SACC task. The two panels on the left in Figure 4.2A show the spike rasters (on top in red) and smoothed mean firing rate (solid black line). The plot shows the temporal profile of the cell's response that rises in response to the cue

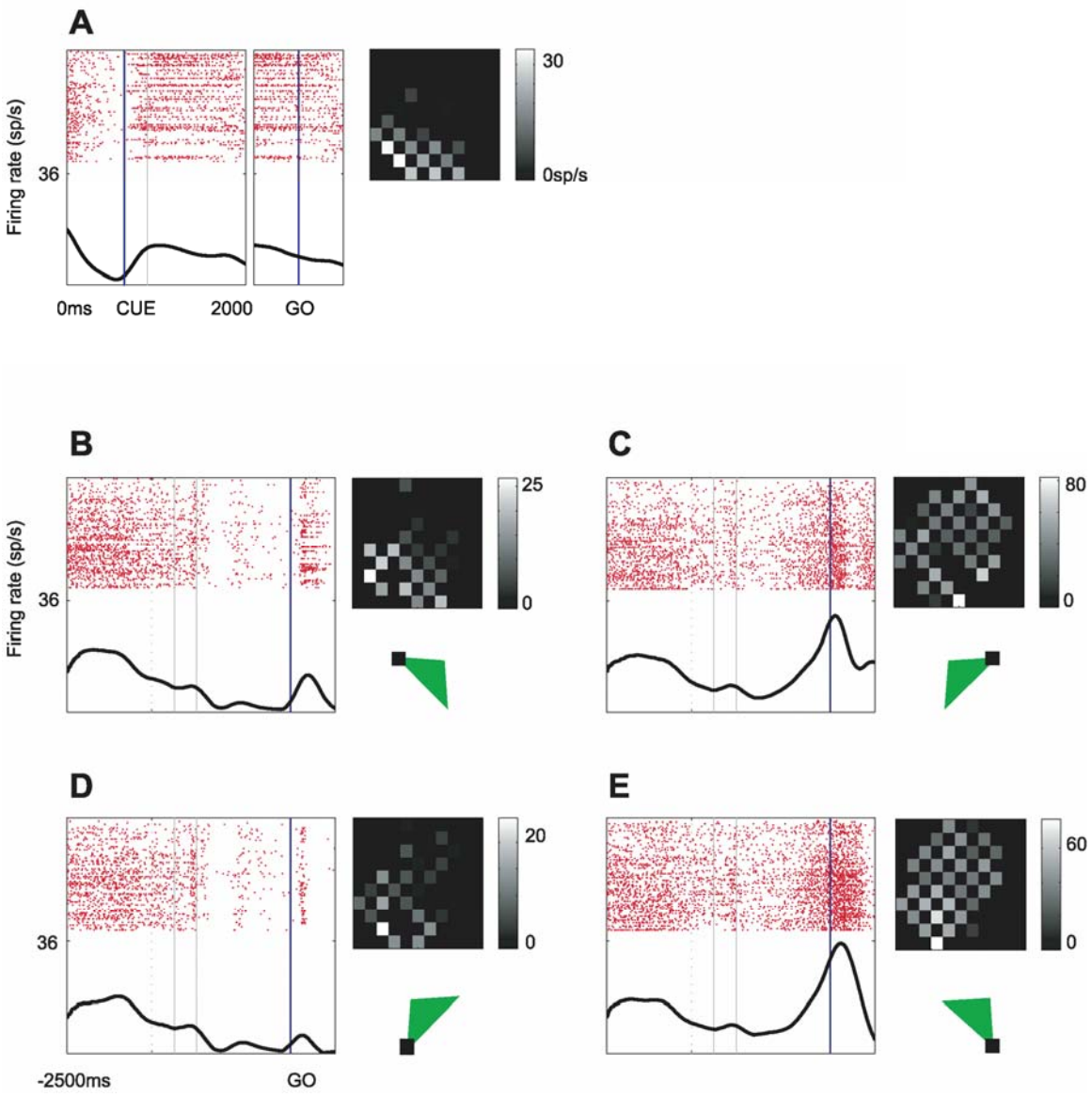

Figure 4.2. *Sample cell recorded form monkey R.* Each subfigure contains two panels: spike rosters (left) and spatial distribution of the mean firing rates (right). The spike rosters show spikes from individual trials as red dots, one line of dots per trial (top). Bellow the spike rosters there is a curve representing smoothed mean firing rate. The right panel shows spatial distribution of mean firing rates. The mean firing rate is taken from 150ms following the GO signal in both tasks. Means are calculated for each target and plotted in the corresponding spatial location. **A.** Data from the MEM-SACC task. Spike rosters are split into two plots: plot on the left is aligned to the acquisition of the fixation point (0ms). Plot on the right is aligned to the GO signal. **B,C,D,E.** Data from OBJ-SACC task split into four contexts. Each context is indicated by a triangle icon showing the object orientation and object-centered cue location for the respective context. Spike rosters are aligned to the GO signal.

presentation and maintains an elevated level of activity during the memory and saccadic periods. The right panel shows the spatial distribution of the mean firing rate calculated

in the saccadic interval. One can see that the cell exhibits a spatially-specific saccadic response, with the response field of the cell in the lower left corner of the visual field. The cue and memory responses of this cell (not shown) had similar spatial tuning. This response is quite typical for an LIP cell in this type of task.

The activity of this cell in OBJ-SACC task is shown in the panels in Figure 4.2B. We separated the spike rasters and tuning plots into four panels according to the task context. By task context we mean the unique combination of object-based cue location, i.e., cue left vs. cue right, and final object orientation, i.e., plus or minus 45 deg. Several features of the cell's response stand out immediately. First, the cell lost its spatial tuning in the saccadic period in one out of four contexts. Although the monkey had to make saccades towards the same set of targets as in the previous task, for the cue right and object orientation +45deg context (Figure 2.2C), the cell does not respond in the same spatially-specific way as it did in the MEM-SACC task. Second, the cell responds differentially to the location of the cue on the object in the memory and saccade periods, with clear preference for the right cue location. Note that the retinal location of the preferred cue position for the initial object position is in the hemifield opposite to the one where the response field of the cell in the MEM-SACC task is located. Finally, the cell also shows modulation of its activity with the final orientation of the object, preferring the -45 degree orientation. These features were present to various degrees in the population of the recorded cells in the two tasks, and in the following paragraphs we will provide a quantitative analysis of each of these phenomena respectively.

The most striking change in the response properties of the cells between the two tasks was the change of the spatial tuning. For the example cell in Figure 4.2, the spatial

tuning is lost in one out of four contexts in the OBJ-SACC task. This was not an unusual phenomenon in the population of recorded cells. To characterize the tuning properties of the cells quantitatively, we used multiple models (see Methods). Since all of them yielded similar results, we will report on the results of only one of the models, i.e., tuning of the cell will be characterized by the preferred angle calculated as the angle of the mean vector. We chose this measure because it allowed us to capture even a very weak spatial preference in the cells' activity, and thus we were sure that we were not excluding any cells that carried spatial information.

To assess the changes in tuning we first calculated the difference between preferred angles in the MEM-SACC task and OBJ-SACC task for the cells tuned in both. Figure 4.3 shows circular histograms of the angle differences of those cells. For the OBJ-SACC task we chose the preferred angle calculated in the 300ms interval aligned at the "go" signal, which is the same interval that was used to plot the spatial distribution of the mean firing rates in Figure 4.2. We subtracted this angle from the preferred angle calculated in two periods in the MEM-SACC task: cue period (Figure 4.3A) and saccadic period (Figure 4.3B). If the cells were similarly tuned in the two tasks, the histograms should be grouped around zero. This is obviously not the case. For comparison, in Figure 4.3C we show a histogram of the angle differences between the preferred angles in the cue and saccadic interval in the MEM-SACC task for the cells tuned in both intervals. Here one can clearly see how the cells maintain the spatial tuning. For Figures 4.3A and B the angle differences were calculated for both monkeys and with all OBJ-SACC context data pooled together. As Figure 4.2 shows, there are cells that maintained tuning in some of the contexts, while losing it in others. Thus we calculated the same kind of

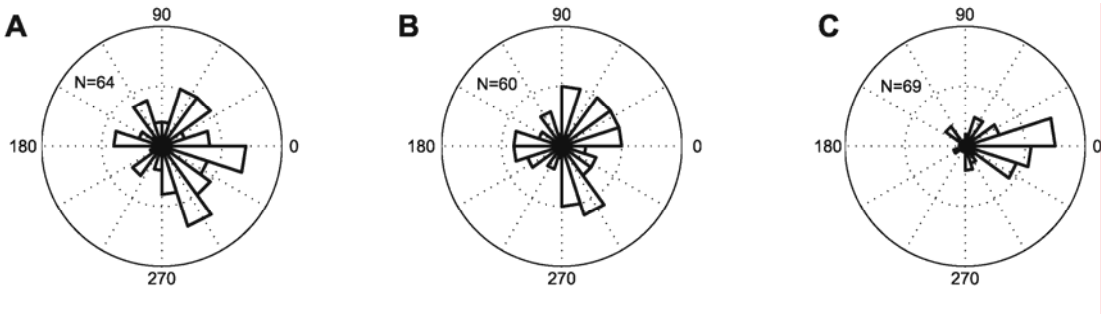

Figure 4.3. *Cells' spatial tuning compared across the two tasks.* Plotted are the circular histograms of the differences between preferred angles in the MEM-SACC task and OBJ-SACC task. **A.** Differences between CUE interval tuning in MEM-SACC and GO interval tuning in OBJ-SACC. **B.** Differences between GO interval tuning in MEM-SACC and GO interval tuning in OBJ-SACC. **C.** For reference: differences between CUE and GO interval tuning in the MEM-SACC task.

histograms for data separated by contexts as well as split by the two animals. The results were the same as in Figures 4.3A and B, i.e., for neither animal and in no context did we find good correspondence between directional preferences in the two tasks.

This analysis shows that the spatial tuning of the cells changes between the two tasks on a cell-by-cell basis. To assess the degree of this change in the entire population of LIP cells, we calculated population vectors to decode the direction of saccades (see Methods). The population vector is a quantity that uses the firing rates of a directionally-tuned pool of neurons to predict the direction of the upcoming saccade. To establish the benchmark for the accuracy of the decode, we first decoded the upcoming saccade in the MEM-SACC task using a leave-one-out method. Figures 4.4 A and B show the distribution of decoding errors in this task for the two monkeys separately. In both cases the errors were clustered around zero (V test $p<0.001$), signifying good performance of the decoding algorithm. We then used the basis vectors calculated in the MEM-SACC task to decode saccade direction in the OBJ-SACC task. The decode errors are plotted in Figures 4.4 C and D. Here the errors are distributed uniformly around the circle (Rayleigh test $p>0.05$), suggesting poor decoding performance. This result confirmed that even at

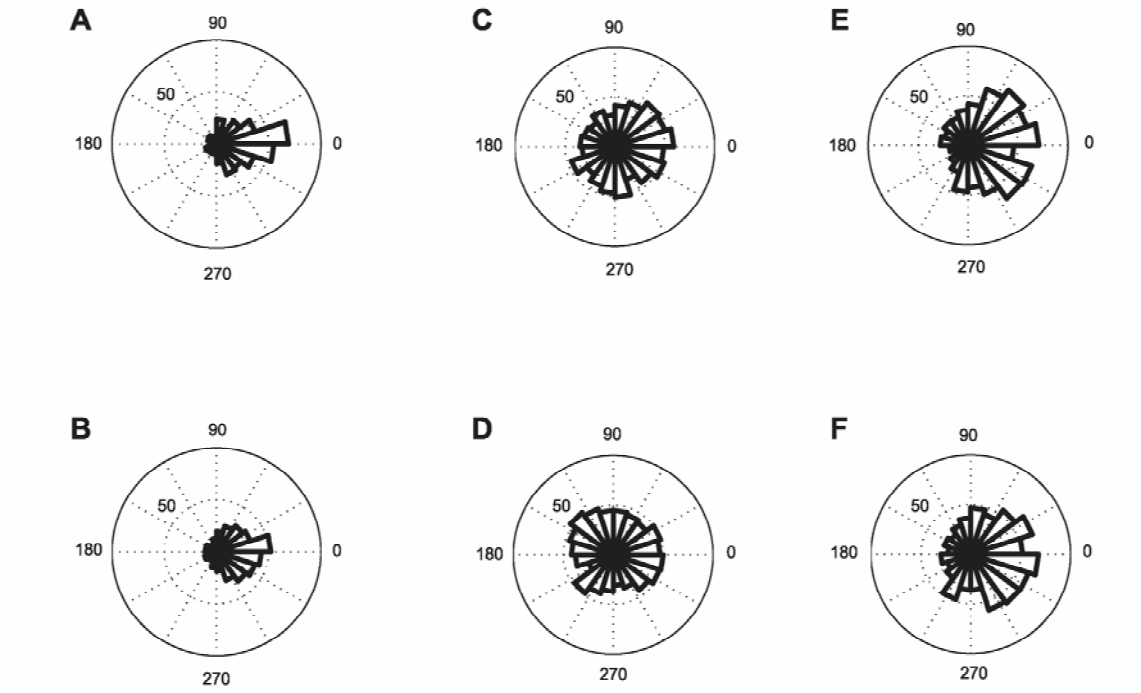

Figure 4.4. *Population vector decode of the direction of saccades.* Plotted are circular histograms of the decoding errors, i.e., the differences between the predicted and actual direction of a saccade. The results are split into two animals, monkey R results are in the top row (**A,C,E**). Monkey S results are in the bottom row (**B,D,F**). **A,B.** Decoding errors in the MEM-SACC task using basis vectors from the same task. **C,D.** Decoding errors in the OBJ-SACC task using basis vectors from the MEM-SACC task. **E,F.** Decoding errors in the OBJ-SACC task using basis vectors from the same task.

the population level there is little correspondence between the tuning of the cells in the two tasks. We noticed, however, that the cells did not lose the spatial tuning in the OBJ-SACC task completely. To establish how much spatial information there is in this task, in the LIP population we again decoded the direction of upcoming saccade, but this time we calculated the basis vectors using a leave-one-out algorithm within the OBJ-SACC task itself. In other words, to decode the saccade direction we used the tuning calculated from the rest of the trials in this task. The results are shown in Figure 4.4 E and F, and one can see a clear improvement in the decode performance as the errors are clustered around zero (V test $p<0.001$). This suggests that LIP cells in both tasks encode the direction of the upcoming saccade, albeit using a different spatial coding.

Besides the spatial information about the planned saccade, the population of LIP cells also represented the information about the object-centered location of the cue. We first used a two-tailed t-test on the mean firing rates in the cue and memory intervals in the OBJ-SACC task to determine how many cells discriminated the object-based cue location. We found that 24 (63%) cells in monkey R and 8 (18%) cells in monkey S had significantly different activity ($p<0.05$) for cue left vs. cue right locations. We then used ROC analysis (see Methods) to track the discrimination during the course of a trial in those cells. Figure 4.5 shows the values of the area under the ROC curve in 100

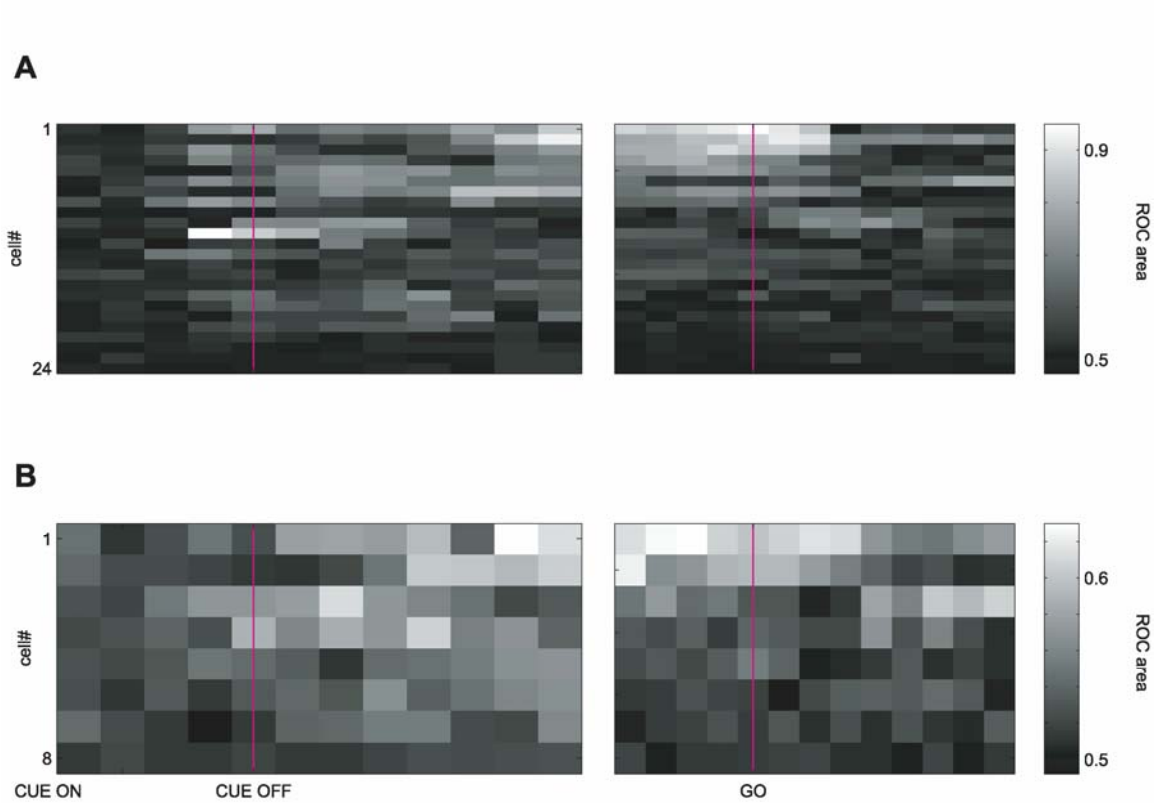

Figure 4.5. *ROC analysis of object-centered location of the cue discriminability* (cue left vs. cue right). For each cell, plotted are areas under ROC curves calculated in 100ms time windows moving in 50ms increments. Left part of both plots shows the data aligned on the CUE on event. Right part shows the data aligned on the GO signal. Included are cells that showed significant differences in the mean firing rates between cue left/right in the memory period of the OBJ-SACC task (two-tailed t-test $p<0.05$). **A.** Monkey R. **B.** Monkey S

millisecond time bins aligned on the onset of the cue. We also analyzed whether the cells kept or switched the preference for the location of the cue on the object during the trial. We found that 91% of the cells maintained the same object side preference.

Since the directional preferences of the neurons in our sample were found to change from one task to the other, we were interested in how the retinotopic tuning of the cells in the MEM-SACC task was related to the preference for the object-based location of the cue. We counted the number of cells that preferred the object-based cue location congruent with hemispheric tuning in the MEM-SACC, i.e., cells with the receptive field in left hemifield preferring the left side of the object and vice versa. For the cue period tuning this was the case for 50% of the cells, and for the saccadic period tuning this was true for 68% of the cells. This means that the preferred location of the cue on the object is only loosely related to the retinotopic tuning in the saccade period of the MEM-SACC task and appears to be unrelated to the visual tuning in that task.

In the saccade interval, the monkey had to take into account the previous cued side of the object, the retiontopic location of the object, and finally its orientation to compute the correct saccade vector. We analyzed the responses of the cells with respect to the orientation of the object at the target position on the screen. Our first analysis was focused on the difference in the mean firing rates corresponding to the two orientations after the object re-appearance. We ran a two-tailed t-test on the mean firing rate in the 500ms aligned on the "go" signal, which also coincided with the re-appearance of the object in one of the peripheral locations. We found that the total of 24 cells had significantly different mean firing rates associated with the two object orientations ($p<0.05$). We also analyzed the temporal profile of the object orientation discrimination

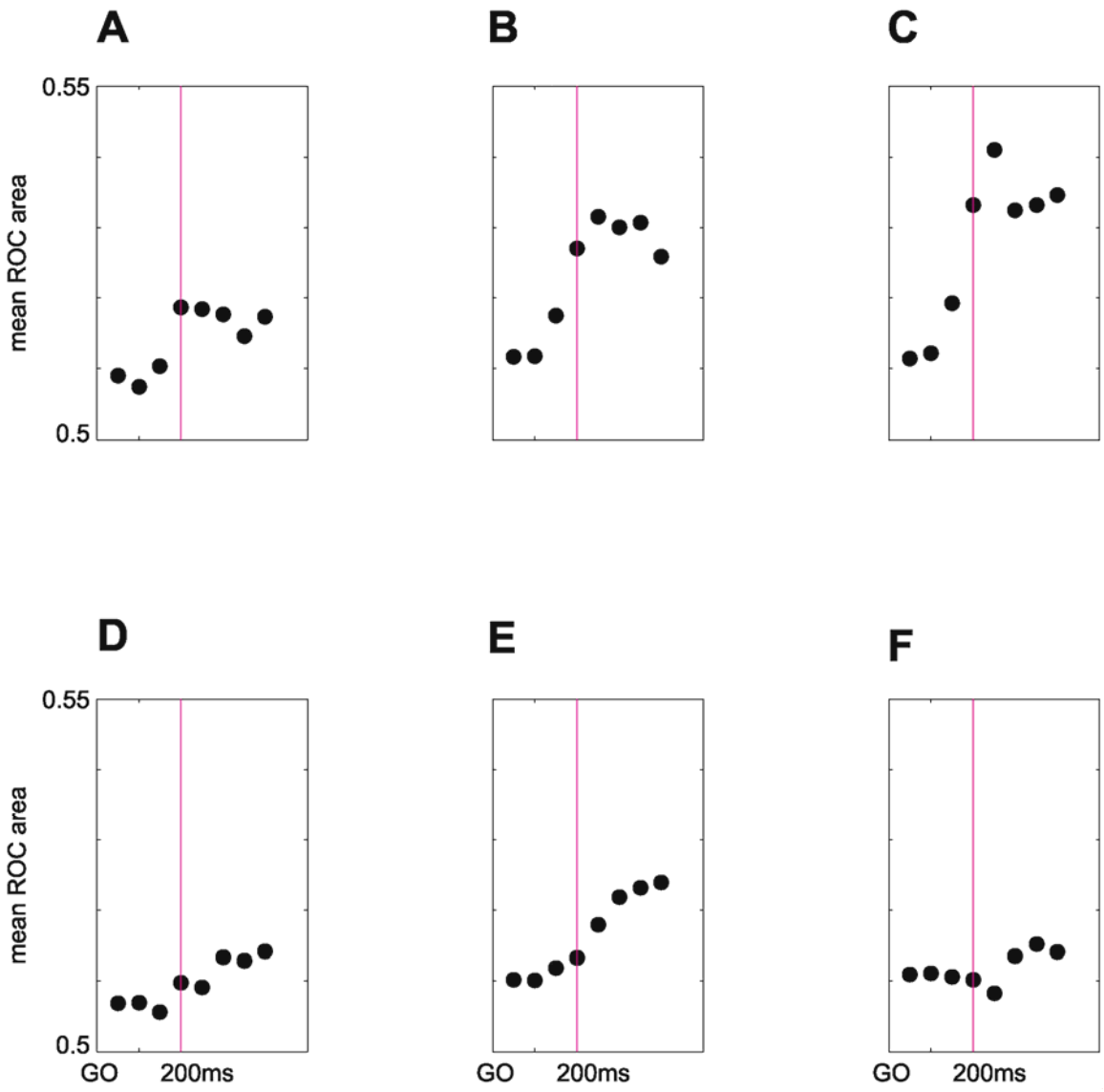

Figure 4.6. Object orientation discrimination. Mean ROC area calculated in 100ms time windows moving by 50ms, aligned on the GO signal. Mean was calculated across all cells with ROC area greater than 0.5. Top row (**A,B,C**) is data from monkey R. Bottom row (**D,E,F)** is data from monkey S. **A,D** Object orientation mean ROC values in all trials. **B,E** Object orientation ROC values in trials with cue left **C,F** same with cue right.

using the ROC analysis in sliding time windows. We found that overall the object orientation is represented only weakly, as already suggested by the low number of significant cells in the t-test. The mean ROC area in the 100ms time windows for all recorded cells for the two monkeys, respectively, is plotted in Figures 4.6A and D. We

noticed, however, that splitting data into two groups according to the object-centered location of the cue actually improves the object orientation discrimination. This happens despite the fact that the number of data points in the two groups is reduced by half, and thus the statistical power of the ROC analysis is weaker. Figures 4.6B, C, E, and F show the mean ROC areas for object orientation discrimination when the data was split to "cue left" and "cue right" groups and analyzed for the two monkeys separately. For three out of four cases the median ROC in the separated groups was higher than in the pooled groups (Wilcoxon ranksum test $p<0.05$). The only group where this test failed was Figure 4.6E, where the p value was 0.07.

DISCUSSION

Eye movements are readily directed to suddenly appearing points of light, such as a lightbulb turning on in a dark room. This is the situation approximated in many oculomotor neurophysiology experiments of LIP or lower-level structures, in which monkeys are instructed to saccade to small spots of light displayed in a dark setting (but see Campos, Cherian, and Segraves, 2006). In such cases, LIP neurons have well-characterized response fields that represent the onset of visual stimuli and intended eye movement plans in a spatially-tuned manner. In more natural circumstances, the oculomotor system is also capable of planning eye movements to portions of larger integrated objects, such as the handle of a coffee cup, and neurological evidence supports the notion that LIP activity serves this allocentric eye-movement encoding scheme as well.

In this study we compared the neural firing activity in the LIP of monkeys performing two tasks in which the same eye movements were instructed in different ways. In the first task, a spot cue was presented at the target location for a subsequent instructed eye movement. In the second task, a cue was presented on a polygonal object, and the appropriate eye movement could only be computed after the object rotated and translated to a new location. Our data give insight into how eye movements are encoded in LIP when they are directed to portions of objects instead of small spots of light. Our main finding was a context-dependence of the neural representation, depending on which task the monkey was performing and depending as well on the combinations of instructions within the tasks. Additionally, we found that object variables were represented in the second task in a way that was not predictable from the responses in the first.

In a review of eye movements in natural environments, Hayhoe and Ballard (2005) concluded that the task at hand has a pervasive role on when and where to fixate. Based on their own psychophysical research, they show that the eyes do not land on the objects that are most visually salient, but rather on those that are the best for the demands of the current task. In search for neural correlates for this context specificity, Hayhoe and Ballard quote the results of Gilbert et al (2001) and Roelfsema et al (2000), showing that even primary visual cortex exhibits task specific neuronal tuning. We submit that our results go further in supporting their psychophysical observations. Since parietal cortex plays a central role in spatial transformations underlying visuomotor behavior, context-specific tuning here, more so than in other peripheral areas, may facilitate flexible cognitive strategies. As we have shown in our experiment, the same movement can be

represented by different neural activity. A corollary to this finding is that the same visual stimulus may evoke context-specific representations, thus leading to task specific visual routines.

Context-dependence of spatial map "basis vectors"

We found that the population of LIP neurons continued to carry decodable retinotopic eye movement planning information in both tasks, but that the preferred spatial direction of the individual neurons often changed between the tasks. Specifically, the spatial preferences defined for individual neurons in the memory-guided saccade task frequently did not correspond to the spatial preferences exhibited by the same neurons in the object-based task. Furthermore, within the object-based task, many neurons would change or lose their directional preferences depending on the specific instruction. There was thus an effect of context on two levels. At the level of which task the monkey was performing, the spatial preferences were found to remap, requiring a new set of basis vectors for the decoding of movement intentions. At the level of which specific configuration of instructions was presented to the monkey in the object-based task, the spatial preferences of the neurons could change direction or be lost altogether. These within-task context changes may be partly attributable to the LIP neurons representing direction information, as well as information about the object-based instructions, at the same time.

Our findings are in line with results from other labs that had discovered modulations in the neuronal tuning as the context of task changes. Rokni and colleagues (Rokni et al. 2003) recorded from the neurons in the primary motor area during

unimanual and bimanual reaches. They first confirmed previous results by establishing that many neurons are tuned for both contralateral and ipsilateral unimanual reaches and that the tuning in those two tasks was similar. In bimanual reaches, however, the tuning of the cells was randomly shifted so that the correlation with the preferred direction that was observed in the unimanual task was lost. Fogassi and colleagues (Fogassi et al. 2005) studied the neurons in Inferior Parietal Lobule when monkeys performed motor acts embedded in different actions. They discovered that if a simple motor act (e.g., grasping a peanut) was embedded in an action comprised of a sequence of such acts (e.g., grasping and eating as opposed to grasping and placing an object into a container), a large majority of the neurons were influenced by the subsequent act. In both of these experiments the context of the task changed the tuning of the neurons that was observed previously. We note that it is a common practice in electrophysiology to establish a "reference" neuronal tuning using an accepted default task and then proceed to test the cells using more complicated tasks. Our results, as well as the results mentioned previously, suggest that there is a limit on the utility of this approach. Particularly, there is no reason to believe that the simplistic tasks used as the reference have any bearing on the behavior of the cells in more complex tasks.

Object-based encoding of eye movement

The eye movement planning circuitry requires three pieces of information to compute the appropriate eye movement in the object-based saccade task: the object's retinotopic position, the object's orientation, and the side of the object that was previously cued. The retinotopic position of the center of mass of the object almost

corresponds to the final target position, however the actual target is 4 degrees away, in a direction determined by the instructed cue side and the object's final orientation. These three important object-based variables were all represented in the population of LIP neurons, indicating that LIP itself contains all of the relevant information for deciding on an eye movement target. Though these variables were observable at the population level, we were surprised to find that for individual neurons the preferences for these object variables were not predictable from the spatial preferences observed in the memory-guided saccade task, as described below.

Representation of object-based instructional cue in visual and memory intervals

The preferences exhibited for the side of the object-based cue was quite strong, became apparent in the visual period of the object task, and continued through the memory period. Surprisingly, this laterality preference had little overlap with the directional preferences when encoding dot stimuli appearing in the periphery in the memory task. The amount of overlap varied according to whether the neuron exhibited primarily visual or saccadic activity in the memory-saccade task. The preferred location of the cue on the object was only loosely related to the preferred direction of the neurons exhibited in the memory task around the time of eye movements, and appeared unrelated (corresponded at chance level) to the visual response fields exhibited around the time of the spatial cue in that task.

Non-separable combination of object-based information in the saccade interval

Since the monkeys were instructed to make an eye-movement as soon as the object was displaced, we expected to see the visual responses related to the object's retinotopic position as well as the object side and orientation-specific responses necessary for computing the appropriate saccade, all in the same saccadic interval. During the saccade interval, we found that orientation tuning was present to a lesser extent compared to the object side preference and was combined with the encoding of the cue side, since our ability to decode the orientation of the object increased with prior knowledge of the side of the object that was cued. In our first example cell figure, Figure 4.2, it is clear that the neuron prefers the -45 degree orientation, but only when comparing the firing activity separately for the cue right versus cue left conditions. When the cue is presented on the left (Figure 4.2B,D), the activity for the -45 degree orientation is higher, and the same is true when the cue is presented on the right (Figure 4.2C,D). However, the activity in 2C (right side, +45 degree) is actually higher than the activity in 2A (left side, -45 degree), since both the side of the object and the orientation of the object are represented simultaneously, and in this neuron the side of the object contributes more to the firing activity than does the orientation. In order to properly decode the orientation of the object from the firing activity of this neuron, it is first important to know the task sub-context, meaning which side of the object was previously cued.

Limitations of the decode algorithm

We found that knowing part of the context (side of object-based cue) improves the decode of other information (orientation of object). We also found that in certain task

contexts the directional preferences of the neurons was lost. It may be a surprise, then, that we collapsed across all task contexts in our saccade direction decode shown in Figure 4.4, leaving context-dependent changes in the spatial tuning patterns to interfere with our directional decode. We attempted to improve the decode by running it separately in the different contexts, only including the data from a given configuration, hoping to eliminate the context-dependent interference. However, in this restricted case we found similar decode results. This may be due to a tradeoff between a more accurate decoding model by taking context into account and the amount of data we could use by collapsing across the different contexts. We leave for future research more sophisticated decode methods that recognize the contexts in which an individual neuron contributes to or interferes with the accuracy of the decode, and then makes use of all of the helpful data, while ignoring all of the data that is presumably encoding other variables.

Possible neural mechanisms of read out

How would downstream neurons accurately read-out context-dependent spatial tuning? Noting that the non-spatial firing activity shown in Figure 4.2C is not substantially higher than it is in the other contexts in which spatial information is present, how does the downstream neuron know that the neural activity in this context does not contain any spatial information and thus should be selectively excluded from the read-out of spatial direction? We can imagine three possibilities. First, there may be a combination of rule- or task- related activity in frontal cortical areas, which combine with the readout of LIP neurons in their projection to FEF or SC, to amplify or suppress the different signals appropriately. Second, the pattern of connections between the axons of LIP and

the dendrites of the downstream areas may themselves manage to segregate the movement command from the object-information processing. And finally, third, it may be possible that the output neurons do indeed have a stable response field mapping, and that the changes in the mapping we observed are only present in neurons engaged in local processing, which do not project outside of LIP.

Implications for Neural Prosthetics

The spatial remapping between tasks and task sub-contexts observed in this study poses a challenge to neuroprosthetic devices that hope to decode movement plans in a variety of situations. This context-dependent result may be found to generalize, such that other contexts have an attendant remapping of the spatial representation of eye movements. As shown here, the basis vectors calculated in one task will not be valid for use in the other task. New basis vectors will need to be computed for each new context, and the decode algorithms for neuroprosthetic applications will be required to take contextual information into account when attempting to decode movement intentions from parietal cortex.

REFERENCES

Andersen, R. A., and C.A. Buneo. "Intentional maps in posterior parietal cortex." *Annu. Rev. Neurosci.* 25: 189-220, 2002.

Andersen R. A., L. H. Snyder, C.S. Li, B. Stricanne. "Coordinate transformations in the representation of spatial information." *Curr Opin Neurobiol.* 3:171-6, 1993.

Andersen, R.A., G.K. Essick, and R.M. Siegel. "Encoding of spatial location by posterior parietal neurons." *Science*. 230: 456-458, 1985.

Breznen, B., M. Campos, and R.A. Andersen. "Parietal coding of saccades to symmetrical objects." Program No. 658.10. *2003 Abstract Viewer/Itinerary Planner.* Washington, DC: Society for Neuroscience, 2003. Online.

Deneve, S., and A. Pouget. "Basis functions for object-centered representations." *Neuron.* 37: 347-359, 2003.

Fogassi L., Ferrari P.F., Geseirich B., Rozzi S., Chersi F. C., and Rizzolatti G. "Parietal Lobe: From Action Organization to Intention Understanding" *Science* 308:662-667, Apr 2005

Georgopoulos A. P., Schwartz A. B., and Kettner R.E. "Neuronal Population Coding of Movement Direction" *Science* 233:1416-1419, Sept 1986

Gilbert C., et al. "The Neural Basis of Perceptual Learning" *Neuron* 31:681-697 (2001)

Goodale M. A., and A. D. Milner. "Separate visual pathways for perception and action." *Trends Neurosci.* 15: 20-25, 1992

Halligan P. W., and J. C. Marshall. "When two is one: a case study of spatial parsing in visual neglect." *Perception.* 22(3):309-12, 1993.

Hayhoe M., and Ballard D. "Eye movements in natural behavior" *Trends in Cognitive Sciences* 9:188-194, 2005.

Moorman, D. E., and C. R. Olson. "Neurons in monkey supplementary eye field exhibit object-centered selectivity even without training on an object-centered task." Program No. 57.12. *2002 Abstract Viewer/Itinerary Planner.* Washington, DC: Society for Neuroscience, 2002. Online.

Olsen, C.R., and Gettner, S.N. "Object-centered direction selectivity in the macaque supplementary eye field." *Science*, 269 (5226): 985-988, Aug 1995

Roelfsema P. et al. "The implementation of visual routines" *Cognition* 18:97-157 (2000)

Rokni U., Steinberg O., Vaadia E., and Sompolinsky H. "Cortical Representation of Bimanual Movements" *The Journal of Neuroscience* 23:11577-11586, 2003

Sabes, P. N., B. Breznen, and R. A. Andersen. "Parietal representation of object-based saccades." *J. Neurophysiol.* 88: 1815-1829, 2002.

Sereno, A. B., and J. H. R. Maunsell. "Shape selectivity in primate lateral intraparietal cortex." Nature. 395: 500-503, 1998.

CONCLUSION

The studies presented here increase our understanding, first, of the ways that different cortical areas involved in eye movement behavior specialize and complement each other, and second, the ways that eye movement signals interface with signals from other functional circuits of the brain. In Chapter 2 we demonstrated a role of SEF in representing sequential states of an instructed task, which is not similarly exhibited by LIP in the simple task context we used, and in Chapter 3 we described complementary roles of LIP and SEF in the process of target selection. Extending the understanding of the relationships between different functional circuits brought together in eye movement behavior, Chapter 1 detailed the coexistence of reward processing and motor representations in supplementary motor cortex, and Chapter 4 characterized the effects of task context on spatial representations in LIP, which is dependent on object recognition. Together these results contribute to our understanding of the mechanisms by which a functioning brain integrates information from a variety of sources to successfully accomplish tasks and achieve rewards.